Section I
Lemke

AN ELECTRON DENSITY INTERPRETATION

OF

THE CHEMICAL BOND

AN ELECTRON DENSITY INTERPRETATION OF THE CHEMICAL BOND

by

WILLIAM HARRISON HENNEKER, B.SC.

A Thesis

Submitted to the Faculty of Graduate Studies

in Partial Fulfilment of the Requirements

for the Degree

Doctor of Philosophy

McMaster University

May 1968

DOCTOR OF PHILOSOPHY
(Chemistry)

McMASTER UNIVERSITY
Hamilton, Ontario.

TITLE: An Electron Density Interpretation of the Chemical Bond

AUTHOR: William Harrison Henneker, B.Sc. (University of Western Ontario)

SUPERVISOR: Professor R. F. W. Bader

NUMBER OF PAGES: ix, 190

SCOPE AND CONTENTS:

This thesis presents the results of an attempt to study the chemical bond in terms of the three-dimensional electronic charge distribution and the force which this charge distribution exerts on the nuclei. The homonuclear diatomic molecules Li_2, B_2, C_2, N_2, O_2, and F_2 are discussed in terms of covalent binding while the heteronuclear diatomic molecules LiF and LiH are discussed in terms of ionic binding.

PREFACE

For approximately one hundred years chemists have been writing structural formulae with lines connecting the atoms which form so-called valence bonds. The concept of valence arose in connection with the development of organic chemistry and originally referred to the combining power of an atom in a molecule. Gradually chemists began to think of these structural formulae as showing the way in which atoms are bonded together in three-dimensional space. With the discovery of the electron, there was much speculation as to the physical basis of the chemical bond. Lewis developed his concepts of the shared-electron-pair and the stable octet to explain respectively the covalent and ionic bonds. The development of quantum mechanics in the late 1920's and its application to chemistry resulted in the valence bond interpretation of ionic character.

Yet the chemical bond so far has evaded precise definition. Indeed it is the considered opinion of many investigators that there is no precise definition for this concept. This study presents a discussion of the chemical bonds in homonuclear and heteronuclear diatomic molecules. The discussion is in terms of the three-dimensional electronic charge distribution and the force

that it exerts on the nuclei. The net force acting on the nucleus in a stable molecule must be zero. The molecular density distribution when compared to the density distributions of the noninteracting atoms gives evidence of the reorganization of charge that occurs during the formation of the molecule in order to achieve this electrostatic equilibrium.

I agree with Polanyi that knowledge is personal and involves the active participation of the one who aspires to know. My stay at McMaster University has allowed me the opportunity of involvement in theoretical chemistry. This thesis is the result of 3.5 years of reading, computer programming, discussions - and more computer programming. Interspersed with these activities were sessions spent at the piano in an attempt to perfect Bachian fugues and the preludes of Rachmaninoff.

In the poem "Ulysses", the hero is quoted as saying, "I am a part of all that I have seen ". Indeed this is true. I thank my parents for their material assistance during the undergraduate portion of my student career and for their encouragement. Also I thank Dr. D. R. Bidinosti of the chemistry department at the University of Western Ontario who first taught me quantum mechanics and directed me to further studies at McMaster University.

I thank Professor R.F.W. Bader for his continued interest in the problems discussed in this thesis. He originally suggested the analysis presented in the following pages and his enthusiastic approach has led to the successful completion of this work. From him I have learned the importance of associating a physical picture with the mathematical description of "l'état des choses". Theoretical chemistry is more than the evaluation of integrals !

I acknowledge the assistance of two graduate students with whom I have been associated during the course of this study. Mr. Andrew Bandrauk with his many statements of disbelief often caused me to re-examine hastily drawn conclusions. Mr. Harry Preston and I redesigned the computer subprogramme FØRINT . He also rewrote the subprogramme ØVLINT for the calculation of overlap force integrals.

Financial assistance was provided by the National Research Council of Canada in the form of one bursary and and three studentships. I acknowledge this monetary aid.

Mr. Paul Curry drew the diagrams and Mrs. H. Kennelly skillfully typed this thesis. To them I say thank you.

Finally I wish to express my thanks to Dr. Paul E. Cade of the Laboratory of Molecular Structure and Spectra at the University of Chicago for supplying us with wave-functions of Hartree-Fock accuracy. The interpretations presented in this thesis would not be possible without the many people who have developed the Hartree-Fock-Roothaan procedure.

TABLE OF CONTENTS

LIST OF TABLES

LIST OF FIGURES

LIST OF FIGURES (continued)

INTRODUCTION

In 1929, Dirac[1] stated "the underlying physical laws necessary for the mathematical theory of a large part of physics and the whole of chemistry are thus completely known and the difficulty is only that the exact application of these laws leads to equations much too complicated to be soluble." This statement has been quoted by numerous theoreticians[2,3] who have devoted themselves to the formidable task of finding solutions to Schroedinger's equation

$$H\Psi = E\Psi$$

where H is the quantum mechanical Hamiltonian, Ψ is the eigenfunction of the system and E is the energy eigenvalue. This equation which, for the quantum chemist, describes the many-body problem presented by a system of nuclei and electrons has not yet been solved exactly. However, progress has been made especially within the framework of a physically well-defined approximation-namely the Hartree-Fock approximation - so that there presently exist electronic wave functions for atoms and diatomic molecules whose energy eigenvalues are close to the Hartree-Fock limit. One particularly important advantage of these wave functions is the fact that they yield one-electron density distributions correct to the second order in perturbation theory. As a consequence of this result, all

properties depending on the one-electron density distribution are also correct to second order. Because the one-electron density is just the three-dimensional electronic charge distribution, an observable of the system being considered, its accuracy warrants its use as the basis for new definitions concerning the chemical bond.

It is the purpose of this thesis to discuss the chemical bond in terms of Hartree-Fock, one-electron density contour maps and to relate these density quantities to the force acting on the nucleus by means of the Hellmann-Feynman theorem[4]. Certain electron density difference contour maps are obtained by subtracting from the total molecular density the density distributions of the constituent atoms. Such contour maps are interpreted as the reorganization of charge attendant upon the formation of the chemical bond. If any correlation exists between these contour maps and the classical ideas concerning the covalent and ionic bonds, then there will be density difference or $\Delta\rho$ maps characteristic of each of these limiting forms of the chemical bond. Does the $\Delta\rho$ map for LiF show a localization of one unit of electronic charge about the fluorine atom ? Does the $\Delta\rho$ map for a homonuclear diatomic molecule present a picture which can be correlated with the classical concept of the shared-electron-pair which Lewis[5] postulated as the important feature of a covalent bond ? Do the density and density

difference maps by themselves predict molecular stability ?

This thesis commences with a general discussion of density matrices and the properties associated with these matrices. Hartree-Fock theory is discussed, and it is shown that the Hartree-Fock, one-electron density distribution and its dependent properties are correct to the second order. Density and density difference contour maps are discussed for the homonuclear diatomic molecules Li_2, B_2, C_2, N_2, O_2, and F_2. Force calculations involving these molecules are analyzed, and a comparison of the terms binding and bonding is presented. Finally a comparative study of the bonds in LiF and N_2 is made. The analysis is in terms of the forces operative in the two molecules and the density and density difference contour maps of the two molecules.

Most of the results of this thesis have been published in the Journal of the American Chemical Society[6,7] and the Journal of Chemical Physics[8].

CHAPTER I

THEORETICAL BACKGROUND

I.1 DENSITY MATRICES

The N-electron wave function is related to the position co-ordinates of each of the N electrons. As Hartree[9] has pointed out, a table listing its values at ten positions of each variable would require 10^{3N} entries. In addition to the fact that for increasing values of N, the size of the table rapidly becomes intractable, the entries in the table are meaningless from a physical point of view. How can such a wave function be interpreted in the light of familiar chemical concepts?

In this section, the first-and second-order density matrices[10] are defined and expressions involving their dependent properties are evaluated. The discussion emphasizes the use of such matrices as interpretive devices.

Consider $\Psi(\vec{x}_1\vec{x}_2\ldots\vec{x}_N)$ as a wave function describing an N-electron system. The co-ordinate $\vec{x}_N$ describes the position $\vec{r}_N$ and the spin s_N of the Nth electron. The product $\Psi^*\Psi$ gives the simultaneous probability of finding electron one at position $\vec{r}_1$ with spin s_1, electron two at position $\vec{r}_2$ with spin s_2, ... and electron N at position $\vec{r}_N$ with spin s_N. The mth-order density matrix is by definition

$$\Gamma^m(1,2\ldots m|1',2'\ldots m') = \frac{N!}{m!(N-m)!} \int \Psi^*(1,2\ldots m,m+1,\ldots N)$$

$$\Psi(1',2',\ldots m',m+1,\ldots N)\,d\vec{x}_{m+1}\ldots d\vec{x}_N \qquad (1)$$

where

$$\Psi(1,2,\ldots,m,m+1,\ldots N) = \Psi(\vec{x}_1,\vec{x}_2,\ldots\vec{x}_m,\vec{x}_{m+1}\ldots\vec{x}_N)$$

In particular, the second-order density matrix is given as

$$\Gamma^2(1,2|1',2') = \frac{N(N-1)}{2} \int \Psi^*(1,2,3\ldots N)\Psi(1',2',3,\ldots N)\,d\vec{x}_3\ldots d\vec{x}_N. \quad (2)$$

The diagonal element of this matrix, $\Gamma^2(1,2|1,2)$ has the following interpretation. The expression $\Gamma^2(1,2|1,2)d\vec{x}_1 d\vec{x}_2$ is equal to the number of pairs of electrons times the probability for finding one electron within the volume element $d\vec{r}_1$ around the point $\vec{r}_1$ with spin s_1 and another electron within the volume element $d\vec{r}_2$ around the point $\vec{r}_2$ with the spin s_2 with all other electrons having arbitrary positions and spins. The diagonal element of the first-order density matrix

$$\gamma(1|1) = N \int \Psi^*(1,2\ldots N)\Psi(1,2,\ldots N)\,d\vec{x}_2\ldots d\vec{x}_N \qquad (3)$$

has the following physical interpretation. It is just the number of electrons, N, times the probability of finding an electron at the position $\vec{r}_1$ with spin s_1 irrespective of the co-ordinates and spins of the other electrons. The expression

$$\rho(\vec{r}_1) = \int \gamma(1|1)\,ds_1 \qquad (4)$$

is now independent of the spin s_1 and is just the total charge density at the position $\vec{r}_1$. Equations (3) and (4) state that, in principle, a one-electron density function which obeys the laws of quantum mechanics can be calculated. Arguments from this point onward can be based upon a three-dimensional function $\rho(\vec{r})$ describing an electronic charge distribution in real space instead of a 4 N-dimensional function Ψ which has no physical interpretation at all.

The discussion of density matrices can be carried further by showing their use in the calculation of atomic and molecular properties. The definition of a one-electron operator is given below as

$$P = \sum_{i=1}^{N} O(i) \tag{5}$$

where the index i refers to the ith electron. The average value of this operator is

$$\langle P \rangle = \int \Psi^*(1,2,\ldots N) \sum_{i=1}^{N} O(i)\, \Psi(1',2,\ldots N)\, d\vec{x}_1 d\vec{x}_2 \ldots d\vec{x}_N$$

$$= \int O(1)\, \gamma(1|1')_{\vec{x}_1'=\vec{x}_1}\, d\vec{x}_1 = \int O(\vec{r})\, \rho(\vec{r})\, d\vec{r} \tag{6}$$

where the last of the three expressions follows if the operator is spin independent. The above equations (6) show that the average value of a one-electron operator depends only on the first-order density matrix where the convention is that the operator operates on unprimed co-ordinates and then primed co-ordinates are set equal to

unprimed co-ordinates. A two-electron operator defined by

$$Q = \frac{1}{2} \sum_{ij} G(i,j) \tag{7}$$

where $i \neq j$ yields for its average value

$$\langle Q \rangle = \frac{N(N-1)}{2} \int \Psi^*(1,2,\ldots N) G(1,2) \Psi^*(1',2',\ldots N) d\vec{x}_1 \ldots d\vec{x}_N$$

$$= \int G(1,2) \Gamma^2(1,2|1',2')_{\vec{x}_1'=\vec{x}_1, \vec{x}_2'=\vec{x}_2} d\vec{x}_1 d\vec{x}_2 \tag{8}$$

From these considerations, the average value of the electronic energy of a molecular system is easily calculated as

$$E = \langle \Psi | H | \Psi \rangle \tag{9}$$

where

$$H = \sum_{i=1}^{N} H_N(i) + \frac{1}{2} \sum_{\substack{i,j \\ i \neq j}} \frac{1}{r_{ij}} \tag{10}$$

and

$$H_N(i) = -\frac{1\nabla_i^2}{2} - \sum_{\alpha} \frac{Z_\alpha}{r_{i\alpha}} \tag{11}$$

Also r_{ij} is the distance between the ith and jth electrons, ∇_i^2 is the Laplacian operator for the ith electron, Z_α is the charge of the αth nucleus and $r_{i\alpha}$ is the distance between the ith electron and the αth nucleus. With these definitions, the energy is

$$E = \int H_N(1) \gamma(1|1')_{\vec{x}_1'=\vec{x}_1} d\vec{x}_1 + \int \frac{\Gamma^2(1,2|1',2')_{\vec{x}_1'=\vec{x}_1, \vec{x}_2'=\vec{x}_2}}{r_{12}} d\vec{x}_1 d\vec{x}_2. \tag{12}$$

Another form for the energy equation is

$$E = \frac{N \int H_N(1) \Gamma^2(1,2|1',2') d\vec{x}_1 d\vec{x}_2 + \frac{N(N-1)}{2} \int \frac{\Gamma^2(1,2|1',2')}{r_{12}} d\vec{x}_1 d\vec{x}_2}{\frac{N(N-1)}{2} \int \Gamma^2(1,2|1',2') d\vec{x}_1 d\vec{x}_2} \tag{13}$$

where the subscripts $\vec{x}_1' = \vec{x}_1$; $\vec{x}_2' = \vec{x}_2$ have been dropped, and the above mentioned convention is still implied. Equation (13) allows for the normalization of the second-order density matrix and shows that, in fact, the energy of the system depends only on the second-order density matrix. Löwdin[10] has suggested that equation (13) be the basis of a minimization procedure that seeks an expression for the density matrix $\Gamma^2(1,2|1',2')$ which produces the lowest energy possible. Then the one-electron density distribution could be calculated from the following equation

$$\rho(\vec{r}) = \frac{(N-1)}{2} \int \Gamma^2(1,2|1',2')\, ds_1 d\vec{x}_2 \quad . \qquad (14)$$

However, in order to proceed in this manner, an analytical form for $\Gamma^2(1,2|1',2')$ must be known. This is by no means a trivial question and is part of the general problem of N-representability[11] which asks the necessary and sufficient conditions that a given density matrix is a representation of the properly antisymmetrized N-body wave function.

Of course, at present the density matrices can be obtained by the more conventional method of integrating the function

$$\Psi^*(1,2,\ldots N)\Psi(1,2\ldots N) \quad . \qquad (15)$$

The following chapter gives a detailed account of the Hartree-Fock approximation to Ψ and the one-electron density derived from this approximate Ψ.

I.2 THE HARTREE-FOCK APPROXIMATION

The electronic wave equation for a polyelectronic, polynuclear system is given below as.

$$\left[-\frac{1}{2}\sum_{i}\nabla_i^2 - \sum_{i\alpha}\frac{Z_\alpha}{r_{i\alpha}} + \sum_{i>j}\frac{1}{r_{ij}}\right]\Psi = E\Psi \qquad (16)$$

where the symbols have been previously defined. As mentioned in the introduction, this wave equation has never been solved exactly. If exact solutions do not present themselves, then approximations are necessary. In particular, the Hartree-Fock formulation seeks an approximate wave function which is antisymmetrized product of one-electron spin functions. Thus

$$\Psi = \sqrt{\frac{1}{N!}}\,\|\, a_1(1)a_2(2).....a_N(N)\,\| \qquad (17)$$

The heavy double bars denote a determinant. If the one electron spin functions obey the following relation

$$\langle a_i | a_j \rangle = \delta_{ij} \qquad (18)$$

where δ_{ij} is the usual diagonal Kronecker δ symbol, then the wave function Ψ is normalized to unity.

The concept of the one-electron spin function arose from an attempt to extend the central field model for the hydrogen atom to the general case of an N-electron system. An electron in the spinorbital a_i moves in a field owing to the nuclei Z_α and the average charge distribution of the remaining N-1 electrons.

Hartree[12] was the first person to formulate the quantum mechanical analogue of the classical central field atom. He calculated the self-consistent field in which a given electron moved, and then obtained the orbital describing this electron by numerical integration techniques. As early as 1927, he obtained an orbital energy for He of -1.835 a.u. which compares favorably with the present day calculation of -1.83592 a.u. published by Clementi[13].

In 1930, Fock[14] extended the Hartree theory to include the Pauli principle and, in the same year, Slater[15] noted the connection between the variation principle and the Hartree-Fock formalism in the case of an antisymmetrized wave function composed of one-electron spin functions.

Consider such a wave function describing the N-electron problem in the case of a diatomic molecule. The Born-Oppenheimer[16] approximation is assumed in this discussion and, as a result, the wavefunction Ψ is labelled with a subscript E for electronic. The energy of such a system is given as

$$E = \langle \Psi_E | H | \Psi_E \rangle \tag{19}$$

where the Hamiltonian H is given in equation (16)
With the definition of $H_N(i)$ as the Hamiltonian describing one electron in the field of the two nuclei Z_1 and Z_2

$$H_N(i) = -\frac{\nabla_i^2}{2} - \sum_{\alpha=1}^{2} \frac{Z_\alpha}{r_{i\alpha}} \tag{20}$$

the total Hamiltonian becomes

$$H = \sum_{i}^{N} H_N(i) + \sum_{i>j} \frac{1}{r_{ij}} \qquad (21)$$

The expression (19) for the electronic energy becomes

$$E=\frac{1}{N!}\langle||a_1(1)....a_N(N)||\left|\sum_{i=1}^{N} H_N(i)+\sum_{i>j}\frac{1}{r_{ij}}\right||a_1(1).....a_N(N)||\rangle$$

$$= \langle a_1(1)....a_N(N)\left|\sum_{i=1}^{N} H_N(i)+\sum_{i>j}\frac{1}{r_{ij}}\right||a_1(1)....a_N(N)||\rangle$$

$$= \sum_{i=1}^{N}\langle a_i(1)\,|H_N(1)\,|a_i(1)\rangle + \sum_{i>j}\left[\langle a_i(1)a_j(2)\,|\frac{1}{r_{12}}|\,a_i(1)a_j(2)\rangle\right.$$

$$\left.-\langle a_i(1)a_j(2)\,|\frac{1}{r_{12}}|\,a_i(2)a_j(1)\rangle\right]$$

$$= \sum_{i=1}^{N} I_i' + \sum_{i>j}^{N}\left[J_{ij}' - K_{ij}'\right] \qquad (22)$$

For a closed shell system where the spinorbital a_i is restricted to be of the form $\phi_i\alpha$ or $\phi_i\beta$, the wave function is given as

$$\Psi_E = \sqrt{\frac{1}{N!}}\,||\phi_1(1)\alpha(1)\phi_1(2)\beta(2).....\phi_{\frac{N}{2}}(N)\beta(N)|| \qquad (23)$$

ϕ_i is the ith molecular orbital and obeys the relation

$$\langle\phi_i|\phi_j\rangle = \delta_{ij} \qquad (24)$$

The symbols α and β refer to the one-electron spin functions. With these definitions, the terms in equation (22) become

$$I_i' = \langle a_i(1)\,|H_N(1)\,|a_i(1)\rangle = \langle\phi_i(1)\,|H_N(1)\,|\phi_i(1)\rangle = I_i \qquad (25)$$

$$J_{ij}' = \langle a_i(1)a_j(2)\,|\frac{1}{r_{12}}|a_i(1)a_j(2)\rangle = \langle\phi_i(1)\phi_j(2)\,|\frac{1}{r_{12}}|\phi_i(1)\phi_j(2)\rangle = J_{ij} \qquad (26)$$

$$K'_{ij} = \langle a_i(1)a_j(2)|\frac{1}{r_{12}}|a_i(2)a_j(1)\rangle = \langle \phi_i(1)\phi_j(2)|\frac{1}{r_{12}}|\phi_i(2)\phi_j(1)\rangle = K_{ij} \quad (27)$$

Equation (27) is true if ϕ_i and ϕ_j have the same spin. Otherwise $K'_{ij}=0$. The energy of such a closed shell system is

$$E = 2\sum_i I_i + \sum_i J_{ii} + \sum_{i>j}\left[4J_{ij}-2K_{ij}\right] \quad (28)$$

where the sums are over the occupied molecular orbitals. The above expression can be rearranged to give

$$E = 2\sum_i I_i + \sum_{ij}\left[2J_{ij}-K_{ij}\right] \quad (29)$$

where $J_{ii} = K_{ii}$.

Under what conditions do the molecular orbitals ϕ_i yield a wave function whose energy is a minimum ? In order to answer this question, the energy must be minimized subject to the restriction that the one-electron functions remain normalized and orthogonal[17]. This is equivalent to minimizing the energy subject to the condition that

$$2\sum_{ij} \varepsilon_{ij} S_{ij} \quad (30)$$

remains constant. The ε_{ij} are constants and

$$S_{ij} = \delta_{ij} = \langle \phi_i|\phi_j\rangle. \quad (31)$$

A new quantity E' is defined and it is required that this E' be stationary with respect to small variations in the ϕ_i. Thus

$$E' = E - 2\sum_{ij} \varepsilon_{ij} S_{ij} \quad (32)$$

and

$$\delta E' = 0 = \delta E - 2\sum_{ij} \varepsilon_{ij}\, \delta S_{ij}$$

$$= 2 \sum_i \delta I_i + \sum_{ij} \left[2\delta J_{ij} - \delta K_{ij} - 2\epsilon_{ij} \delta S_{ij} \right] \qquad (33)$$

It is necessary to evaluate all the expressions in equation (33)

$$\delta S_{ij} = \delta \langle \phi_i(1) | \phi_j(1) \rangle = \langle \delta\phi_i(1) | \phi_j(1) \rangle + \langle \phi_i(1) | \delta\phi_j(1) \rangle \qquad (34)$$

$$\delta I_i = 2 \langle \delta\phi_i(1) | H_N(1) | \phi_i(1) \rangle \qquad (35)$$

Further, $$J_{ij} = \langle \phi_i(1)\phi_j(2) | \frac{1}{r_{12}} | \phi_i(1)\phi_j(2) \rangle$$

$$= \langle \phi_i(1) | J_j(1) | \phi_i(1) \rangle = \langle \phi_j(2) | J_i(2) | \phi_j(2) \rangle \qquad (36)$$

where $$J_j(1) = \langle \phi_j(2) | \frac{1}{r_{12}} | \phi_j(2) \rangle \qquad (37)$$

$$J_i(2) = \langle \phi_i(1) | \frac{1}{r_{12}} | \phi_i(1) \rangle \qquad (38)$$

J_j is the interaction of electron one with electron two where the position of electron one is held constant and the integration is carried out over the charge distribution of electron two. It is the average field acting on electron one because of the remaining N-1 electrons. The assumption that this average field does not change as electron one moves is implicit in the Hartree-Fock formalism. Thus

$$\delta J_{ij} = 2\langle \delta\phi_i(1) | J_j(1) | \phi_i(1) \rangle + 2\langle \delta\phi_j(1) | J_i(1) | \phi_j(1) \rangle \qquad (39)$$

Also $$K_{ij} = \langle \phi_i(1)\phi_j(2) | \frac{1}{r_{12}} | \phi_i(2)\phi_j(1) \rangle =$$

$$= \langle \phi_i(1) | K_j(1) | \phi_i(1) \rangle = \langle \phi_j(2) | K_i(2) | \phi_j(2) \rangle \qquad (40)$$

K_j is an exchange operator which reflects the inclusion of the Pauli principle in the theory. Thus

$$\delta K_{ij} = 2\langle\delta\phi_i(1)|K_j(1)|\phi_i(1)\rangle + 2\langle\delta\phi_j(2)|K_i(2)|\phi_j(2)\rangle \quad (41)$$

With these relations $\delta E'$ in equation (33) becomes

$$\delta E' = 0 = \sum_{i=1}\left[\langle\delta\phi_i(1)|\left[4H_N(1)+\sum_j(8J_j(1)-4K_j(1))\right]|\phi_i(1)\rangle - \langle\delta\phi_i(1)|2\sum_j\varepsilon_{ij}\,\phi_j(1)\rangle\right] \quad (42)$$

Since $\delta\phi_i(1)$ represents an arbitrary variation of the ith molecular orbital ϕ_i, then

$$\left[H_N(1) + \sum_j (2J_j(1)-K_j(1))\right]\phi_i(1) = \sum_j \varepsilon_{ij}\,\phi_j \quad (43)$$

An orthogonal unitary transformation of the type

$$\phi_i' = \sum_j \phi_j C_{ji} \quad (44)$$

can be executed where here and in all future references the index one indicating the single particle nature of ϕ_i is dropped. Such molecular orbitals ϕ_i' lead to an electronic wave function

$$\Psi_E = \sqrt{\frac{1}{N!}}\,||\phi_1'(1)\alpha(1)\phi_1'(2)\beta(2).....\phi_{\frac{N}{2}}'(N)\beta(N)||$$

$$= \Psi_E \det\{\bar{C}\} \quad (45)$$

where $\det\{\bar{C}\}$ is the determinant of the matrix $\bar{C}$.

Since $\bar{C}$ is a unitary matrix, $\det\{\bar{C}\}=\pm 1$,

$$\Psi_E' = \pm \Psi_E \tag{46}$$

and such a unitary transformation does not change the total electronic energy of the system. In particular, the unitary transformation $\bar{U}$ which diagonalizes the matrix $\bar{\varepsilon}$ is sought. The Hartree-Fock operator is defined below as

$$F = H_N + \sum_j (2J_j - K_j) \tag{47}$$

and is invariant to this transformation. The transformed molecular orbitals and $\bar{\varepsilon}$ matrix become

$$\bar{\phi}' = \bar{\phi}\bar{U} \tag{48}$$

$$\bar{\varepsilon}' = \bar{U}^{-1}\bar{\varepsilon}\bar{U}. \tag{49}$$

$\bar{\phi}'$ and $\bar{\phi}$ are row vectors, $\bar{U}$ is the required $p\times p$ matrix where $p=\frac{N}{2}$ is the number of occupied molecular orbitals, $\bar{U}^{-1}$ is the inverse of this matrix and $\bar{\varepsilon}'$ is a diagonal matrix. The placement of these results in the matrix equivalent of equation (43)

$$F\bar{\phi} = \bar{\phi}\bar{\varepsilon} \tag{50}$$

yields the result

$$F\phi_i' = \varepsilon_i'\phi_i' \tag{51}$$

or

$$\left[H_N + \sum_j (2J_j - K_j)\right]\phi_i' = \varepsilon_i'\phi_i' \tag{52}$$

Equation (52) describes the Hartree-Fock integro-differential equations. In future references to this result, all primes

will be dropped and ϕ_i will be used to represent the ith Hartree-Fock molecular orbital. The equation is essentially the same as that one proposed intuitively by Hartree. The average potential in which the electron moves is given by

$$V = -\frac{Z_1}{r_{i1}} - \frac{Z_2}{r_{i2}} + \sum_j (2J_j - K_j) \qquad (53)$$

In order to calculate this average potential, a charge distribution must be assumed. Thus a self-consistent approach to the problem is adopted in which it is required that the final calculated charge distribution be the same as that one assumed in order to make the calculation.

The term ε_i' in equation (52) is called the orbital energy. It has been shown by Koopmans[90] that ε_i (with the prime dropped) is an approximation to the ionization energy I_i of an electron in the ith molecular orbital; that is

$$I_i = -\varepsilon_i \qquad (54)$$

Also

$$\varepsilon_i = -\langle\phi_i|\tfrac{1}{2}\nabla_i^2|\phi_i\rangle - \langle\phi_i|\frac{Z_1}{r_{i1}} + \frac{Z_2}{r_{i2}}|\phi_i\rangle + \sum_j (2J_{ij} - K_{ij}) \qquad (55)$$

The orbital energy is equal to the kinetic energy of electron i and the interaction potential $\langle\phi_i|V|\phi_i\rangle$. This interaction potential consists of the coulomb attraction between electron i and the two nuclei Z_1 and Z_2 plus the coulomb repulsion between the electron i and the charge distribution describing the remaining N-1 electrons. In the case of j=i, $J_{ii}=K_{ii}$ and the coulomb repulsion is equal to J_{ii}, the

repulsion between two electrons in the ith molecular orbital. In this particular case, the exchange integral K_{ii} is seen as preventing the inclusion in the total potential energy of a term describing the repulsive self-potential of an electron ; that is, the repulsive potential of an electron due to its own charge distribution. For $i \neq j$, the term $2J_{ij}$ describes the potential between electron i and the 2 electrons in the orbital ϕ_j. Since the exchange potential K_{ij} is non zero only for electrons of the same spin, the factor two is in this case deleted. It is difficult to ascribe a simple, classical, physical picture to the term K_{ij}. All that can be said about this term is that it arises because of the antisymmetric nature of the electronic wave function. It represents an additional interaction between a pair of electrons with parallel spins.

Although Hartree originally obtained his one-electron functions by numerical integration techniques, Roothaan[18] has more recently formulated the expansion method for the solution of the Hartree-Fock equation. In the case of diatomic molecules, he obtains the molecular orbitals as linear combinations of Slater-type functions centred on each nucleus.

Thus $$\phi_{i\lambda\alpha} = \sum_{p} \chi_{p\lambda\alpha} C_{i\lambda p} \qquad (56)$$

where $\chi_{p\lambda\alpha}$ is a Slater-type function denoted by $S_{n\ell\alpha}$*

$$S_{n\ell\alpha} = \frac{(2\zeta)^{n+\frac{1}{2}}}{[(2n)!]^{\frac{1}{2}}} r^{n-1} Y_{\ell}^{\alpha} e^{-\zeta r} \qquad (57)$$

Similarly the one-electron atomic orbitals are approximated as

$$\chi'_{i\lambda\alpha} = \sum \chi_{p\lambda\alpha} C_{i\lambda p} \qquad (58)$$

The index lambda refers to the symmetry species of the one-electron orbital and α is the symmetry subspecies which becomes important if λ is degenerate. The index i is an integer which numbers the nondegenerate functions within a given symmetry species. For instance, in atoms the electrons are classified according to their angular momentum quantum number as

$$\ell=0 \longrightarrow s$$

$$\ell=1 \longrightarrow p$$

$$\ell=2 \longrightarrow d$$

Thus for neon in the configuration $1s^2 2s^2 2p^6$, the atomic Hartree-Fock orbitals are labelled

$$\chi'_{1s}, \chi'_{2s}, \chi'_{2po}, \chi'_{2pl}, \chi'_{2p-1}$$

In linear molecules, the electrons are classified according to their angular momentum along the z axis as

$$\ell_z=0 \longrightarrow \sigma$$

$$\ell_z=1 \longrightarrow \pi$$

---

*The symbol ζ represents the orbital screening coefficient. Y_{ℓ}^{α} is a spherical harmonic.

Hence, LiF, in the configuration $1\sigma^2 2\sigma^2 3\sigma^2 4\sigma^2 1\pi^4$ has associated with it the molecular orbitals

$$\phi_{1\sigma}, \phi_{2\sigma}, \phi_{3\sigma}, \phi_{4\sigma}, \phi_{1\pi+}, \phi_{1\pi-} \quad .$$

From the expansion equation (56) above, it is seen that the choice of Slater-type functions depends on the symmetry of the molecular orbital in question. Non-degenerate molecular orbitals of the same symmetry species have the same basic Slater-type functions. However, the linear coefficients $C_{i\lambda p}$ depend on the index i but are independent of the symmetry subspecies α. If equation (56) is substituted into equation (51), the canonical Hartree-Fock equations become in matrix notation

$$F\bar{\phi}_{\lambda\alpha} = \bar{\bar{\varepsilon}}\bar{\phi}_{\lambda\alpha} \tag{59}$$

Thus for molecular orbital $\phi_{i\lambda\alpha}$,

$$F\bar{\chi}_{\lambda\alpha}\bar{C}_{\lambda} = \varepsilon_i \bar{\chi}_{\lambda\alpha}\bar{C}_{\lambda} \tag{60}$$

$\bar{\chi}_{\lambda\alpha}$ is a row vector, $\bar{\phi}_{\lambda\alpha}$ is a row vector, and $\bar{C}_{\lambda}$ is a column vector. The indices $\lambda\alpha$ in equation (59) imply that in the case of σ electrons, there will be one matrix equation of the form

$$F\bar{\phi}_{\sigma} = \bar{\bar{\varepsilon}}\bar{\phi}_{\sigma} \tag{61}$$

and that, in the case of π electrons, there will be two identical matrix equations of the form

$$F\bar{\phi}_{\pi} = \bar{\bar{\varepsilon}}\ \bar{\phi}_{\pi} \tag{62}$$

Consider equation (60) and premultiply both left and right hand sides by $\bar{\chi}_{\lambda\alpha}^{*}$. Then

$$\bar{\chi}_{\lambda\alpha}^{*}\ F\ \bar{\chi}_{\lambda\alpha}\ \bar{C}_{\lambda} = \varepsilon_i\ \bar{\chi}_{\lambda\alpha}^{*}\ \bar{\chi}_{\lambda\alpha}\ \bar{C}_{\lambda} \tag{63}$$

or $$[\bar{F}_\lambda - \varepsilon_i \bar{S}_\lambda]\bar{C}_\lambda = 0 \tag{64}$$

The matrix F_λ has elements F_{pq} such that

$$F_{pq} = \langle \chi_p | F | \chi_q \rangle \tag{65}$$

The matrix S_λ has elements S_{pq} such that

$$S_{pq} = \langle \chi_p | \chi_q \rangle \tag{66}$$

Again for σ electrons there will be one such matrix equation. For π electrons there will be two identical matrix equations. The above matrix equation has a nontrivial solution if the determinant

$$||\bar{F}_\lambda - \varepsilon_i \bar{S}_\lambda|| = 0 \tag{67}$$

Here is the clue for solving the matrix equation to self-consistency. Initial vectors $\bar{C}_\lambda$ are assumed and an initial basis set is proposed. The matrix $\bar{F}$, of the Hartree-Fock operator, and the overlap matrix $\bar{S}$ are calculated. The matrix $|\bar{F}-\varepsilon\bar{S}|$ is diagonalized, the orbital energies ε_i are obtained and new sets of vectors C_λ are generated. The cycle is continued until the calculated $\bar{C}_\lambda$ agree with the assumed $\bar{C}_\lambda$ to a given degree of accuracy. The total energy is then given as

$$E_T = \sum_i (\varepsilon_i + \langle \phi_i | H_N | \phi_i \rangle). \tag{68}$$

The sum is over all occupied molecular orbitals

The total energy calculated is not yet necessarily the minimum or Hartree-Fock energy. Many calculations must be done in the search for a completely flexible basis set which allows for full atomic polarization and the excitation of the atoms within the molecule to higher quantum states. The former effect (polarization) has been treated in a different way by Hurley[19]. Also within each calculation the nonlinear exponential parameters are varied to minimize the energy.

In 1955, C. W. Scherr[20] performed the first nonempirical calculation with the expansion method on the molecule N_2. He used a basis set of single 1s, 2s and 2p Slater-type functions on each centre, chose nonlinear coefficients according to Slater's rules and obtained a total energy of -108.574 a.u. In 1960, Ransil[21] used the first generation[3] of molecular structure electronic computer programmes in a set of calculations on closed shell structures including Li_2, Be_2, C_2, N_2, F_2; LiH, BH, NH, HF; CO, BF; and LiF. He again used a minimum basis set but allowed his nonlinear parameters to be varied in the energy minimization process. A variation of the orbital exponent on one centre can have the effect of increasing the polarization of charge at the other centre. Ransil's total energy for N_2 was -108.63359 a.u. In 1961, Richardson[22] made the next significant improvement on the energy of N_2 by

using a double zeta basis set in which each of the valence Slater-type functions was doubled; that is, he used 2s, $2s'$, $2p_\sigma$, $2p_\sigma'$, $2p_\pi$ and $2p_\pi'$ Slater-type functions on each centre. With variation of the nonlinear parameters, he reduced the error in the total energy by 4.1 e.v. to -108.785 a.u. Using the second generation[3] of molecular structure computer programmes developed by Wahl, Huo and others[23], Cade, Wahl, Huo and their associates have done extensive calculations on CO, BF, N_2 and its ionization products, the remaining homonuclear diatomic molecules, and the first and second row hydrides. They have used large flexible basis sets with higher quantum Slater-type functions such as 3s, 3p, 3d and 4f, and have also varied the nonlinear exponential parameters to obtain what they feel to be results close to the Hartree-Fock limit. For example, in the case of N_2[24], they obtain a total energy of -108.9928 a.u. This computed energy is still in error from the total experimental energy by 16.1 e.v. while D_e, the dissociation energy is in error by 4.70 e.v. This error is called the correlation error and results in part from an overestimation of the field acting on a given electron because of electrons of opposite spin.

Löwdin[10] has shown that, given a complete set of one-electron functions, a true solution to Schrödinger's equation can be given as

$$\Psi = \sum_i C_i \Psi_i \qquad (69)$$

Ψ_i describes the ith configuration and is an antisymmetrized product of N of these one-electron functions where N is the number of electrons in the system. This is the method of configuration interaction and is just an extension of the single-configuration wavefunction that has already been discussed. In the Laboratory of Molecular Structure and Spectra at the University of Chicago, a third generation[3,25] of computer programmes based on multiconfigurational self-consistent field theory is being constructed. It is expected that expansions of a relatively few number of configurations will yield wave functions of high quality.

1.3 BRILLOUIN'S THEOREM[26] AND THE HARTREE-FOCK ONE-ELECTRON DENSITY

In the case of an orbital approximation to the electronic wavefunction, the diagonal element of the first-order density matrix is given as

$$\gamma(1|1) = \sum_i a_i^*(1) a_i(1) \qquad (70)$$

The sum is over all occupied molecular spin orbitals. In this section it will be shown that the Hartree-Fock one-electron density is correct to second order[27].

The Hartree-Fock model for an electronic system is essentially a single particle model in which each electron moves in an average field owing to the nuclei and the other electrons. It has been pointed out that the energy of such a system is never equal to the experimental energy. There is a difference between the two which is called the correlation energy*. This correlation energy is just a reflection of the fact that the instantaneous field that an electron experiences owing to the remaining N-1 electrons is not the same as the average field that it experiences in the Hartree-Fock approximation.

---

* The correlation energy is the difference between the Hartree-Fock energy and the theoretical energy. This theoretical energy is the experimental energy of the system minus the relativistic corrections.

Suppose there exists a complete set of one-electron spin functions such that each member of this set obeys the relation

$$\langle a_i | a_j \rangle = \delta_{ij} \tag{71}$$

Since these functions depend only on the coordinates of one electron, they must be eigenfunctions of some Hartree-Fock operator; that is,

$$F\, a_i = \varepsilon_i a_i \tag{72}$$

F is the Hartree-Fock operator and ε_i is the orbital energy. If these eigenfunctions are arranged in order of increasing orbital energy then the first N spin functions can be used to form an antisymmetrized product wavefunction which describes the ground state of an N-electron system. This wavefunction is given as

$$\Psi^o = \sqrt{\frac{1}{N!}}\, ||a_1(1)a_2(2)\ldots a_i(i)a_j(j)\ldots a_N(N)|| \tag{73}$$

For this ground state wavefunction, the Hartree-Fock operator is[29]

$$F = H_N + \sum_j [J_j' - K_j'] \tag{74}$$

where

$$H_N = -\frac{1}{2}\sum_i \nabla_i^2 - \sum_{i\alpha} \frac{Z_\alpha}{r_{i\alpha}} \tag{75}$$

J_j' and K_j' are defined by the relations

$$J_{ij}' = \langle a_i | J_j' | a_i \rangle = \langle a_i(1)a_j(2) | \frac{1}{r_{12}} | a_i(1)a_j(2) \rangle \tag{76}$$

$$K_{ij}' = \langle a_i | k_j' | a_i \rangle = \langle a_i(1) a_j(2) | \frac{1}{r_{12}} | a_i(2) a_j(1) \rangle \quad (77)$$

The Hartree-Fock energy is given as

$$E_{H.F.} = \sum_i I_i' + \sum_{i>j} [J_{ij}' - K_{ij}'] \quad (78)$$

where

$$I_i = \langle a_i | H_N | a_i \rangle \quad (79)$$

Also[28]

$$E_{H.F.} = \sum_i \varepsilon_i - \frac{1}{2} \sum_{\substack{ij \\ i \neq j}} [J_{ij}' - K_{ij}'] \quad (80)$$

Thus there is some H^O such that

$$H^O \psi^O = E_{H.F.} \psi^O \quad (81)$$

An inspection of equation (80) shows that

$$H^O = \sum_i F(i) - \frac{1}{2} \sum_i \sum_j (J_j'(i) - K_j'(i))_{i \neq j} \quad (82)$$

F(i) is defined by equation (74). Further

$$\langle \psi^O | \sum_i F(i) | \psi^O \rangle = \sum_i \varepsilon_i \quad (83)$$

where the index i runs from one to N.

The ab ove discussion can be made the basis of an analysis of the accuracy of the Hartree-Fock one-electron density. The total electronic Hamiltonian is given as

$$H = \sum_i H_N(i) + \frac{1}{2} \sum_{\substack{ij \\ i \neq j}} \frac{1}{r_{ij}}$$

$$= H^O + \frac{1}{2} \sum_{\substack{ij \\ i \neq j}} \frac{1}{r_{ij}} - \frac{1}{2} \sum_i \sum_j [J_j'(i) - K_j'(i)]$$

$$= H^O + \lambda V \quad (84)$$

H^o is defined in equations (81) and (82). V is the difference between the exact operator H and the operator H^o which possesses eigenvalues $E_{H.F.}$. It is here regarded as a small perturbation. The energy of the system correct through first-order perturbation theory is given as

$$E = \langle\Psi|H|\Psi\rangle = \langle\Psi^o+\lambda\Psi^1|H^o+\lambda V|\Psi^o+\lambda\Psi^1\rangle$$

$$= \langle\Psi^o|H^o|\Psi^o\rangle+\lambda\,[\langle\Psi^1|H^o|\Psi^o\rangle+\langle\Psi^o|H^o|\Psi^1\rangle+\langle\Psi^o|V|\Psi^o\rangle] \qquad (85)$$

where λ is a perturbation parameter. Ψ^1 is a first-order correction to the Hartree-Fock ground state Ψ^o.

An excited state configuration in which a_i is replaced by a_k is called a one-electron excitation and is described by the antisymmetrized product

$$\Psi_{i:k} = \sqrt{\frac{1}{N!}}\;||a_1(1)a_2(2)\ldots a_k(i)\ldots a_j(j)\ldots a_N(N)|| \qquad (86)$$

An excited state configuration in which a_i is replaced by a_k and a_j is replaced by a_ℓ is called a two-electron excitation and is described by the antisymmetrized product

$$\Psi_{ij:k\ell} = \sqrt{\frac{1}{N!}}\;||a_1(1)a_2(2)\ldots a_k(i)\ldots a_\ell(j)\ldots a_N(N)|| \qquad (87)$$

Ψ^1, the first-order correction to Ψ^o will contain determinants that differ from Ψ^o by one-and two-electron excitations. This is so because the perturbation term V will connect states differing from each other by one- and two-electron excitations. Therefore

$$\Psi^1 = \sum_{ik} a_{i:k} \Psi_{i:k} + \sum_{ijk\ell} a_{ij:k\ell} \Psi_{ij:k\ell} \qquad (88)$$

From perturbation theory

$$a_{i:k} = \frac{\langle \Psi_{i:k} | V | \Psi^o \rangle}{E_{H.F.} - E_{i:k}} \qquad (89)$$

$$a_{ij:k\ell} = \frac{\langle \Psi_{ij:k\ell} | V | \Psi^o \rangle}{E_{H.F.} - E_{ij:k\ell}} \qquad (90)$$

$E_{i:k}$ is the Hartree-Fock energy of the determinantal wavefunction $\Psi_{i:k}$ and $E_{ij:k\ell}$ is the Hartree-Fock energy of the determinantal wavefunction $\Psi_{ij:k\ell}$. The scalar product

$$\langle \Psi_{i:k} | V | \Psi^o \rangle = \langle \Psi_{i:k} \Big| \frac{1}{2} \sum_{\substack{ij \\ i \neq j}} \frac{1}{r_{ij}} - \frac{1}{2} \sum_{\substack{i \\ i \neq j}} \sum_{j} (J_j'(i) - K_j'(i)) \Big| \Psi^o \rangle \qquad (91)$$

$$= 0$$

Thus the wavefunction correct through first order is given as

$$\Psi = \Psi^o + \sum_{ijk\ell} a_{ij:k\ell} \Psi_{ij:k\ell} \qquad (92)$$

With these relations, the various portions of equation (85) can be evaluated. The scalar product $\langle \Psi^1 | H^o | \Psi^o \rangle$ involves only the term $\langle \Psi_{ij:k\ell} | H^o | \Psi^o \rangle$ which is equal to zero Thus

$$\langle \Psi^1 | H^o | \Psi^o \rangle = \langle \Psi^o | H^o | \Psi^1 \rangle = 0 \qquad (93)$$

There remains the term $\langle \Psi^o | V | \Psi^o \rangle$. A straightforward calculation shows that it is zero. With this information equation (85) yields the energy of the system correct through first-order as

$$E = \langle \Psi^o | H^o | \Psi^o \rangle = E_{H.F.} \tag{94}$$

There is a second-order correction to the Hartree-Fock energy which is given by

$$E^{(2)} = [\langle \Psi^2 | H^o | \Psi^o \rangle + \langle \Psi^o | H^o | \Psi^2 \rangle + \langle \Psi^1 | H^o | \Psi^1 \rangle + \langle \Psi^1 | V | \Psi^o \rangle \tag{95}$$

$$+ \langle \Psi^o | V | \Psi^1 \rangle]$$

This expression can easily be seen to reduce to

$$E^{(2)} = \langle \Psi^1 | H^o | \Psi^1 \rangle + \langle \Psi^1 | V | \Psi^o \rangle + \langle \Psi^o | V | \Psi^1 \rangle \tag{96}$$

where $E^{(2)}$ represents the second-order correction to the energy. The wavefunction correct through first order is written as

$$\Psi^1 = \Psi^o + \sum_{ijk\ell} a_{ij:k\ell} \Psi_{ij:k\ell} \tag{92}$$

The diagonal element of the first-order density matrix correct through first-order perturbation theory can be calculated from the expression

$$\gamma(1|1) = \int \left| \Psi^o + \sum_{ijk\ell} a_{ij:k\ell} \Psi_{ij:k\ell} \right|^2 d\vec{x}_2 \, d\vec{x}_3 \ldots d\vec{x}_N$$

$$= \int \Psi^o \Psi^o \, d\vec{x}_2 \, d\vec{x}_3 \ldots . \, d\vec{x}_N \, . \tag{97}$$

There is no first-order correction to the density and equation (70) is correct to second order. If Ψ^o is written in the restricted Hartree-Fock scheme and is a closed shell determinant, then the expression for the electron density distri-

bution is

$$\rho(\vec{r}) = \sum_{i\lambda\alpha} n_{i\lambda\alpha}\, \phi_{i\lambda\alpha}\, \phi_{i\lambda\alpha} \qquad (98)$$

The symbol $n_{i\lambda\alpha}$ is the occupation number of the orbital $\phi_{i\lambda\alpha}$. Equation (98) is also correct to second order. However in the case of an open shell system, there is some disagreement as to whether $\rho(\vec{r})$ is or is not correct to the second order[30,31,32].

A one-electron operator has previously been defined and it has been shown that such an operator is dependent only on the first-order density matrix. The average value of the one-electron operator

$$P = \sum_i O(i) \qquad (99)$$

correct through the first order is given as

$$\langle P\rangle = \langle \Psi^o + \lambda\Psi^1 | \sum_i O(i) | \Psi^o + \lambda\Psi^1 \rangle$$

$$= \langle \Psi^o | \sum_i O(i) | \Psi^o \rangle + \lambda \langle \Psi^1 | \sum_i O(i) | \Psi^o \rangle + \lambda \langle \Psi^o | \sum_i O(i) | \Psi^1 \rangle \qquad (100)$$

Since Ψ^1 involves only two-electron excitations, it is easily seen that

$$\langle \Psi^1 | \sum_i O(i) | \Psi^o \rangle = \langle \Psi^o | \sum_i O(i) | \Psi^1 \rangle = 0 \qquad (101)$$

and

$$\langle P\rangle = \langle \Psi^o | \sum_1 O(i) | \Psi^o \rangle = \int O(1)\ \gamma(1|1')\, d\vec{x}_1 \qquad (102)$$

The average value of this one electron operator has no first-order corrections[33]. The statement that all properties dependent on the first-order density matrix are correct to second-order has thus been proven.

I.4 THE CONCEPTS OF BINDING AND ANTIBINDING IN DIATOMIC MOLECULES

(a) The Hellmann-Feynman Theorem

The force acting on the nucleus in a molecule is, according to the Hellmann-Feynman theorem[4], rigorously determined by the first-order density matrix. Thus, a Hartree-Fock wavefunction should yield a force correct to second order in perturbation theory. Consider the proof of the Hellmann-Feynman theorem. Ψ is the wavefunction describing a molecular system, and the energy of this system is given as

$$E = \langle\Psi|H|\Psi\rangle \tag{103}$$

where

$$H\Psi = E\Psi \tag{104}$$

and

$$\langle\Psi|\Psi\rangle = 1 \quad . \tag{105}$$

The derivative $\frac{dE}{d\lambda}$ is obtained as

$$\frac{dE}{d\lambda} = \langle\Psi|\frac{dH}{d\lambda}|\Psi\rangle + \langle\frac{d\Psi}{d\lambda}|H|\Psi\rangle + \langle\Psi|H|\frac{d\Psi}{d\lambda}\rangle \tag{106}$$

$$= \langle\Psi|\frac{dH}{d\lambda}|\Psi\rangle + E\,\frac{d}{d\lambda}\,[\langle\Psi|\Psi\rangle] \tag{107}$$

$$= \langle\Psi|\frac{dH}{d\lambda}|\Psi\rangle = \langle\frac{dH}{d\lambda}\rangle \tag{108}$$

since

$$\frac{d}{d\lambda}\langle\Psi|\Psi\rangle = \frac{d}{d\lambda}(1) = 0 \tag{109}$$

Figure 1. The co-ordinate system describing a diatomic molecule AB. The distance x_{Ai} represents the component of $\vec{r}_{Ai}$ along the internuclear axis. The distances r_{Ai} and x_{Ai} are measured with respect to a co-ordinate system centred on nucleus A. The symbol e represents an electronic charge.

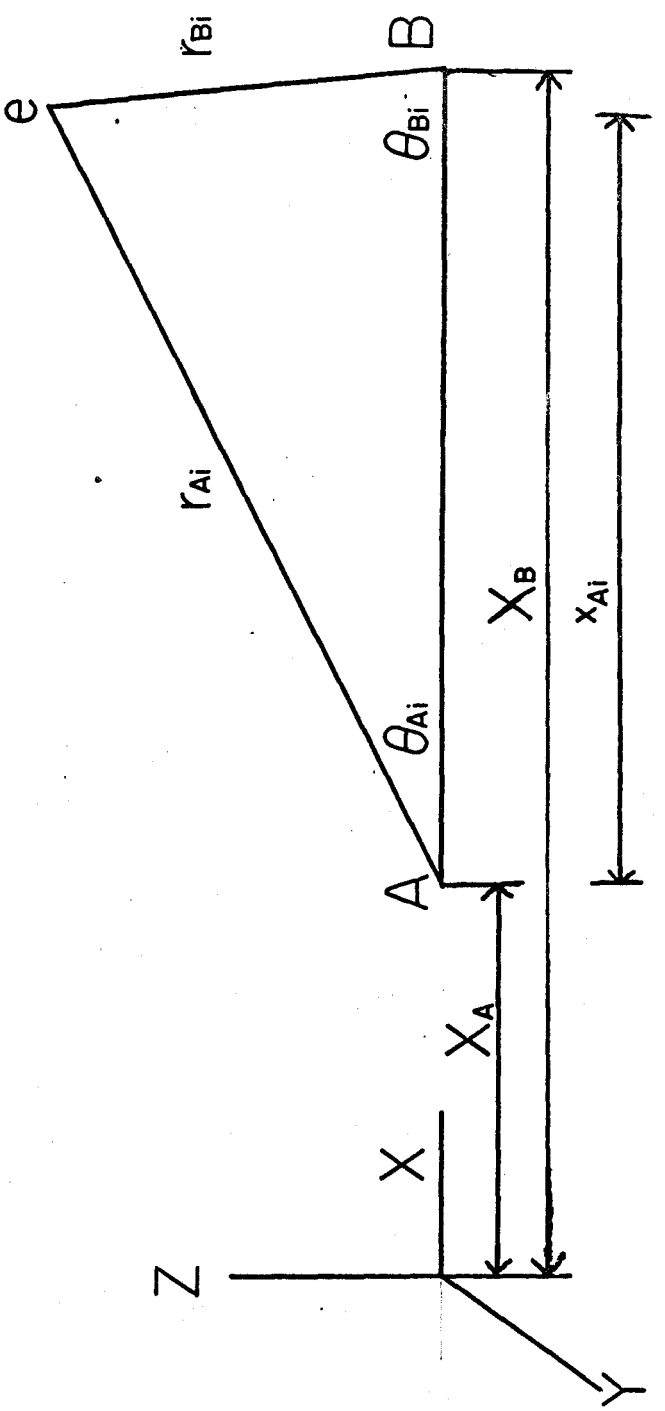
e
r_{Bi}
B
θ_{Bi}
r_{Ai}
θ_{Ai}
A
X_B
x_{Ai}
X_A
X
Z
Y

This is the mathematical statement of the generalized Hellmann-Feynman theorem. If Ψ describes a diatomic molecule and is obtained within the framework of the Born-Oppenheimer[16] approximation, then

$$\Psi = \Psi_E(\vec{x}_1,\vec{x}_2.....\vec{x}_N,R)\Psi_{AB}(\vec{X}_A,\vec{X}_B) \quad . \tag{110}$$

R is the internuclear distance and Ψ_{AB} is the nuclear wavefunction which depends on the nuclear co-ordinate $\vec{X}_A$ and $\vec{X}_B$. The Hamiltonian which includes the nuclear-nuclear potential term is given as

$$H = -\frac{1}{2}\sum_i^N \nabla_i^2 - \sum_i \frac{Z_A}{r_{Ai}} - \sum_i \frac{Z_B}{r_{Bi}} + \sum_{i>j} \frac{1}{r_{ij}} + \frac{Z_A Z_B}{R} \tag{111}$$

The indices i and j run from one to N where N is the number of electrons.

The parameter λ is defined to be the nuclear co-ordinate X_A and the derivative $\frac{dH}{d\lambda}$ is taken with r_{Bi} held constant. Figure 1 shows the above described situation

$$\frac{dH}{dX_A} = \sum_i \frac{Z_A}{r_{Ai}^2} \left(\frac{dr_{Ai}}{dX_A}\right)\Big|_{r_{Bi}} - \frac{Z_A Z_B}{R^2} \left(\frac{dR}{dX_A}\right)\Big|_{r_{Bi}} \tag{112}$$

$$\left(\frac{dR}{dX_A}\right)\Big|_{r_{Bi}} = -1 \tag{113}$$

$$\left(\frac{dr_{Ai}}{dX_A}\right)\Big|_{r_{Bi}} = -\left(\frac{dr_{Ai}}{dx_{Ai}}\right)\Big|_{r_{Bi}} = -\cos\theta_{Ai} \tag{114}$$

Therefore

$$\frac{dH}{dX_A} = -\sum_i^N \frac{Z_A \cos\theta_{Ai}}{r_{Ai}^2} + \frac{Z_A Z_B}{R^2} \tag{115}$$

and

$$\frac{dE}{dX_A} = F_A = \langle \Psi_E \left| -\sum_i \frac{Z_A \cos\Theta_{Ai}}{r_{Ai}^2} \right| \Psi_E \rangle + \frac{Z_A Z_B}{R^2} \qquad (116)$$

where F_A is the definition of the Hellmann-Feynman force on nucleus A. If Ψ_E is an unrestricted Hartree-Fock wavefunction, then

$$F_A = \frac{Z_A Z_B}{R^2} - Z_A \int \frac{\cos\Theta_A}{r_A^2} \gamma(1|1') \, d\vec{x}_1 \qquad (117)$$

or if Ψ_E is obtained within the restricted Hartree-Fock formalism then

$$F_A = \frac{Z_A Z_B}{R^2} - Z_A \int \frac{\cos\Theta_A}{r_A^2} \rho(\vec{r}) d\vec{r} \qquad (118)$$

Similarly, the force acting on nucleus B is

$$F_B = \frac{Z_A Z_B}{R^2} - Z_B \int \frac{\cos\Theta_B}{r_B^2} \rho(\vec{r}) d\vec{r} \qquad (119)$$

If F_A and F_B are added together and the result is divided by two then the equation

$$\frac{F_A + F_B}{2} = \frac{Z_A Z_B}{R^2} - \frac{1}{2} \int \rho(\vec{r}) \left[\frac{Z_A \cos\Theta_A}{r_A^2} + \frac{Z_B \cos\Theta_B}{r_B^2} \right] d\vec{r} \qquad (120)$$

is obtained. The quantity

$$Q = \frac{Z_A \cos\Theta_A}{r_A^2} + \frac{Z_B \cos\Theta_B}{r_B^2} \qquad (121)$$

is just the sum of the force acting on nucleus A and the force acting on nucleus B because of a point charge at a distance r_A from the nucleus A and a distance r_B from the

Figure 2. Binding and antibinding regions in diatomic molecules. The curves passing through the nuclei represent the nodal surfaces of revolution defined by Q=0. Charge density placed in the antibinding regions behind the nuclei exerts a force tending to separate the nuclei. Charge density placed in the binding region between the nuclei exerts a force tending to displace the nuclei towards each other. In the case of a homonuclear molecule, the two antibinding regions are identical and the curve Q=0 is open. In the case of a heteronuclear molecule, the figure shows that the curve Q=0 is closed in the region of nucleus B. This nucleus has a smaller charge than does nucleus A.

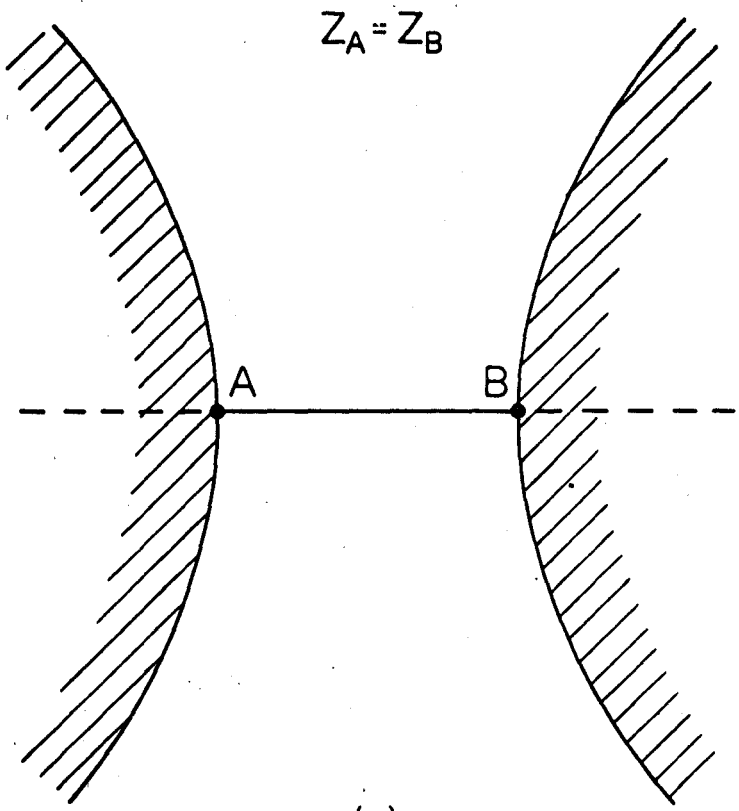

(a)

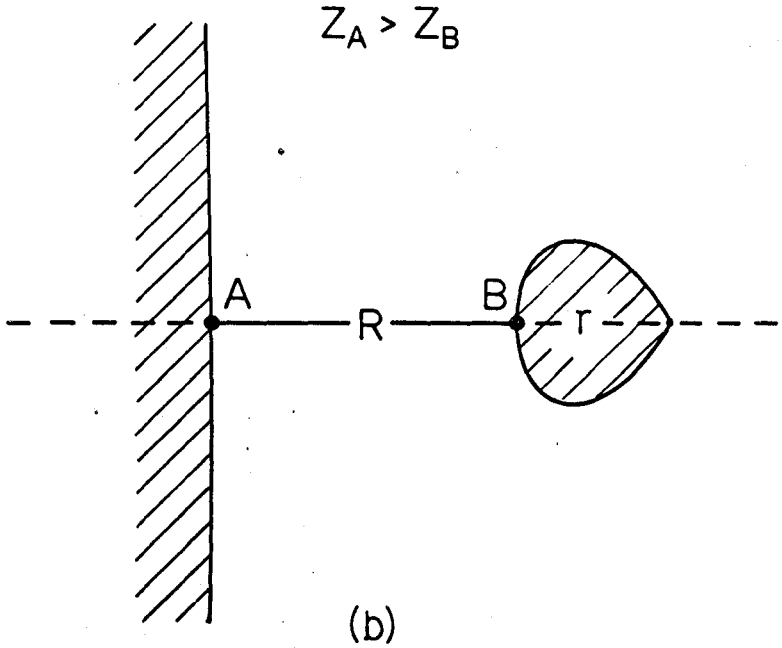

(b)

nucleus B. The situation is the same as that shown in Figure 1. Berlin[34] used th e relation (121) to define binding and antibinding regions in diatomic molecules. In the region of positive Q, the total electronic force is such that it tends to pull the nuclei toward each other in opposition to the force of nuclear repulsion. Such a region, Berlin termed the binding region. In the region of negative Q, the total electronic force is such that it tends to pull each nucleus in the same direction. However, it tends to pull one nucleus more strongly than the other with the result that the nuclei separate. Such a region is termed the antibinding region. The binding and antibinding regions are separated by nodal surfaces of revolution where

$$Q = 0 \quad . \tag{122}$$

Figure 2 shows a homonuclear and a heteronuclear diatomic molecule. The lined regions behind the nuclei are the antibinding regions while the internuclear area is defined as the binding region.

(b) The Density-Difference Function-An Interpretive Device.

One of the purposes of this thesis is to discuss diatomic molecules in terms of their electron density distribution functions $\rho(\vec{r})$. These functions are easily pictured in terms of electron density contour maps. A description of the computational techniques required to plot these contour maps is presented in the appendix.

It is also of use to compare the density of a given molecule with the densities of its atomic constituents. This is done by means of the electron density difference function[35-44], $\Delta\rho(\vec{r})$ defined as

$$\Delta\rho(\vec{r}) = \rho_M(\vec{r}) - \rho_A(\vec{r}). \qquad (123)$$

The molecular density is designated by $\rho_M(\vec{r})$ while $\rho_A(\vec{r})$ is the sum of the atomic densities calculated as if the non-interacting atoms were brought to the observed internuclear distance. Such $\Delta\rho$ functions can also be pictured in the form of contour maps. These $\Delta\rho$ contour maps can be interpreted as th e redistribution of charge which accompanies the formation of a chemical bond. The Hellmann-Feynman theorem as it applies to diatomic molecules gives a firm basis for this interpretation.

Consider two spherical atomic charge distributions. Label the nuclei of the respective charge distributions A and B. The force acting on nucleus A is given as

$$F_A = \frac{Z_A}{R^2}\,[Z_B - f_A] \qquad (124)$$

where Z_A and Z_B are the nuclear charges of A and B respectively, R is the distance between the nuclei, and f_A is an effective electronic charge situated on the nucleus B. From Gauss's Law, this effective charge is equal to the total amount of charge within a sphere whose centre is nucleus B and whose radius is R. At large internuclear dis-

tances the nucleus A is outside the charge distribution of B and

$$Z_B = f_A \qquad (125)$$

with the result that

$$F_A = 0 \qquad (126)$$

As nucleus A penetrates the electronic charge distribution surrounding nucleus B

$$Z_B > f_A \qquad (127)$$

and

$$F_A > 0 \qquad (128)$$

For all degrees of penetration, there is a net force of repulsion acting on nucleus A. Similarly there is always a net force of repulsion acting on nucleus B. The overlap of two spherical charge distributions does not place enough charge in the region between the nuclei or more precisely in the binding region to balance the electrostatic force of repulsion owing to the nuclei A and B.

The $\Delta\rho$ map, which describes a stable diatomic molecule must show an accumulation of electron density in the binding region - an accumulation sufficient to offset the electrostatic force of repulsion owing to the nuclei.

CHAPTER II

THE ELECTRON DENSITY DISTRIBUTIONS IN HOMONUCLEAR DIATOMIC MOLECULES

II.1 INTRODUCTION

In this section, an interpretive discussion of one-electron density and density difference distributions in terms of contour maps is presented. Although such topographical maps have previously been documented in the literature, the density quantities which they represent have been derived from crude Ψ. A comparison of the difference density maps shown here with those published by Roux[38] is sufficient to underline the importance of an accurate representation of the one-electron density for both atoms and molecules. After the publication of these density contour maps, an interpretive paper by Ransil and Sinai[45] appeared in the literature. Their analysis is similar to that espoused in this discussion and the results reported here can be compared with their data.

The analysis of $\rho(\vec{r})$ presented here is neither the first nor the only analysis to be exploited. For some time now, Mulliken's[46,47] molecular orbital population count, an integrated form of $\rho(\vec{r})$, has been used to gain an idea of the distribution of electrons within a molecule. The population analysis gives quantitative meaning to concepts such

as electron promotion, hybridization, bond orders, atomic and overlap populations; and the results of such calculations are presented as effective electron configurations for atoms within the molecule under consideration. The increasing complexity of molecular orbitals approximated as linear combinations of atomic orbitals makes precise definitions of these concepts difficult to formulate. Indeed, the population analysis appears to be meaningful only when the molecular orbitals are approximated by minimal basis sets of atomic orbitals. Davidson[48] has realized this and has attempted to fit density distributions obtained from extended basis set approximations to a minimal basis set of atomic orbitals having some intuitive significance He constrains the approximate densities so that their mean square error relative to the "true" densities is a minimum, and, in this way, attempts to recover a meaning for the terms hybridization and electron promotion.

The analysis of molecular charge density contour maps by Ransil and Sinai[45] results in the division of such maps into regions of localized and delocalized charge defined respectively as that charge contained within contours that encircle both nuclei separately and that charge excluding the core regions which spans the entire molecular space. A classification of these charge regions in terms of their binding, nonbinding or antibinding nature is made, and electron populations within given localized contours

are calculated. A comparison of these populations with those found within the same contours in the isolated atoms from which the molecule is formed gives an idea of the charge transferred to the core regions during the formation of the molecule.

Ruedenberg[49] has proposed an extensive interpretation of the physical nature of the chemical bond using the first- and second-order density matrices. He relates these density quantities to energy changes accompanying certain hypothetical processes occurring as the chemical bond develops. Another approach to establish a nonarbitrary link between rigorous molecular orbital wavefunctions and chemical concepts has been formulated by Edmiston and Ruedenberg[50,51]. Beginning with the canonical molecular orbitals ϕ_i these authors determine localized molecular orbitals λ_i which correspond to conventional localized inner shell, lone pair, and bond orbitals. These localized molecular orbitals are determined by the unitary transformation

$$\lambda_i = \sum_p \phi_p T_{pi}$$

which maximizes the sum

$$D(\lambda) = \sum_i \langle \lambda_i^2 | \frac{1}{r_{12}} | \lambda_i^2 \rangle$$

The term $\langle \lambda_i^2 | \frac{1}{r_{12}} | \lambda_i^2 \rangle$ represents the repulsion of two electrons in the orbital λ_i. The index i runs over all

occupied localized molecular orbitals. It is possible to compare the diagrams derived by Edmiston and Ruedenberg with the density difference diagrams shown here.

The direct determination of electron density distributions in molecules from x-ray and electron diffraction of the relevant gases is theoretically possible. Elastic scattering depends on the one-electron density distribution while inelastic scattering depends on the two-electron density[52,53,54]. At present, Bartell [55] and his associates are attempting to reproduce experimental intensity measurements for the molecules N_2 and O_2 by employing the $\Delta\rho(\vec{r})$ contours shown in this thesis for these molecules. In the past, their calculations have been based upon the density distributions of the undistorted atoms oxygen and nitrogen and have not agreed with the experimental data at low angle scattering. Such $\Delta\rho(\vec{r})$ contour maps should help to determine whether the disagreement occurs as a result of correlation effects or the chemical bond. As of yet, the density contour maps discussed here have not been reproduced by experiment.

Figure 3. The total molecular charge density contours for the first row homonuclear diatomic molecules. The values of the contours in this and the following maps are quoted in atomic units (1 a.u.=e/a_o^3 = 6.749$e/\AA^3$). The same scale of length applies to all the maps in this figure. The innermost circular contours centred on the nuclei have been omitted for the sake of clarity. The value of the total density at the position of the nuclei is given in Table I.

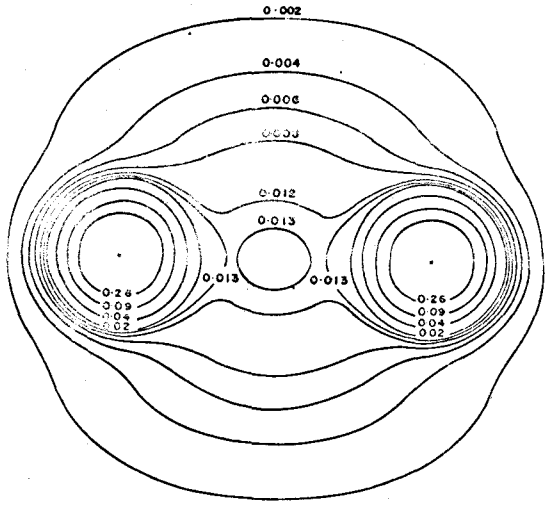

$Li_2\ {}^1\Sigma_g^+$

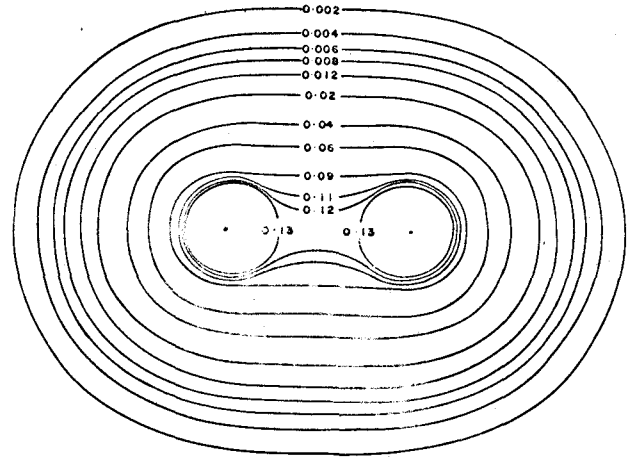

$B_2\ {}^3\Sigma_g^-$

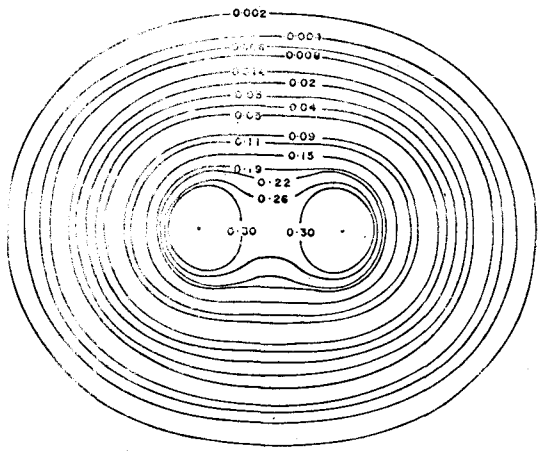

$C_2\ {}^1\Sigma_g^+$

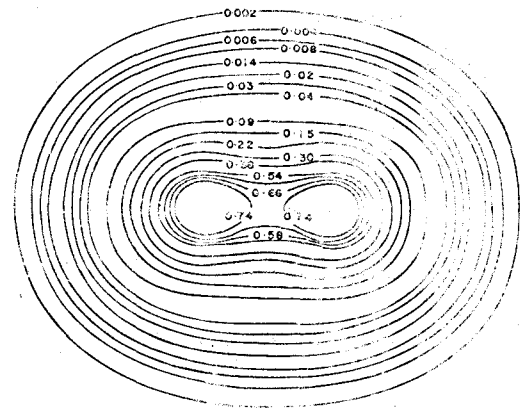

$N_2\ {}^1\Sigma_g^+$

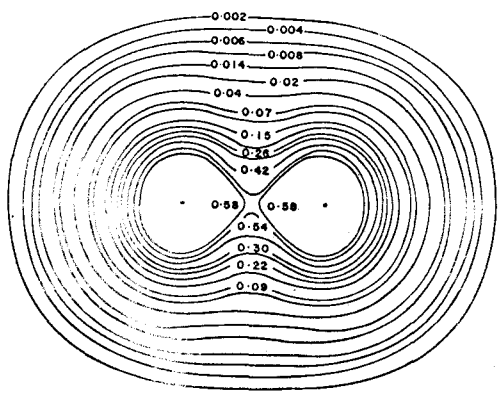

$O_2\ {}^3\Sigma_g^-$

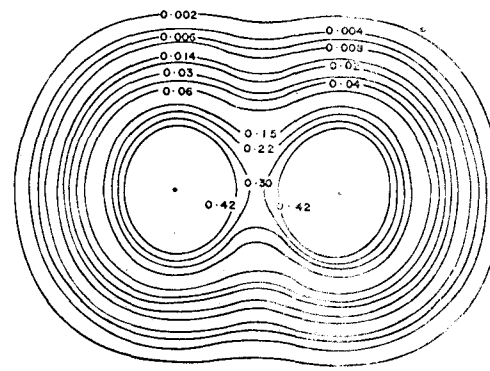

$F_2\ {}^1\Sigma_g^+$

II.2 THE TOTAL MOLECULAR CHARGE DISTRIBUTIONS

Contour maps of the total molecular charge density distributions for Li_2, B_2, C_2, N_2, O_2 and F_2 all drawn to the same scale are shown in Figure 3. The wave function for Li_2 ($X^1\Sigma_g^+$) is from Cade, Sales and Wahl[56]; for B_2($X^3\Sigma_g^-$) and C_2($a^1\Sigma_g^+$)[57] from Greenshields; for N_2($X^1\Sigma_g^+$) from Cade, Sales and Wahl[58]; for O_2 ($X^3\Sigma_g^-$) from Cade and Malli[59]; and for F_2($X^1\Sigma_g^+$)[60] from Wahl. The contours connect points of equal density in a plane containing the two nuclei and are continuous in nature. The total density is distinct from the various orbital densities in that it possesses no nodal contours.

A cursory examination of these density diagrams shows that Li_2 differs from the remaining members of the series in two aspects. The Li_2 density along the internuclear axis possesses two saddlepoint minima while the remaining molecular densities possess only one such saddlepoint. The density of the lithium molecule, especially that in the binding region, is diffuse in nature; that is, the outer contours are separated by greater distances in Li_2 than, for example, in O_2. This has the effect of giving Li_2 an overall width greater than that found for the other molecules. The diffuse nature of the density in Li_2 can be correlated with its bond type as predicted by simple molecular orbital theory. The bond in Li_2 is seen as resulting from the over-

lap of two lithium 2s orbitals,one on each nuclear centre. The overlap of such s orbitals is not highly effective in concentrating density in the internuclear region along the bond axis. The diffuse nature of the electron density in this molecule also correlates with its bond strength. Li_2 has the lowest dissociation energy of any of the homonuclear diatomic molecules studied in this thesis.

Molecular dimensions have long been inferred from measurements of virial coefficients or transport properties such as viscosity. The assumption of the empirical Lennard-Jones (6-12) intermolecular potential[61] yields one effective molecular diameter. More complicated empirical potential expressions such as those by Kihara and Corner[61] for molecules with cylindrical symmetry yield two "effective dimensions". An examination of the density distributions in Figure 3 provides a basis for different definitions concerning the lengths and widths of molecules. Molecular size here is defined with reference to a specific contour inside of which most of the electron density is contained. Calculations carried out during these studies indicate that the 0.002 contour contains over 95% of the total electronic charge, and thus the 0.002 contour appears to be a good cut-off contour in terms of which the length and width of a given molecule can be measured. Such a contour choice is arbitrary to some extent, and there is no a priori reason why the results reported here should agree with the "experimental

TABLE I

Characteristics of the Total Density Distributions

Molecule	Li_2	B_2	C_2	N_2	O_2	F_2
Width (a.u.)	7.8	7.2	7.0	6.4	6.0	5.4
Length (a.u.)	8.7	9.8	8.5	8.2	7.9	7.9
Re (a.u.)	5.051	3.005	2.3481	2.068	2.282	2.268
Distance of 0.002 contour from nucleus						
In molecule (a.u.)	1.8	3.4	3.1	3.1	2.8	2.6
In atom (a.u.)	3.2	3.4	3.2	3.0	2.9	2.8
Fraction of total electronic charge in the binding region	0.59	0.58	0.60	0.56	0.55	0.54
Charge density at the nuclei* (a.u.)	13.855	71.856	127.323	205.591	311.312	448.760
Dissociation Energy e.v.	1.12	3.0	6.36	9.902	5.213	1.647

*1 a.u. of density = e/a_o^3 = 6.749 $e/\text{Å}^3$

diameters" of the respective molecules. The length and width of each molecule defined respectively as the distance between the intercepts of the 0.002 contour on the molecular axis and on a line perpendicular to the molecular axis and passing through its mid-point are given in Table I. These data in Table I are similar to results reported by Ransil[45] except for the case of N_2. His total density contour map for N_2 shown in Figure 3 of his text differs from that one reported here although the same molecular wavefunction was used in each case. As a result he reports a molecular width of 4.70 a.u. for N_2 while this study indicates a width of 6.4 a.u. for the same molecule . The experimental values of the diameters of the N_2 and O_2 molecules as determined by a Lennard-Jones (6-12) potential are 7.84 and 7.32 a.u.[61] respectively. These results are slightly smaller than the lengths and slightly larger than the widths of the molecules N_2 and O_2 shown in Table I. With a more complicated potential expression Kihara obtains for N_2 a width of 6.57 or 7.73 a.u. and a length of 8.64 or 9.81 a.u. for spherocylindrical or ellipsoidal molecules[61] respectively. The spherocylindrical values agree quite well with those reported in Table I.

Table I also shows for each of the molecules the fraction of the total charge that lies in the binding region.

There appears to be no correlation between this fraction and the strength of the bond as determined by the dissociation energy. Neither does there appear to be any correlation with the number of electron-pair bonds predicted by the Lewis model. However a population number by itself does not give a complete picture. More important than the total number of charges in the binding region is the placement of this charge relative to the nuclear axis. Density concentrated on and near the molecular axis is the most effective in binding the nuclei together. The diffuse nature of the Li_2 molecular density shows that there is no strong concentration of this density along the molecular axis and consequently that, relatively speaking, more charge must be placed in the binding region of this molecule in order to obtain electrostatic equilibrium. Similarly C_2 has an abnormally large fraction of the total electronic charge in its binding region. Simple molecular orbital theory predicts that this molecule is held together by two pi bonds - bonds which do not concentrate density on the molecular axis. It is true that the studies reported here indicate that, even in the case of C_2 there is a concentration of density in the internuclear region typical of a p_σ bond. However the abnormally large binding region population and further data to be discussed presently indicate that there is a considerable amount of density characteristic of π

character in the off-axis internuclear regions - an amount of density larger than that found in the case of N_2,O_2 and F_2.

Also shown in Table I are the experimental bond lengths and the electron densities at the nuclei. There seems to be no definite correlation between the bond length and the overall molecular length. There are two factors which must be considered in understanding the length of a molecule, the bond length and the rate at which density falls off from the nucleus on the side away from the bond. Table I lists the distance from the nucleus to the 0.002 contour in the molecule and the radius of the same contour in the isolated atom. With the exception of Li_2 this distance in the molecule is almost identical to the value in the isolated atom. Thus the contribution of the two end lengths, beyond the nuclear separation to the overall length of the molecule is largely determined by how tightly the density is bound in the unperturbed atom. The binding of the atomic density increases from Li across to F so that Li and Be are large and diffuse while N,O and F are progressively tighter and more compact. Therefore F_2 is smaller in size than N_2 or C_2 even though possessing a greater bond length owing to the fact that the density in the F atom is more tightly bound than that in the C or N atoms. The Li_2 molecule differs from the others in that its length is considerably less than expected considering

Figure 4. A diagram to illustrate a method of estimating the size of a peripheral atom.

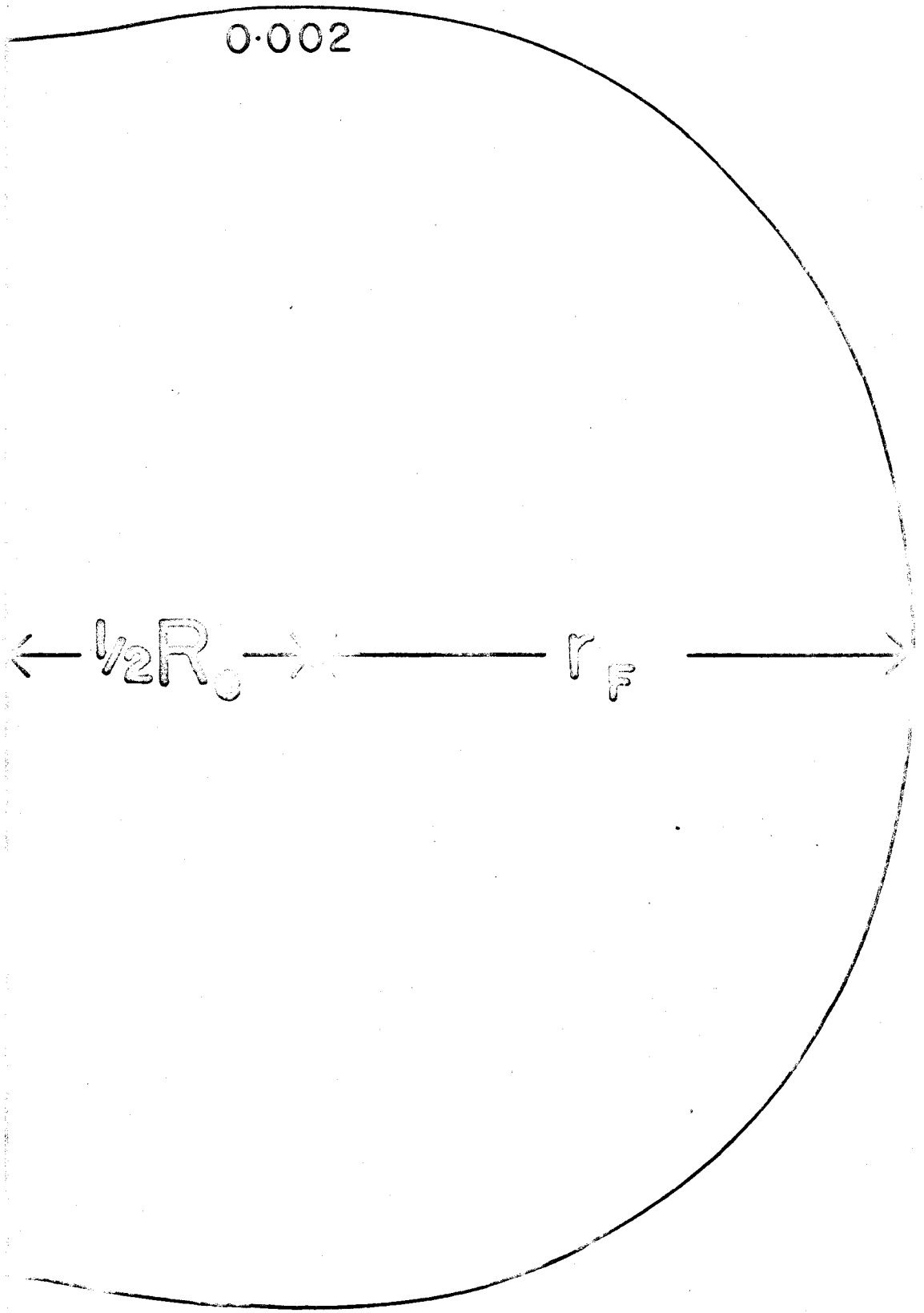
0·002
½R₀
r_F

the diffuse nature of its atomic density or in this case the molecular length is not approximately equal to the sum of R_e and twice the "atomic" radius. This is however easily understood since in the Li atom only one valence shell electron is present so that no atomlike residual charge in the valence shell remains in the molecule as is the case in B_2, C_2, N_2, O_2 and F_2. This is further illustrated by using instead of the 0.002 contour of Li the 0.002 contour of the $1s^2$ shell of Li which yields a relevant atomic radius of 1.7 a.u. in good agreement with the molecular value of 1.8a.u.

An accurate estimate of the size of a peripheral atom is <u>tentatively</u> proposed as the sum of $\frac{1}{2} R_e$ from a suitable source and the atomic "radius" as defined by the 0.002 contour of the atom (except for Li, Na, etc., where the core radius should be used). For example, Figure 4 shows the length of a peripheral fluorine fragment.

Figure 5. The density difference contour maps for the stable first-row homonuclear diatomic molecules. The same scale of length applies to all the maps. The dotted lines (shown in full for N_2) separate the binding from the antibinding regions.

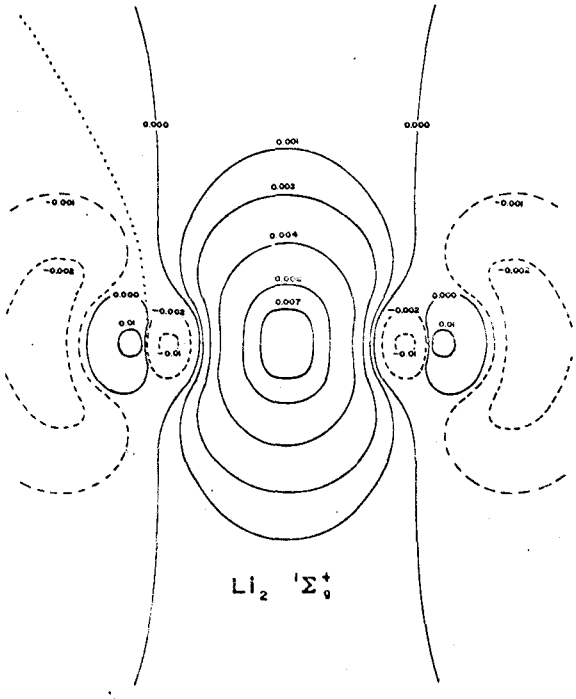

$Li_2\ {}^1\Sigma_g^+$

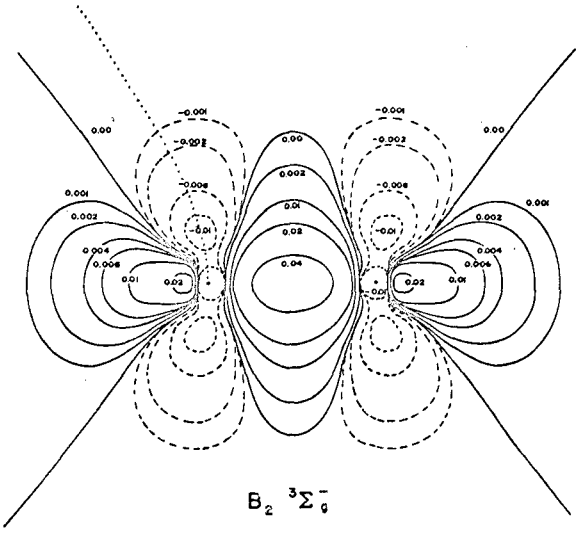

$B_2\ {}^3\Sigma_g^-$

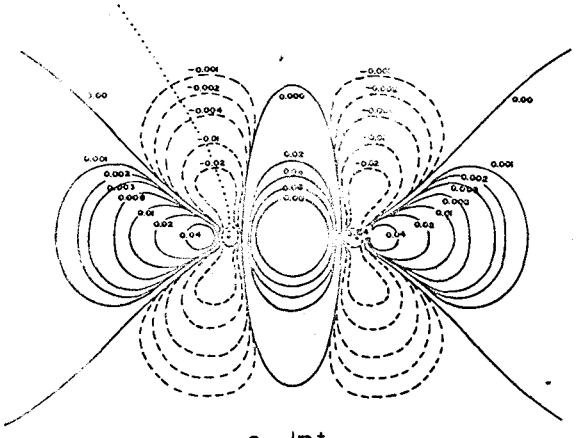

$C_2\ {}^1\Sigma_g^+$

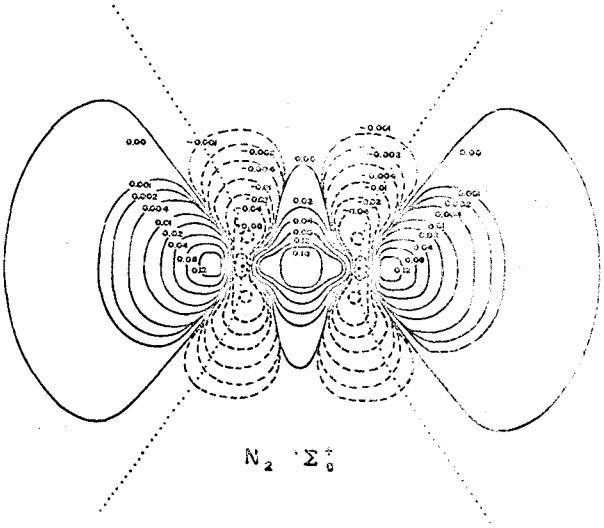

$N_2\ {}^1\Sigma_g^+$

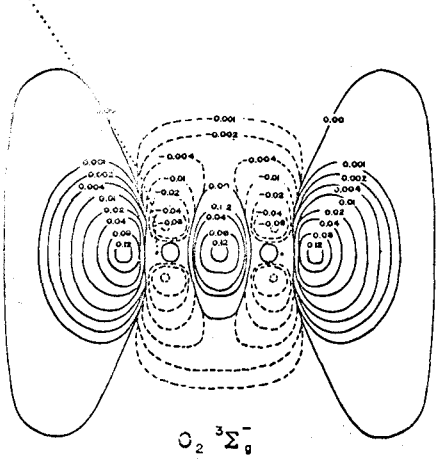

$O_2\ {}^3\Sigma_g^-$

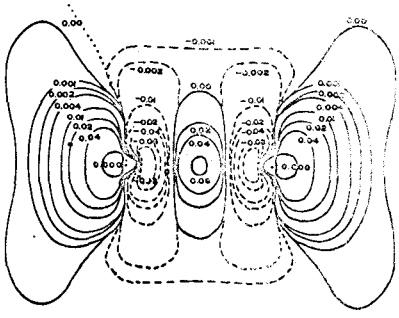

$F_2\ {}^1\Sigma_g^+$

II.3 THE DENSITY DIFFERENCE CHARGE DISTRIBUTIONS

Figure 5 shows the $\Delta\rho(\vec{r})$ contour maps for the series of homonuclear diatomic molecules Li_2, B_2, C_2, N_2, O_2 and F_2. As mentioned in the introduction, these $\Delta\rho(\vec{r})$ maps provide a useful picture of the net redistribution of charge that takes place during the formation of the chemical bond. Also, in the case of stable molecular arrangements such $\Delta\rho(\vec{r})$ contour maps should evidence a net transfer of charge to the binding region. The overlap of two atomic densities at the observed internuclear distance does not place sufficient charge in the binding region to balance the electrostatic force of repulsion owing to the nuclei[62].

The $\Delta\rho(\vec{r})$ function is a significant quantity independent of the orbital representation of the wave function as it is invariant to orthogonal, unitary, orbital transformations. $\Delta\rho(\vec{r})$ maps identical to those shown in Figure 5 would be obtained if the molecular orbitals were first transformed into equivalent or localized orbitals. The $\Delta\rho(\vec{r})$ function is dependent on the quality of the orbital representation in both the molecular and atomic wavefunctions.* A consistent approximation perspective has been adopted in this approach with wave functions of Hartree-Fock accuracy being used to calculate both the molecular density and the

---

*The $\Delta\rho$ map is independent of the atomic basis set for basis sets of equally high quality. The use of the "accurate basis sets" of P.Bagus and T.Gilbert (unpublished results) leaves the $\Delta\rho$ maps of the first-row homonuclear diatomic molecules unaltered except in the case of Li. In this latter case a small change in the zero contour is evident in the region of the Li nucleus.

Figure 6. A density difference contour map for the molecule Li_2. Here the molecular density is derived from a multi-configurational wavefunction. The $\Delta\rho(\vec{r})$ map for Li_2 in figure 5 involves the molecular density derived from a Hartree-Fock approximation to the wavefunction.

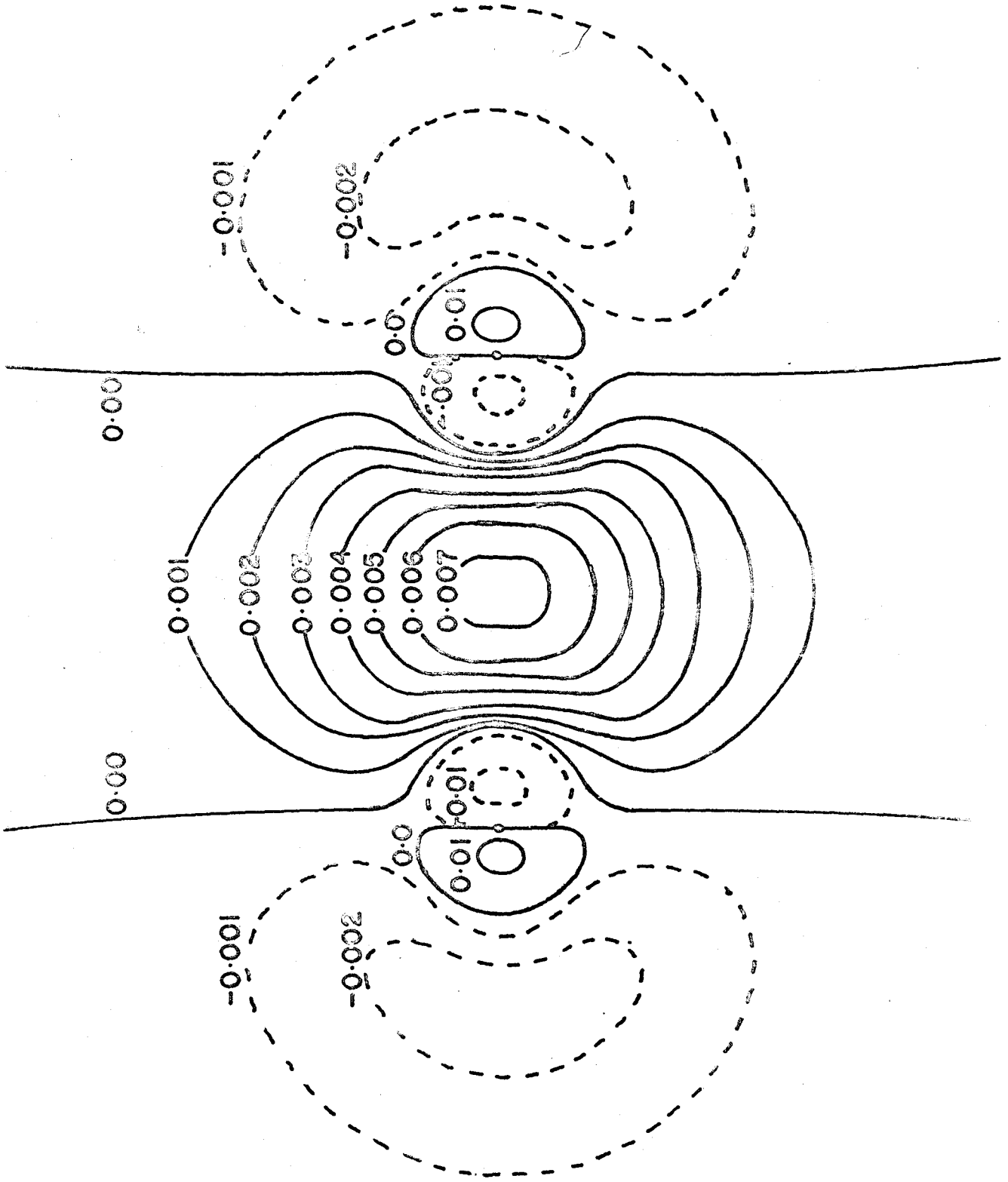
-0.001
-0.002
-0.01
0.00
0.00
0.001
0.002
0.003
0.004
0.005
0.006
0.007
0.00
0.00
-0.01
-0.001
-0.002

atomic densities[63] that are needed to construct the $\Delta\rho(\vec{r})$ function. Such an approach neglects the electronic correlation in both the atomic and molecular systems. It might be argued that the $\Delta\rho(\vec{r})$ function which is defined as the result of a subtraction of two Hartree-Fock densities is essentially accurate. The correlation errors in each density tend to cancel each other with a resultant error of less than 1% in $\Delta\rho(\vec{r})$. However, as the separated atoms approach each other to form a molecule, there is a pairing of electrons with a resultant correlation effect that is not present in the atomic densities. Hence the above argument is not totally valid. Although it is not known how best to treat this problem at present, preliminary studies[64] employing a configuration interaction wavefunction[65] for the Li_2 molecule yield a $\Delta\rho(\vec{r})$ contour map shown in Figure 6. This $\Delta\rho(\vec{r})$ map is similar in every detail to the $\Delta\rho(\vec{r})$ contour map shown for Li_2 in Figure 5.

The atomic densities used to construct these $\Delta\rho(\vec{r})$ maps describe the atoms in their valence states. This approach foresees the formation of the electron-pair bond and is considered to yield the chemically most interesting results. As an example, consider the formation of the F_2 molecule. At large internuclear distances, where the two fluorine atoms just begin to interact, their orbitals can be classified in terms of the quantum number λ, the orbital

angular momentum along the bond axis. In the limit where λ just begins to be a good quantum number, the two fluorine atoms can be described by the configuration $1s^2 2s^2 2p_\pi^4 2p_\sigma^1$. Hence the bond in F_2 is foreseen as the overlap of two $2p_\sigma$ orbitals each with a single electron. A spherical average over the ground state configuration for the atomic densities would neglect this preferred direction towards the other atom. There is no difference between the valence state density and the average ground state density for Li and N, but B and C are placed in valence states with one and two p_π electrons respectively while O and F are placed in states with a single p_σ electron, the remaining p electrons being averaged over the π orbitals.

An examination of the diagrams shows that there are two characteristic regions of charge buildup in each molecule - one being in the internuclear region and one being in the region behind the nuclei. The charge increase behind the nuclei is small in the case of Li_2 but quite extensive in the remaining molecules. The dotted contours on the N_2 $\Delta\rho(\vec{r})$ map indicate the boundaries between the binding and the antibinding regions. Similar dotted contours appear in the upper left region of each remaining diagram and serve the same purpose as those contours in N_2. A consideration of these observations in terms of the concepts of binding and antibinding[34] leads to the surprising fact

TABLE II

Increase in the Number of Electronic Charges in Berlin's binding and antibinding regions*

	Binding Region	Antibinding Region
Li_2	0.41	~0.01
Be_2	0.17	0.11
B_2	0.30	0.05
C_2	0.50	0.06
N_2	0.25	0.13
O_2	0.10	0.14
F_2	0.08	0.10

*Since the charge which is concentrated in these regions is removed from both the binding and antibinding regions these figures do not represent the changes in total electron population for these regions. The calculation of these numbers is described in the appendix.

that charge is not only concentrated in the binding region but also in the antibinding regions. Only Li_2 corresponds to the simple picture of charge transfer from the antibinding to the binding region. From Li_2 on across the series, the charge density is increasingly removed from the binding region until, for F_2, practically the whole of the decrease occurs in the binding region. Table II shows a series of population numbers obtained by integrating the $\Delta\rho(\vec{r})$ function over the various regions where it is positive. The table shows two columns - one corresponding to a buildup of charge in the binding region and one corresponding to a buildup of charge in the antibinding region. In agreement with the interpretation derived from the total density contour maps, Li_2 and C_2 show the greatest increase of charge in the binding region. The data for O_2 and F_2 shows that here a greater amount of charge is transferred to the antibinding region than to the binding region. Again it must be noted that the $\Delta\rho(\vec{r})$ contour maps and population numbers do not give a complete picture. Although the charge accumulated in the binding region is concentrated along the internuclear axis while the charge accumulated in the antibinding region is more diffuse in nature, it is evident that an examination of these maps and population numbers will lead to no conclusions regarding the stability of the respective molecules. A force analysis will however show

that each of these molecules has reached a state of electrostatic equilibrium. In fact, the force exerted by the charge density in the binding region, the overlap density, is greater than that required to balance the force of nuclear repulsion. Consequently, the atomic density on each nucleus is strongly polarized away from the binding region.

The difference maps do give an idea of the bond type. Li_2 is certainly distinct from the other members of the series and is characteristic of the increase in the internuclear region that is expected because of the overlap of s functions. Indeed, in the wave function for Li_2 the coefficients describing the p orbital contributions are quite small. The remaining $\Delta\rho(\vec{r})$ maps show the increased p character of the resulting bonds. Even B_2 and C_2 which are seen in simple molecular orbital theory as possessing respectively one and two π bonds, show maximum increases in their respective $\Delta\rho(\vec{r})$ maps along the internuclear axis. If the π character of the bond remained strongly evident, the maximum increase in $\Delta\rho(\vec{r})$ would be above and below the bond axis. However the π character of these bonds is evidenced by the relatively larger distance separating the two portions of the zero contour as measured along a line at the molecular midpoint and perpendicular to the internuclear axis. The relatively larger populations in C_2 and B_2 - firstly describing the charge increase in the

Figure 7. The total density and density difference contour maps for the ground state of Be_2 at an internuclear separation of 3.5 a.u.

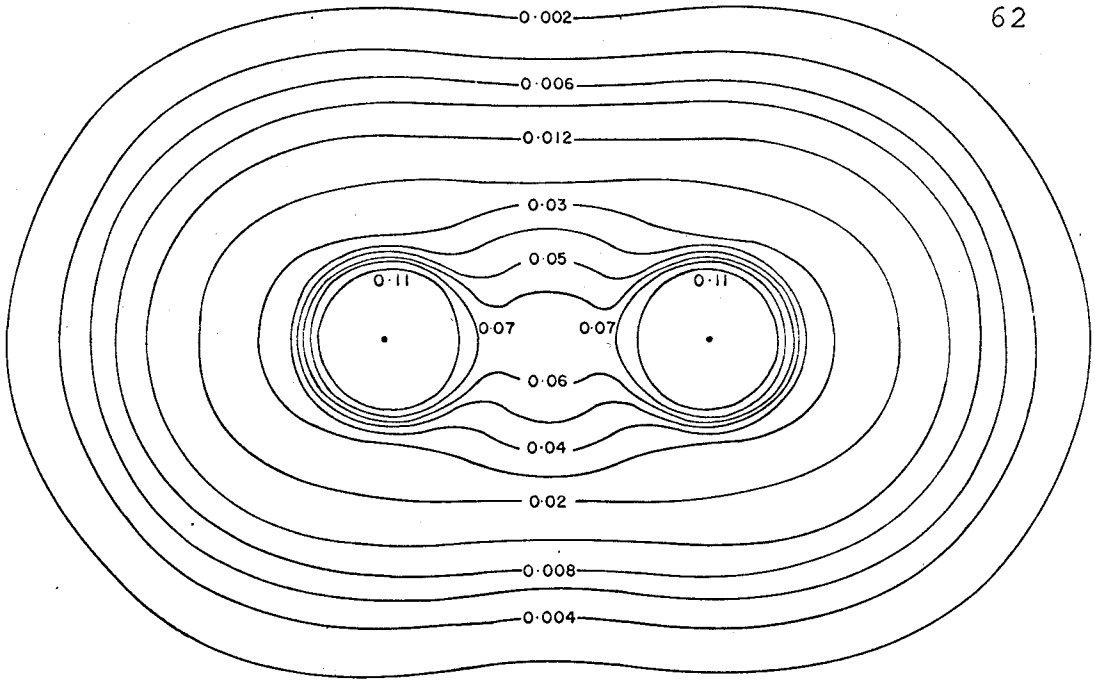
0·002
0·006
0·012
0·03
0·05
0·11
0·11
0·07
0·07
0·06
0·04
0·02
0·008
0·004

$Be_2\ ^1\Sigma_g^+$

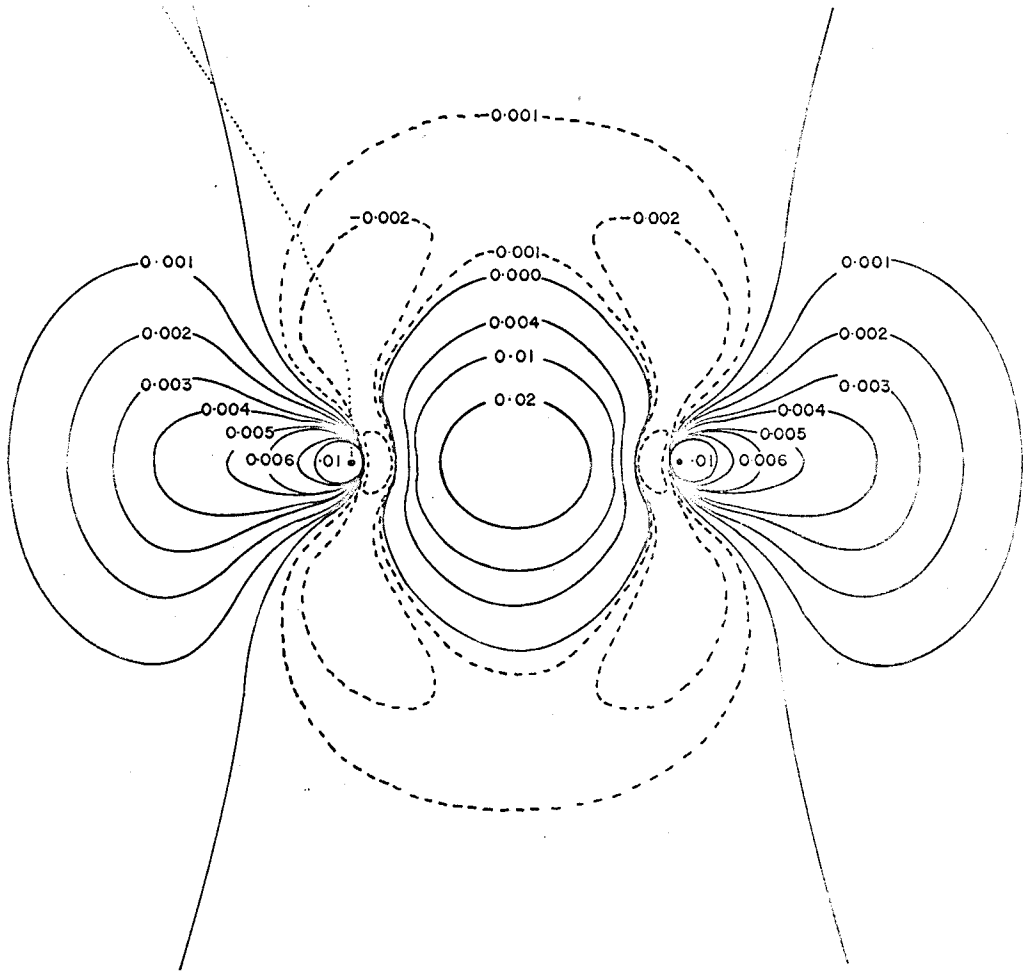
0·001
0·002
0·001
0·002
0·001
0·000
0·004
0·01
0·02
0·001
0·002
0·003
0·004
0·005
0·006
·01
·01
0·006
0·005
0·004
0·003
0·002
0·001

binding region and secondly describing the total fraction of the charge in the binding region, together with the relatively smaller increases of charge in the antibinding regions of these molecules also evince their π character. With the filling of the $3\sigma_g$ and π_g orbitals in N_2, O_2 and F_2, the internuclear increase becomes even more concentrated along the axis while the increase behind the nuclei becomes more diffuse.

The molecule Be_2 in its ground state has the configuration $1\sigma_g^2 1\sigma_u^2 2\sigma_g^2 2\sigma_u^2$. As this state is not bound, its electron density contour map should be investigated to determine if this type of information is predicted by such an analysis. Figure 7 shows the total density and density difference contour maps for Be_2 at an internuclear distance of R = 3.5 a.u. The wavefunction for Be_2 is from Cade and Sales[66]. The internuclear distance is approximately the value obtained for a nuclear charge of 4 when R_e is graphed versus Z for the stable members of the series. The density contour map does not indicate the instability of Be_2 in its ground state. The diagram, as it stands, has one feature reminiscent of Li_2 - namely the manner in which the contours bulge out from the internuclear axis. Presumably, there is a double saddlepoint minimum along the internuclear axis. Even the density difference contour map for Be_2 shows the same general features as those describing the other members

of the series,including two regions of charge increase, one in the internuclear region and one behind the nuclei. The simple picture of charge transferred from the binding region to the antibinding region as depicted for the molecule He_2[67] in its unstable ground state is no longer evident. From another point of view, Table II shows that compared to the neighbouring members in the series Li_2 and B_2 there is an abnormally large buildup of charge in the extranuclear region while, in addition to this, there is an abnormally small buildup of charge in the internuclear region. Similarly, the total fraction of charge in the binding region of Be_2 is only 0.53 compared to 0.59 for Li_2 and 0.58 for B_2. These facts suggest and a force calculation shows that the amount of charge transferred to the binding region in Be_2 is insufficient to balance the electrostatic force of repulsion owing to the nuclei However, the difference in the density distributions for a stable and an unstable molecule is clearly one of degree and not one of kind.

A question was posed in the introduction concerning the compatibility of this approach with the Lewis concept of the electron-pair bond. Herzberg[68] has pointed out that the difference between the number of bonding orbitals and the number of antibonding orbitals in the molecular orbital description gives the number of electron-pair bonds in the system. It would be satisfying to obtain some correlation

between this electron-pair bond concept and the number of charges accumulated in the binding region. A casual inspection seems to indicate no overall relationship. There is approximately twice as much charge accumulated in the binding region of C_2 as there is in the case of B_2. Similarly N_2 has a charge accumulation in the binding region three times that of F_2. These facts can be rationalized and a partial correlation can be obtained if it is recognized that there are essentially three different bond types in the series of molecules Li_2, B_2, C_2, N_2, O_2 and F_2. The first bond type is here represented by Li_2, the second bond type is represented by B_2 and C_2 while the third type is characteristic of the bonds found in N_2, O_2 and F_2. Li_2 appears to be bound together by a relatively large diffuse accumulation of charge in its binding region. This can be interpreted as evidence of a bond formed by the overlap of s orbitals. The accumulation of charge in the binding region of B_2 and C_2 is not as diffuse as that of Li_2; neither is it as concentrated as the charge accumulation in N_2, O_2, and F_2. This can be taken as evidence of the partial π character of the bonds in these two molecules. The concentrated nature of the charge buildup in the binding region of N_2, O_2, and F_2 seems to indicate the strong p_σ nature of the bonding. Molecular orbital theory predicts these molecules to have one sigma bond and respectively two, one and zero π bonds.

The change in bond type after C_2 to one which is more contracted along the axis accounts for the lack of correlation of the charge accumulation in the binding region and the number of electron-pair bonds. A discussion of bonding solely in terms of a population count is misleading. As important as the amount of charge is the exact disposition of the charge in the molecule; that is, whether it is diffuse or contracted in nature. Both of these features, the amount of charge and its disposition are taken into account in a determination of the forces which bind the nuclei together to form a molecule.

Figure 8. Electron density difference profiles for the first-row homonuclear diatomic molecules. The vertical axis shows the $\Delta\rho(\vec{r})$ values. The horizontal axis represents the internuclear axis.

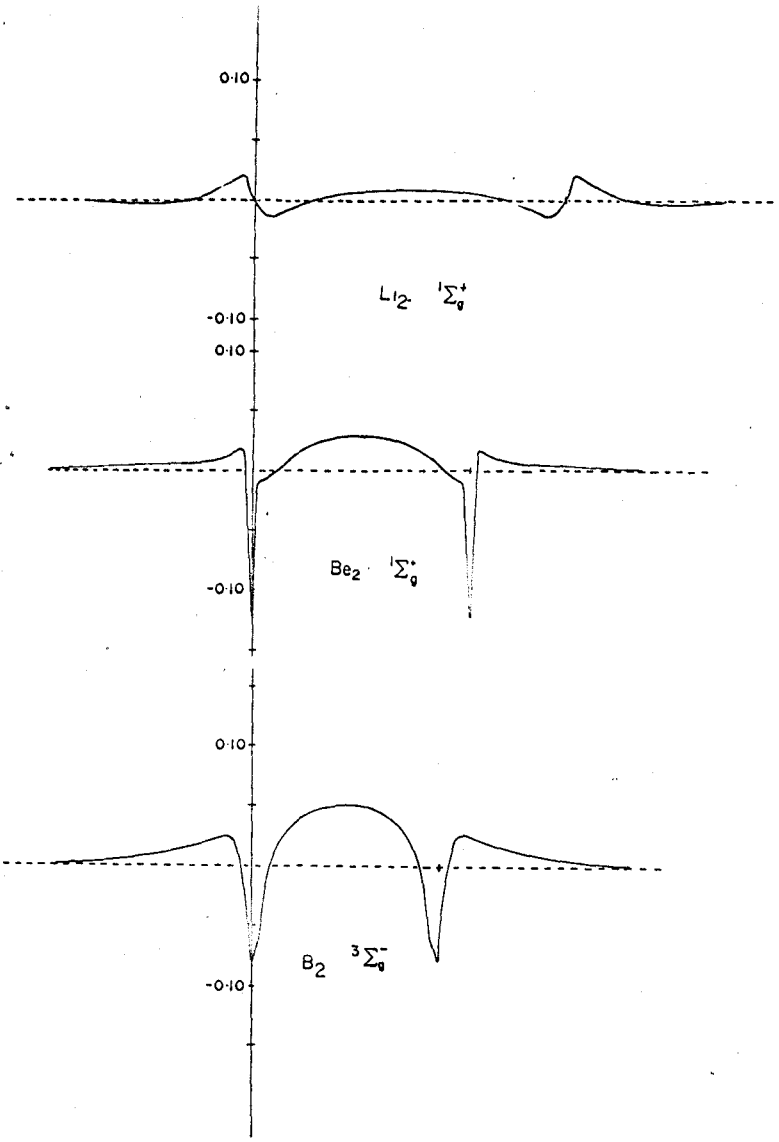
0·10
-0·10
Li_2 $^1\Sigma_g^+$
0·10
-0·10
Be_2 $^1\Sigma_g^+$
0·10
-0·10
B_2 $^3\Sigma_g^-$

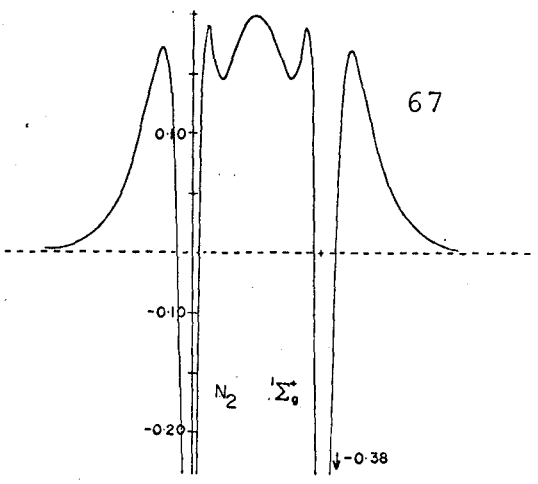
0·10
-0·10
-0·20
N_2 $^1\Sigma_g^+$
-0·38

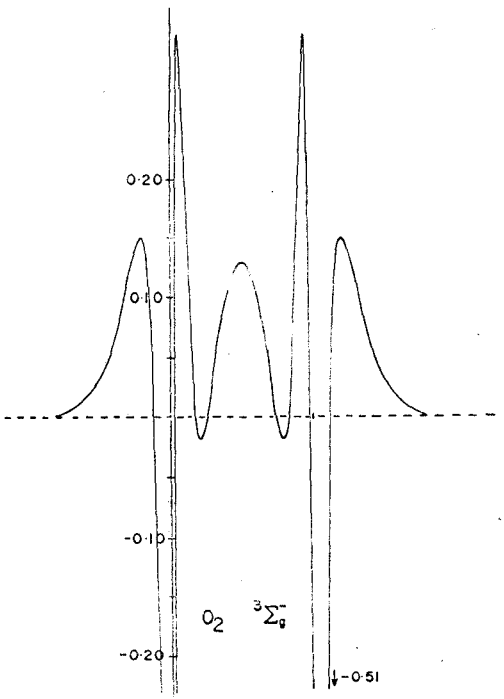
0·20
0·10
-0·10
-0·20
O_2 $^3\Sigma_g^-$
-0·51

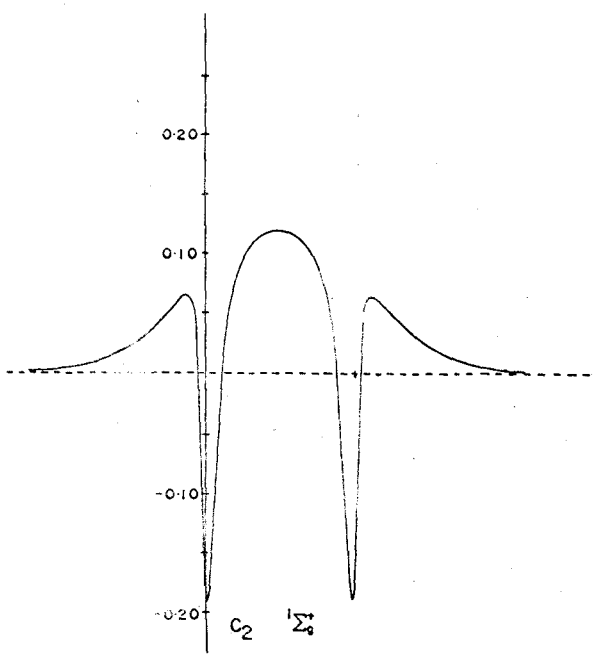
0·20
0·10
-0·10
-0·20
C_2 $^1\Sigma_g^+$

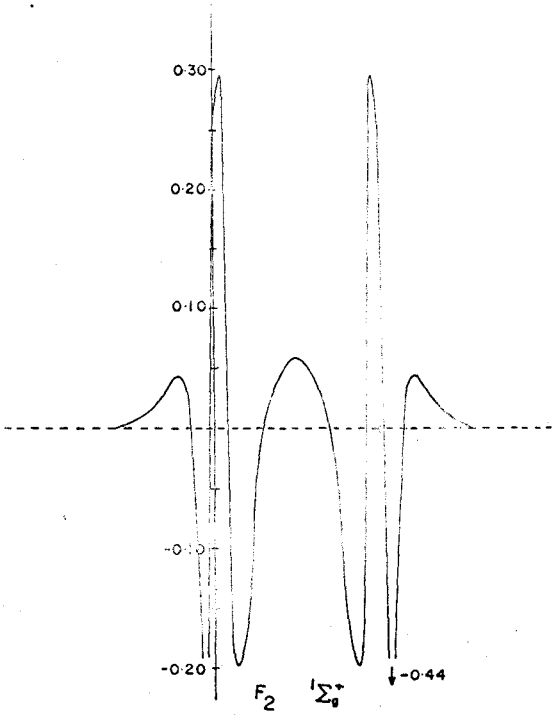
0·30
0·20
0·10
-0·10
-0·20
F_2 $^1\Sigma_g^+$
-0·44

II-4 THE ELECTRON DENSITY DIFFERENCE PROFILES

Figure 8 shows electron density difference profile maps for the molecules Li_2, Be_2, B_2, C_2, N_2, O_2 and F_2. These graphs summarize the value of the $\Delta\rho(\vec{r})$ function at various points along the internuclear axis. The scale of density difference values is shown along the vertical axis. There seems to be a correlation between the value of $\Delta\rho(\vec{r})$ at the molecular midpoint ($R_e/2$) and the value of the dissociation energy. Thus C_2 has a dissociation energy two times that of B_2 and the difference density accumulated at the molecular midpoint in C_2 is twice that of B_2. Rosenfelt[42] has suggested that there is a correlation between the dissociation energy calculated from a given approximate molecular wavefunction and the density difference at the molecular midpoint. In fact, if the experimental dissociation energy is plotted against the value of $\Delta\rho(\vec{r})$ calculated at th e molecular midpoint, there is a straight line relationship for the molecules Li_2, B_2, C_2 and N_2. However O_2 and F_2 do not fall on this straight line but lie above it.

The profiles again evidence the three distinct bond types previously discussed . Li_2 shows only a very small increase of density along the bond axis. Indeed there is a greater increase of $\Delta\rho(\vec{r})$ behind the nuclei than there is in the internuclear region. The profiles for B_2 and C_2 are

quite similar. There is a larger increase of $\Delta\rho(\vec{r})$ along the internuclear axis in the binding region than there is in the antibinding region. The diagrams make evident the p_σ character of the bonds in these molecules. Although simple molecular orbital theory predicts that the bonds in B_2 and C_2 should result from the overlap of p_π orbitals centred on each nucleus, the profiles show a large increase of charge density along the internuclear axis. There is necessarily a transfer of charge from orbitals of π symmetry to orbitals of σ symmetry. The profiles describing N_2, O_2 and F_2 are all quite similar. Further these profiles are distinct from those describing the other molecules. Each of these profiles shows three $\Delta\rho(\vec{r})$ maxima in the binding region along the internuclear axis. The maximum $\Delta\rho(\vec{r})$ contours describing the charge buildup in the antibinding region are similar in value to those $\Delta\rho(\vec{r})$ contours at the molecular midpoint. The remaining two $\Delta\rho(\vec{r})$ maxima in the binding region appear because of the filling of the $3\sigma_g$ orbital. The density contours of this orbital show maxima along the internuclear axis in close proximity to the nuclei.

The profile for Be_2 shows larger positive $\Delta\rho(\vec{r})$ contours in the binding region than in the antibinding region. It appears quite similar to those profile graphs describing the molecules B_2 and C_2 with the exception that there is

a larger amount of density removed from the nuclei in Be_2 than there is removed from the nuclei in B_2. However the instability of Be_2 is not predicted by its profile map.

CHAPTER III

THE FORCES OPERATIVE IN HOMONUCLEAR DIATOMIC MOLECULES

The preceding section presented an analysis of the density distributions in the first row homonuclear diatomic molecules. From a comparison of these density distributions with their separated atom components in terms of the density difference function $\Delta\rho(\vec{r})$, a picture of the charge redistribution attendant upon the formation of the chemical bond was gained. The study of such $\Delta\rho(\vec{r})$ maps led to the conclusion that their use in predicting molecular stability was limited. The physical features of the $\Delta\rho(\vec{r})$ contour map for the unstable ground state of Be_2 were found to be similar to those of the stable members of the series.

To attempt an understanding of binding in a molecule, it is useful to consider the change in the force which the total density exerts on the nuclei in the molecule relative to the situation in the separated atoms. Label the nuclei in a diatomic molecule A and B with nuclear charges Z_A and Z_B respectively. From the Hellmann-Feynman[4] theorem, the total force acting on A for any internuclear separation is

$$F_A(R) = \frac{Z_A Z_B}{R^2} - Z_A \sum_{\mu} \int \Psi^*_{AB}(\vec{x}^n) \frac{\cos\theta_{\mu A}}{r^2_{\mu A}} \Psi_{AB}(\vec{x}^n) d\vec{x}^n \quad (1)$$

$$= \frac{Z_A}{R^2} \left[Z_B - R^2 \sum_{\mu} \int \Psi^*_{AB}(\vec{x}^n) \frac{\cos\theta_{\mu A}}{r^2_{\mu A}} \Psi_{AB}(\vec{x}^n) d\vec{x}^n \right] \quad (2)$$

where

$$\Psi_{AB}(\vec{x}^n) = \Psi_{AB}(\vec{x}_1, \vec{x}_2 \ldots\ldots \vec{x}_n) \quad (3)$$

$$d\vec{x}^n = d\vec{x}_1 d\vec{x}_2 \ldots\ldots d\vec{x}_n \quad (4)$$

The index μ runs over all values from one to n where n is the number of electrons in the molecule AB. At very large R such that R>>Re (the equilibrium bond length)

$$\Psi_{AB}(\vec{x}^n) \simeq \Psi_A (\vec{x}^{n_A}) \Psi_B(\vec{x}^{n_B}). \quad (5)$$

This implies that electron exchange between A and B is negligible. The electronic force integral now becomes

$$F_A^{(Elec)}(R) = -Z_A \int \Psi_{AB}(\vec{x}^n) \left[\sum_{\mu} \frac{\cos\theta_{\mu A}}{r^2_{\mu A}} + \sum_{\nu} \frac{\cos\theta_{\nu A}}{r^2_{\nu A}} \right] \Psi_{AB}(\vec{x}^n) d\vec{x}^n \quad (6)$$

$$= - Z_A \int \Psi_A(\vec{x}^{n_A}) \left[\sum_{\mu} \frac{\cos\theta_{\mu A}}{r^2_{\mu A}} \right] \Psi_A(\vec{x}^{n_A}) \, d\vec{x}^{n_A}$$

$$- Z_A \int \Psi_B(\vec{x}^{n_B}) \left[\sum_{\nu} \frac{\cos\theta_{\nu A}}{r^2_{\nu A}} \right] \Psi_B(\vec{x}^{n_B}) \, d\vec{x}^{n_B} \quad (7)$$

The index μ runs from one to n_A where n_A is the number of electrons associated with atom A. The index ν runs from one to n_B where n_B is the number of electrons associated with the atom B. For large R

$$F_A(R>>R_e) = \frac{Z_A}{R^2} \left[Z_B - \sum_{\mu} (1 - \delta_{\mu\mu}) - \sum_{\nu} \delta_{\nu\nu} \right.$$

$$\left. - R^2 \sum_{\nu} \int \Psi_B(\vec{x}^{n_B}) \left(\frac{\cos\theta_{\nu A}}{r^2_{\nu A}} - \frac{\delta_{\nu\nu}}{R^2} \right) \Psi_B(\vec{x}^{n_B}) d\vec{x}^{n_B} \right] \quad (8)$$

where $\delta_{\mu\mu}$ and $\delta_{\nu\nu}$ are the usual diagonal Kronecker δ symbols. In equation (8), the contribution to the force on nucleus A from electrons on A is given as

$$\sum_{\mu} (1-\delta_{\mu\mu})$$

This is a sum of zeros and results from the fact that, in this limit, the electronic density is spherically placed about nucleus A. The electrons on B contribute an attractive force just balancing the repulsive force resulting from the nuclear charge Z_B except for the electronic force occurring in the last term in equation (8). This last expression becomes negligible by choosing R large enough; that is, as

$$R \to \infty$$

then

$$\cos\theta_{\nu A} \to 1$$

$$\vec{r}_{\nu A} \to R \ .$$

In the general case

$$F_A(R\to\infty) = \frac{Z_A}{R^2} \left[Z_B - \sum_{\mu} (1-\delta_{\mu\mu}) - \sum_{\nu} \delta_{\nu\nu}\right] = 0 \qquad (9)$$

or

$$Z_B = \sum_{\mu} (1-\delta_{\mu\mu}) + \sum_{\nu} \delta_{\nu\nu} \qquad (10)$$

At the equilibrium internuclear distance, R_e, the force on nucleus A is also zero so that

$$\sum_{\mu} R^2 \int \Psi_{AB}(\vec{x}^n) \frac{\cos\theta_{\mu A}}{r^2_{\mu A}} \Psi_{AB}(\vec{x}^n) d\vec{x}^n = Z_B \qquad (11)$$

If a Hartree-Fock wavefunction is used to calculate the integral on the left hand side of equation (11), then

$$\sum_{\mu} R^2 \int \Psi_{AB}(\vec{x}^n) \frac{\cos\theta_{\mu A}}{r^2_{\mu A}} \Psi_{AB}(\vec{x}^n) d\vec{x}^n = \sum_{i=1} R^2 N_i \int \phi_i(\vec{r}_\mu) \frac{\cos\theta_{\mu A}}{r^2_{\mu A}} \phi_i(\vec{r}_\mu) d\vec{r}_\mu$$

$$= \sum_i f_i \qquad (12)$$

The index i runs over all occupied molecular orbitals and N_i is the occupation number of orbital ϕ_i. Equation (2) now becomes

$$F_A(R) = \frac{Z_A}{R^2} [Z_B - \sum_i f_i] \qquad (13)$$

At all internuclear distances, the equation

$$F_A(R) = - F_B(R) \qquad (14)$$

holds. In an orbital description, equation (11) becomes

$$Z_B = \sum_i f_i \qquad (15)$$

and equation (10) becomes

$$Z_B = \sum_k N_k(1-\delta_{kk}) + \sum_\ell N_\ell \delta_{\ell\ell} \qquad (16)$$

The indices k and ℓ run over the atomic orbitals on A and B respectively. The kth and ℓth atomic orbitals correlate with the ith molecular orbital at large internuclear distances. N_k is the occupation number of the k^{th} atomic orbital on A and N_ℓ is the occupation number of the ℓth atomic orbital on atom B. The f_i value is a measure of the

Figure 9. The Hellmann-Feynman force on nucleus A and its variation with internuclear separation. $F_A^{(e)}$ is the electronic force acting on nucleus A. $F_A^{(n)}$ is the force of nuclear repulsion. $F_B(R)$ is the Hellmann-Feynman force on nucleus B.

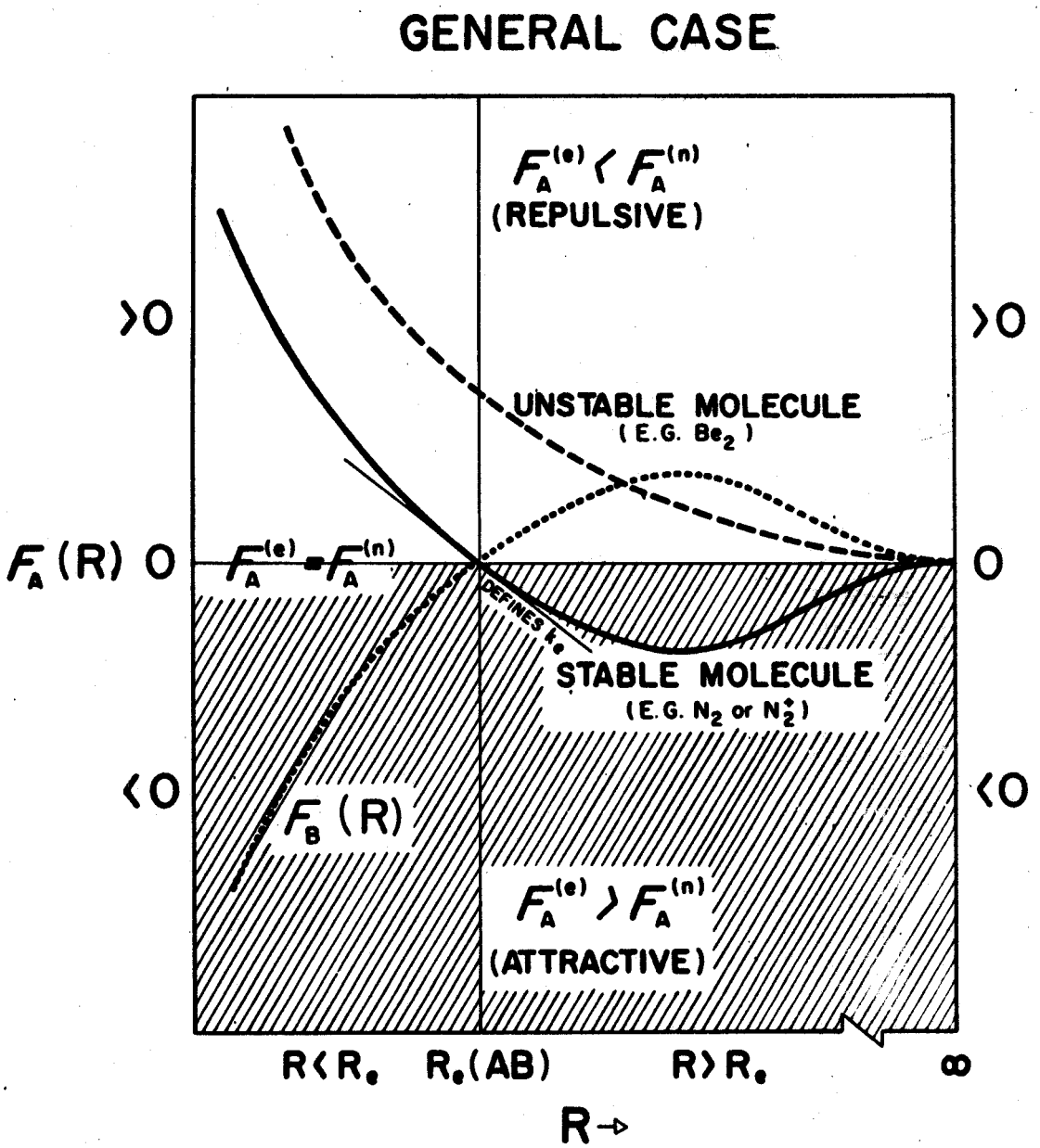
GENERAL CASE
$F_A^{(e)} < F_A^{(n)}$
(REPULSIVE)
UNSTABLE MOLECULE
(E.G. Be_2)
$F_A^{(e)} = F_A^{(n)}$
DEFINES R_e
STABLE MOLECULE
(E.G. N_2 or N_2^+)
$F_B(R)$
$F_A^{(e)} > F_A^{(n)}$
(ATTRACTIVE)
$F_A(R)$
>0
0
<0
$R < R_e$
R_e(AB)
$R > R_e$
∞
R→

TABLE III

Summary of Behaviour of the Forces on the Nuclei with Internuclear Separation[a]

R-Range	Force on Nuclei	Electronic Versus Nuclear Force	Net Effect of All Forces	Remarks
$R>>R_e$	$F_A=-F_B=0$	$\sum_{\ell}^{N_B} \delta_{\ell\ell} = Z_B$	Nil	Electronic contribution cancels nuclear repulsion
$R > R_e$	$F_A=-F_B\neq 0$	$\sum_i f_i > Z_B$	Attraction	Electronic attractive force exceeds nuclear repulsive force
$R = R_e$	$F_A=-F_B=0$	$\sum_i f_i = Z_B$	Equilibrium	Electronic attractive force balances nuclear repulsive force
$R < R_e$	$F_A=-F_B\neq 0$	$\sum_i f_i < Z_B$	Repulsion	Nuclear repulsive force exceeds electronic attractive force

[a]This table is complimentary to Figure 9 and assumes AB forms a stable molecule.

degree of the attractive or repulsive contribution to F_A from electrons in the ith molecular orbital.

The general schematic behavior of F_A graphed against R is shown in Figure 9 for both a stable and an unstable molecule. Table III describes the force acting on nucleus A in terms of the f_i values for given ranges of the internuclear separation. At large R, $F_A = -F_B = 0$, so that the total electronic charge on B is completely effective in cancelling the repulsive force due to nucleus B. For $R>R_e$, the attractive electronic force exceeds the nuclear repulsive force due to nucleus B. At R_e, there is electrostatic equilibrium, and again $F_A = -F_B=0$ with the result that

$$\sum_i f_i = Z_B \qquad (15)$$

For $R<R_e$, the repulsive force due to nucleus B becomes larger than the attractive force due to the electronic charge cloud although $F_A = -F_B$ is still valid.

The foregoing straightforward equations and remarks are valid for the exact wavefunction and for a select group of approximate wavefunctions including the Hartree-Fock wavefunction ,but for crude approximate wavefunctions $F_A(R_e)\neq 0$ and $F_A(R)\neq -F_B(R)$ except fortuitously. Hurley[69] has discussed in some detail in a survey article the conditions for which the Hellmann-Feynman theorem is satisfied.

Since the net force on nucleus A is zero both at R_e and in the limit as R approaches infinity, then

$$\sum_i f_i = \sum_k N_k(1-\delta_{kk}) + \sum_\ell N_\ell \delta_{\ell\ell} = Z_B \qquad (17)$$

For a homonuclear diatomic molecule, the molecular orbital ϕ_i correlates with the same atomic orbitals on both A and B for large internuclear separations. In this limit, the atomic density on A makes no contribution to the electronic force acting on A. Thus at large R, each f_i has a value of unity; that is

$$f_i(\infty) = 1 \qquad (18)$$

As the atoms approach there is a redistribution of charge in each molecular orbital with the result that the f_i values are in general[70] no longer equal to one. If $f_i>1$, then relative to the separated atoms, the charge density in the ith molecular orbital has been built up in the region between the nuclei such that it more than screens one unit of nuclear charge; that is, there is an attractive force in excess of the repulsion of one nuclear charge. Such a molecular orbital is denoted as a <u>binding molecular orbital</u>. If $f_i<1$, then relative to the separated atoms, the charge density of the ith molecular orbital has been built up in regions behind the nuclei. This density no longer screens one unit of nuclear charge on B as it did in the separated atoms. Such a molecular orbital is denoted as an <u>antibinding molecular orbital</u>. If the density in such

a molecular orbital has an f_i value less than zero, then this density is strongly antibinding. In a strongly antibinding molecular orbital, the density is so placed to actually pull the nuclei apart. If $f_i \sim 1$ then the density in the molecular orbital ϕ_i continues to screen one unit of nuclear charge on nucleus B from nucleus A. The density in this type of molecular orbital is termed nonbinding as it plays the same role in the molecule as in the separated atoms. Inner shell molecular orbitals possess f_i values close to unity. This observation indicates that the density in such molecular orbitals is indeed tightly bound to each nucleus in close to spherical distributions. In summary, the force on nucleus A is given as

$$F_A = \frac{Z}{R^2} \sum_i (\delta_{ii} - f_i) \qquad (19)$$

where the sum is over each of the occupied orbitals. The $\pm\lambda$ components of a doubly degenerate orbital are counted separately. If an f_i value is less than unity, the quantity $(1-f_i)$ determines the net positive electric field at the two nuclei and hence the net force of repulsion acting on the molecule because of the ith molecular orbital. If an f_i value is greater than unity, then the quantity $(1-f_i)$ is a quantitative measure of the net negative electric field and of the binding exerted by the density of this molecular orbital over and above the screening of one nuclear charge.

TABLE IV

Orbital Forces in Homonuclear Diatomic Molecules

Ground State	Molecule	$f(1\sigma_g)$	$f(1\sigma_u)$	$f(2\sigma_g)$	$f(2\sigma_u)$	$f(1\pi_u)$	$f(3\sigma_g)$	$f(1\pi_g)$	$\Sigma_i f_j$	Net force in a.u.
$^1\Sigma_g^+$	Li_2	0.706	0.658	1.591					2.955	0.005
$^1\Sigma_g^+$	Be_2[a]	1.051	1.028	2.003	-0.399				3.683	0.103
$^3\Sigma_g^-$	B_2	0.979	0.971	2.305	-0.492	1.188			4.951	0.027
$^1\Sigma_g^+$	C_2	0.969	0.954	2.250	-0.436	1.125[b]			5.987	0.015
$^1\Sigma_g^+$	N_2	1.160	1.085	2.682	-0.463	1.216[b]	0.150		7.046	-0.075
$^3\Sigma_g^-$	O_2	1.232	1.138	2.934	-0.518	1.302[b]	0.174	0.426	7.990	0.016
$^1\Sigma_g^+$	F_2	1.243	1.123	2.447	-0.168	1.232[b]	0.516	0.656[b]	8.937	0.080

[a] The $X^1\Sigma_g^+$ state of Be_2 is a repulsive one. These results refer to an internuclear distance of 3.5 bohr.

[b] All of the f_i values are quoted for double occupation of the orbitals for comparative purposes. The values marked by b are to be doubled to obtain the total electronic force as they refer to filled pi-orbitals.

Table IV lists the f_i values for the homonuclear diatomic molecules formed from atoms in the first row of the periodic table. These values are calculated from the same Hartree-Fock ground state wave functions used to obtain ρ and $\Delta\rho$ for these molecules. With the exception of Be_2, the sum of the f_i values is close to Z in each case, as required for electrostatic equilibrium[71]. For Be_2 the sum is less than Z, a result which correctly predicts the ground state of this molecule to be a repulsive one. The method of calculation of these numbers is described in the appendix.

A quantitative measure of the binding or antibinding nature of each m.o. is obtained by comparing its f_i value with unity. With the exception of the $1\sigma_g$ and $1\sigma_u$ orbitals, the binding or antibinding nature of a given molecular orbital is the same for all the molecules in the series. Several factors indicate that the molecules in this series can be divided into three groups, one containing the molecules N_2, O_2 and F_2, one containing the molecules B_2 and C_2, and one involving only Li_2. For N_2, O_2, and F_2, both the $1\sigma_g$ and the $1\sigma_u$ orbitals are slightly binding. For Be_2, B_2, and C_2, these orbitals are essentially non-binding while for Li_2, $1\sigma_g$ and $1\sigma_u$ are definitely antibinding. For Li_2, the overall disposition of the 1σ density results in a force of repulsion equivalent to placing approximately

six-tenths of a positive charge on each nucleus. The $2\sigma_g$ orbital is uniformly binding for the whole series. The $f(2\sigma_u)$ values are negative in every case and thus the $2\sigma_u$ molecular orbitals are all strongly antibinding. The density in these orbitals does not shield one unit of charge on nucleus B from nucleus A and is so placed as to draw the nuclei apart.

Again the classification described above is seen. The overall 2σ density is binding in the case of N_2, O_2, and F_2 while it is slightly antibinding in the case of B_2 and C_2. For Be_2 $f(2\sigma_g) + f(2\sigma_u)$ is considerably less than 2. From these observations, it is clear that the Be_2 molecule in its ground state configuration will be unstable as the nuclei in this molecule will be imperfectly screened and will experience a net force of repulsion.

The $1\pi_u$ orbital is only weakly binding for the molecules in this series. In the case of N_2, O_2, and F_2, $1\pi_u$ is of comparable strength to the $1\sigma_g$ orbital. The $f(3\sigma_g)$ values are all less than one with the result that the $3\sigma_g$ orbital is antibinding. The density in this molecular orbital while it does draw the nuclei together, does not shield one unit of nuclear charge on B from A. The $1\pi_g$ orbital is slightly more antibinding than the $1\pi_u$ orbital is binding. The complete filling of the π_u and π_g orbitals in F_2 leads to a small net force of repulsion

as the electric field exerted by the eight electrons in these π orbitals no longer balances the field due to four positive charges on each nucleus.

As explained in the appendix, each molecular orbital in this work is approximated by a linear combination of Slater-type functions. Thus each f_i value can be written as a sum

$$f_i = f_i^{(AA)} + f_i^{(AB)} + f_i^{(BB)} . \qquad (20)$$

The term $f_i^{(AA)}$ designated by A and referred to as the atomic force is a measure of the electronic force acting on nucleus A because of density situated about the A nucleus. If this density is spherically disposed about A, then the resultant electronic force is zero. However, any polarization of the atomic charge distribution as described by s-p or p-d hybridization results in a force on the A nucleus in the same direction as the polarization. The term $f_i^{(AB)}$ designated by O and referred to as the overlap force is a measure of the electronic force acting on the A nucleus as a result of the overlap distribution. The positive overlap of orbitals centred on A and B results in the transfer of charge density to the region between the nuclei and the overlap force provides a quantitative measure of the effectiveness of this transferred density in binding the two nuclei together. The term $f_i^{(BB)}$ designated by S and referred to as the screening force is a measure of the elec-

Figure 10: Contour maps and various force contributions for the orbital densities of $O_2(X^3\Sigma_g^-)$ at $R = R_e$ (experimental) after Wahl (Ref. 72). A ≡ atomic force, $f_i^{(AA)}$; O ≡ overlap force, $f_i^{(AB)}$ and S ≡ screening force $f_i^{(BB)}$.

$1\sigma_g$

A = 0·231
O = 0·000
S = 1·001
f = 1·232

$1\sigma_u$

A = 0·129
O = 0·010
S = 0·999
f = 1·138

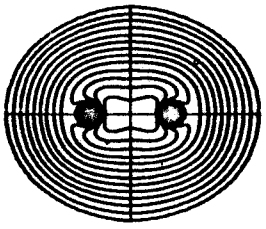

$2\sigma_g$

A = 0·404
O = 1·628
S = 0·902
f = 2·934

$2\sigma_u$

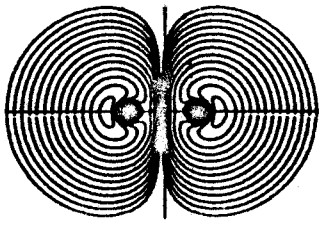

A = -1·048
O = -0·267
S = 0·797
f = -0·519

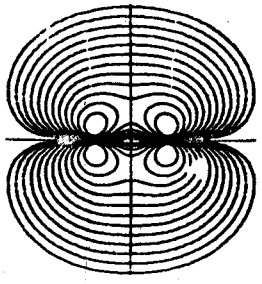

$1\pi_u$

A = 0·217
O = 0·421
S = 0·664
f = 1·302

$3\sigma_g$

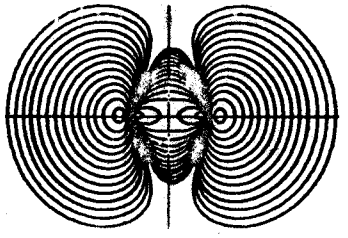

A = -2·334
O = 1·693
S = 0·815
f = 0·174

$1\pi_g$

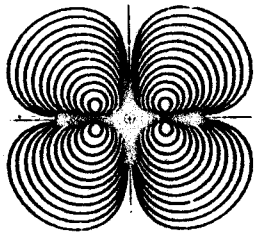

A = -0·100
O = -0·419
S = 0·945
f = 0·426

tronic force acting on the A nucleus as a result of density situated entirely on the B nucleus. It is a measure of the electronic shielding of nucleus B from nucleus A by electrons on B. The screening force provides the sole contribution to the f_i values at large R

Figure 10 shows the orbital density diagrams given by Wahl[72] for the O_2 molecule using the wave function of Cade and Malli[59]. The caption under each diagram gives the force exerted by each orbital density and its breakdown into atomic, overlap, and screening contributions as described above. The various populations for the remaining molecules of the series are given in the appendix.

The density contour maps for the $1\sigma_g$ and $1\sigma_u$ orbitals appear similar in nature to those describing inner shell atomiclike orbitals centred on each nucleus. There is no overlap force and each "core" density shields one unit of nuclear charge. However each core density is slightly polarized into the internuclear region. It is this polarization that makes $\phi_{1\sigma_g}$ and $\phi_{1\sigma_u}$ binding in the case of N_2, O_2 and F_2, For C_2, B_2 and Li_2 the polarization is in the opposite direction with the result that for these molecules, $\phi_{1\sigma_g}$ and $\phi_{1\sigma_u}$ are antibinding.

The density contours of the $2\sigma_g$ orbital encircle the entire molecule in contrast to the contours of the $1\sigma_g$ orbital. The strong binding character of this molecular

orbital is a result of two factors, the large transfer of density into the overlap region and the polarization of the remaining atomic density. As a result of this large overlap force, the screening value is less than unity. This disposition of the $2\sigma_g$ charge density is characteristic for all the molecules but C_2 and N_2 for which the atomic force contribution is small and negative.

The nodal surface passing through the midpoint of the internuclear axis half way between each oxygen nucleus is strongly evident in the density contour map describing the $2\sigma_u$ molecular orbital. The strongly antibinding nature of this molecular orbital is a result of a strong back polarization of the density surrounding each nucleus and a negative overlap force. The negative overlap force indicates that the charge in this molecular orbital is redistributed to regions behind the nuclei during the formation of the chemical bond. The strong back polarization of the atomic densities results in a considerable reduction of the screening contribution and thus in an unshielding of the nuclei relative to the separated atoms. A comparison of the $2\sigma_g$ and $2\sigma_u$ orbitals shows that the total overlap force is attractive and tends to pull the nuclei together while the total atomic force is negative and tends to pull the nuclei apart. These two resultant properties of the $2\sigma_g$ and $2\sigma_u$ orbital densities dominate the $\Delta\rho$ maps for B_2 and C_2 with the result as noted earlier that their bonds can be con-

sidered sigma bonds rather than pi bonds. In B_2, for example, the binding force exerted by the overlap density in the $2\sigma_g$ orbital is three times larger than that exerted by the $1\pi_u$ overlap density.

The $1\pi_u$ orbital contains a nodal surface perpendicular to the plane of the contour map and passing through the internuclear axis. The nuclei are descreened in the formation of this molecular orbital and the resultant charge density is transferred to the overlap region where it exerts a positive force on each nucleus. However, because of the nodal plane, the overlap density is placed above and below the internuclear axis where it only exerts a minimal binding effect as compared to the overlap density in the $2\sigma_g$ orbital. In fact the sum of the overlap and screening contributions is approximately equal to one the nonbinding result. The slight binding nature of the molecular orbital can be considered a result of the net inward polarization of the remaining atomic density.

The $3\sigma_g$ molecular orbital contains one nodal surface. The antibinding nature of this molecular orbital is a result of the strong back polarization of the atomic densities centred on each oxygen nucleus. Even the large overlap force which reflects the transfer of charge into the binding region and its localization along the bond axis is not sufficient to counteract this strong polarization. The strong atomic force

results in a descreening of the oxygen nuclei.

The appearance of the density lobes pictured for the $1\pi_g$ orbital is the result of a transfer of overlap charge density to the antibinding region and of a direct polarization of the atomic densities. In both O_2 and F_2 the $1\pi_g$ orbital is slightly more antibinding than the $1\pi_u$ orbital is binding.

Finally it should be noted that an orthogonal unitary transformation of the canonical Hartree-Fock molecular orbitals will change the individual f_i values but will leave their sum invariant. Thus in going from "canonical" molecular orbitals to "equivalent" or "localized" molecular orbitals, the new set of f_i values can also be analyzed in the above fashion in parallel with the new sets of localized or equivalent orbital densities. Thus using f_i values in an interpretive sense violates a desirable tenet of any acceptable interpretive approach but the valuable perspective outweighs this shortcoming.

CHAPTER IV

A COMPARISON OF THE TERMS BINDING AND BONDING

An interpretation of the force acting on the nucleus in a homonuclear diatomic molecule was presented in the preceding chapter. The interpretation was in terms of certain f_i values which measure the degree of the attractive or repulsive contribution to the force acting on the nucleus from electrons in the ith molecular orbital. Although the f_i values were derived from an orbital representation of the molecular wavefunction they were found to provide a meaningful discussion of the chemical bond in terms of the definitions binding and antibinding.

This chapter presents the results of force calculations involving three states of N_2^+, namely $X^2\Sigma_g^+$, $A^2\Pi_u$ and $B^2\Sigma_u^+$. An attempt is made to relate the two definitions bonding and binding. The bonding character of an electron removed from the ith molecular orbital of AB depends on the nodal characteristics of that molecular orbital. A bonding molecular orbital possesses no nodal surface passing between the nuclei while an antibonding molecular orbital does possess such a nodal surface The degree of bonding or antibonding character is related

to the state of promotion of the ith molecular orbital in the correlation scheme connecting the separated and united atoms[73,74]. The $2\sigma_g$ and $1\pi_u$ orbitals are binding as they both possess f_i values greater than one. These orbitals are also classified as bonding according to the previous definition. Similarly the $2\sigma_u$ and $1\pi_g$ orbitals are antibinding as they possess f_i values less than one. These orbitals are also antibonding because they possess nodal surfaces between the nuclei. These nodal surfaces are perpendicular to the plane containing the nuclei. The only qualitative discrepancy between the two sets of definitions concerns the $3\sigma_g$ orbital which is classed as a bonding orbital in terms of orbital energies and an antibinding orbital in terms of orbital forces. The $3\sigma_g$ orbital is only weakly bonding because of its incipient promotion to a united atom $3s_\sigma$ orbital. In like manner the $3\sigma_g$ orbital is not strongly antibinding as it does not exert a force tending to pull the nuclei apart. The attractive force that this orbital exerts on the nuclei is not sufficient to counteract the repulsive force contribution of one positive charge situated on each nucleus. The definition of binding could be changed so that a binding orbital would have an f_i value greater than zero while an antibinding orbital would have an f_i value less than zero. Even in this case the correlation between the two definitions binding and bonding is not perfect as the $1\pi_g$ orbital is now classi-

fied as binding and antibonding. Furthermore restricting the term antibinding to cases where f_i is less than zero results in a loss of the most useful feature of the definition binding. A molecular state will be unstable as long as the sum of the f_i values is less than the nuclear charge and the attractive force of the electrons fails to balance the nuclear repulsive force.

The definitions of bonding and antibonding correlate remarkably well with the empirical definition regarding observed changes in bond length which accompany the removal of an electron in a diatomic molecule[73,74]. The ionization of an electron leads to an increase in R_e if removed from a bonding orbital and to a decrease in R_e if removed from an antibonding orbital. An analysis of the force acting on the nucleus in a diatomic molecule should lead to an even more direct physical interpretation of the ionization process.

For this purpose, it is convenient to define certain $\tilde{f}_i$ values by the following equation

$$-\tilde{f}_i = \frac{R_e^2}{Z_A}\left[F_A^{(AB)}(R_e) - F_A^{(AB+)}(R_e)\right]. \qquad (1)$$

$F_A^{(AB)}$ is the force acting on nucleus A in the molecule AB while $F_A^{(AB+)}$ is the force acting on nucleus A in the molecular ion. Both molecular species have the same internuclear distance so the ionization is termed vertical. R_e is the equilibrium internuclear distance of AB. The $\tilde{f}_i$ value is a measure of the change in the force on A accompanying the loss of an

electron from the molecule AB.

Equation (1) can be expanded by the use of equation (2) in the preceding section. The result is

$$-\tilde{f}_i = \frac{R_e^2}{Z_A}\left[-Z_A \sum_{\mu}^{n} \int \Psi_{AB}^{*}(\vec{x}^n)\,\frac{\cos\Theta_{\mu A}}{r_{\mu A}^2}\,\Psi_{AB}(\vec{x}^n)\,d\vec{x}^n\right.$$

$$\left. - Z_A \sum_{\mu}^{n-1} \int \Psi_{AB}^{*}{}^{+}(\vec{x}^{n-1})\,\frac{\cos\Theta_{\mu A}}{r_{\mu A}^2}\,\Psi_{AB}{}^{+}(\vec{x}^{n-1})\,d\vec{x}^{\,n-1}\right] \qquad (2)$$

$$= - R_e^2 \int \Psi_{AB}^{*}(\vec{x}^n)\,\frac{\cos\Theta_{\mu A}}{r_{\mu A}^2}\,\Psi_{AB}(\vec{r}^n)\,d\vec{x}^n$$

$$-(n-1)R_e^2 \int \left[\Psi_{AB}^{*}(\vec{x}^n)\,\Psi_{AB}(\vec{x}^n)\,d\vec{x}^n - \Psi_{AB}{}^{+}(\vec{x}^{n-1})\,\Psi_{AB}{}^{+}(\vec{x}^{n-1})\,d\vec{x}^{n-1}\right]\frac{\cos\Theta_{\mu A}}{r_{\mu A}^2} \qquad (3)$$

If distinct Hartree-Fock wavefunctions are used for Ψ_{AB} and $\Psi_{AB}{}^{+}$, then equation (3) becomes

$$-\tilde{f}_i = - f_i + f_i{}' - \sum_{j\neq i} (f_j - f_j{}') \qquad (4)$$

The index j runs over all molecular orbitals common to Ψ_{AB} and $\Psi_{AB}{}^{+}$. For $i\neq j$

$$N_j = N_j{}' \qquad (5)$$

The f_j and $f_j{}'$ are defined by

$$f_j = R_e^2 N_j \int \phi_j^{*}\,\frac{\cos\Theta_{\mu A}}{r_{\mu A}^2}\,\phi_j\,d\vec{r}_{\mu} \qquad (6)$$

Figure 11. The Hellmann-Feynman force and its change upon ionization. These are idealized schematic sketches to indicate general characteristics. The lower shaded regions correspond to the case in which attractive forces exceed repulsive forces.

LOSS OF A BONDING ELECTRON

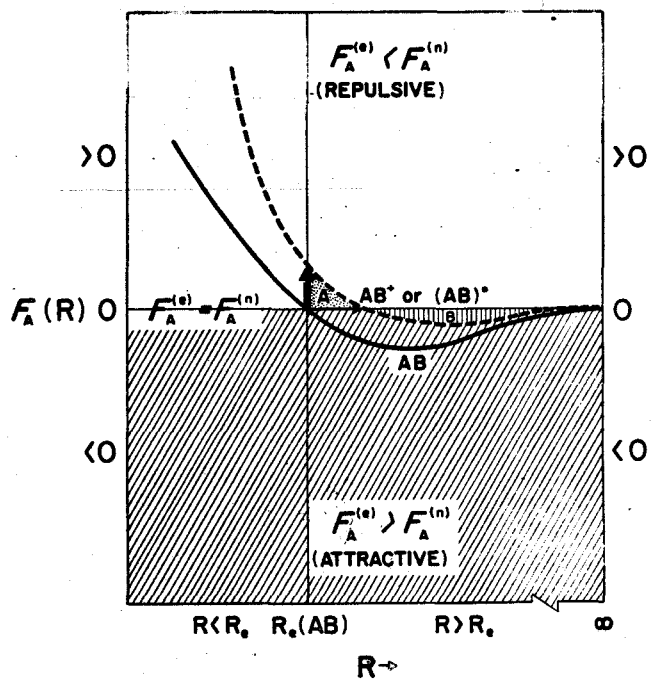

a

LOSS OF AN ANTIBONDING ELECTRON

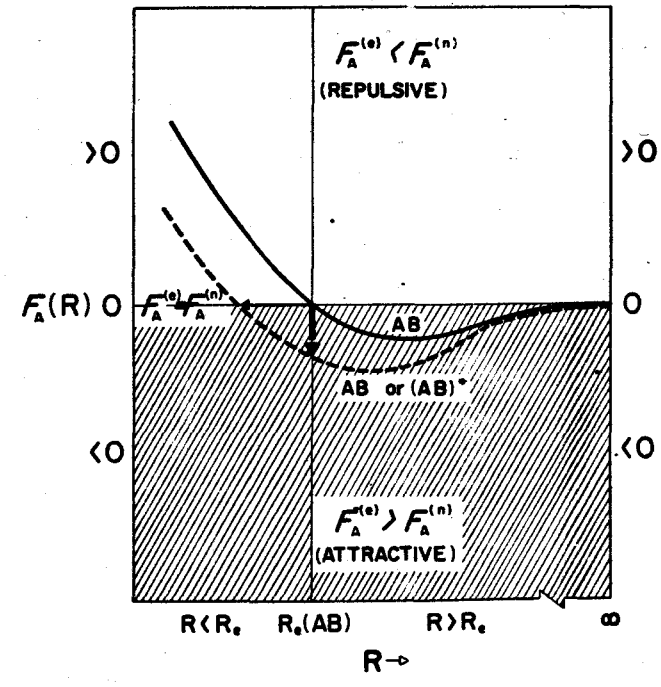

b

$$f_j' = R_e^2 N_j' \int \phi_j'^* \frac{\cos\theta_{\mu A}}{r_{\mu A}^2} \phi_j' d\vec{r}_\mu \qquad (7)$$

where ϕ_j' are the molecular orbitals describing the AB^+ molecule. In this description the electron is ionized from the ith molecular orbital. If ϕ_i is doubly occupied then

$$N_i' = 1 \qquad (8)$$

If ϕ_i is only singly occupied, then

$$N_i' = 0 \qquad (9)$$

and the second term on the right hand side of equation (4) is absent.

Figures 11a and b show the Hellmann-Feynman force, $F_A(R)$ and its variation with internuclear distance. The change in this force which accompanies an ionization process is also shown. The vertical arrows are a measure of the f_i values. The horizontal arrows involve adiabatic ionization processes for which the force on the nucleus always remains zero. The loss of a bonding electron is depicted in Figure 11a. The force curve for the product of ionization intersects the $F_A=0$ axis at a larger value of the internuclear distance and the $R=R_e$ axis at a positive value of the net force. The vertical arrow from the AB curve at R_e strikes the AB^+ curve at a repulsive point so that a net force of repulsion occurs. If the area defined by A in the diagram is less than the area defined by B, then a stable

ion AB^+ exists and its equilibrium bond length is larger than R_e. The loss of an antibonding electron is depicted in Figure 11b . The force curve for the product of ionization intersects the $F_A=0$ axis at a smaller internuclear distance and the $R=R_e$ axis at a negative value of the Hellmann-Feynman force. The vertical arrow from the AB curve at R_e strikes the AB^+ curve at an attractive point so that a net force of attraction occurs. The stable ion AB^+ has an equilibrium internuclear distance smaller than R_e. The foregoing comments imply that the bonding or antibonding nature of an electron can be determined by the respective positive or negative sign of the $\tilde{f}_i$ value associated with that electron. An examination of equation (4) shows that the sign of f_i does not necessarily determine the sign of $\tilde{f}_i$. This is an important point and will be illustrated later in a discussion of the binding nature of the $1\pi_g$ orbital in O_2. The observed change in the bond length which occurs as the result of the ionization of an electron from the ith molecular orbital is not in general indicative of the role of that orbital in the binding of the neutral molecule.

Clinton and Hamilton[75] have attempted to calculate a force curve for the molecular ion $O_2^+(X^2\Pi_g)$ which results from the removal of an electron from $O_2(X^3\Sigma_g^-)$. From equation (1) such a force curve can be calculated as

$$F_O^{(O_2^+)}(R) = F_O^{(O_2)}(R) + \frac{Z_O \tilde{f}_i}{R^2} \qquad (10)$$

TABLE V

Ionization Energies

	Hartree-Fock Energy	"True" Ionization Energy	Rigid Orbital Ionization energy
$N_2\ ^1\Sigma_g^+$	-108.9956		
$N_2\ ^2\Sigma_g^+$	-108.4073	0.5883	0.6379
$N_2\ ^2\Pi_u$	-108.4196	0.5760	0.6285
$N_2\ ^2\Sigma_u^+$	-108.2631	0.7325	0.7687

$F_O^{(O_2)}(R)$ was calculated from spectroscopic data and $\tilde{f}_i$ was determined with the aid of a rigid orbital model. In such a model, the core orbitals are not allowed to adjust themselves to the changing field which occurs during the vertical ionization process. With reference to equation (4), this approximation allows f_j and f_j' to be equated to each other. For double occupation of the ith molecular orbital in the molecule AB, the relation

$$\tilde{f}_i = \frac{1}{2} f_i \tag{11}$$

is obtained. If ϕ_i is only singly occupied in the ground state of AB, then

$$\tilde{f}_i = f_i \tag{12}$$

Hurley[69] has recently used this rigid orbital approximation to derive formulae describing the energy difference between a molecular ion and its parent neutral molecule.

The simple idea of rigid orbitals unfortunately does not hold because of a significant reorganization of the charge density in orbitals other than the one involved in the ionization process.

Cade et al[58,59] have determined the molecular orbitals for certain of the ionized states of N_2 and O_2 by a complete reoptimization of the ground state wavefunctions. Table V shows a comparison of the ionization energies for various N_2^+ states obtained both in the rigid orbital approximation and as the result of a subtraction of the Hartree-Fock

Figure 12. Density difference contour maps describing the loss of an electron from various molecular orbitals in N_2 during vertical ionization processes. If a rigid orbital approximation is used then the density difference contour map describing the loss of a $3\sigma_g$ electron from N_2 is just equal to the density distribution of one electron in the $3\sigma_g$ orbital of N_2. The positive contours of this $3\sigma_g$ molecular orbital density indicate regions from which electron density is removed during a vertical ionization to the $X^2\Sigma_g^+$ state of N_2^+. If the density difference contour map describing the loss of a $3\sigma_g$ electron from N_2 involves a subtraction of the Hartree-Fock densities describing $N_2(X^1\Sigma_g^+)$ and $N_2^+(X^2\Sigma_g^+)$, then both positive and negative contours are present. The positive contours describe regions from which electron density is removed during the vertical ionization process. The negative contours describe regions which gain electron density as a result of the vertical ionization process. This figure permits a comparison of $\Delta\rho(\vec{r})_I$ calculated with the aid of the rigid orbital approximation and the accurate $\Delta\rho_I(\vec{r})$ calculated by subtracting the Hartree-Fock density of the ionized molecule from the Hartree-Fock density of the parent molecule.

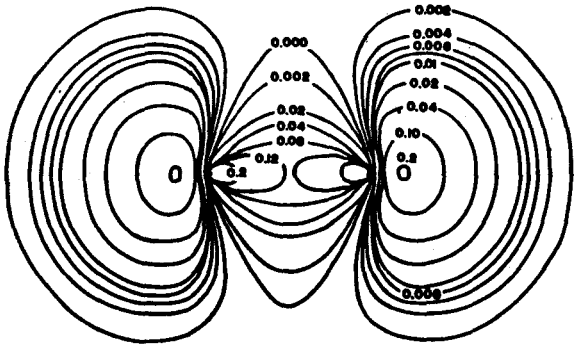

$N_2(X^1\Sigma_g^+)$ $3\sigma_g$

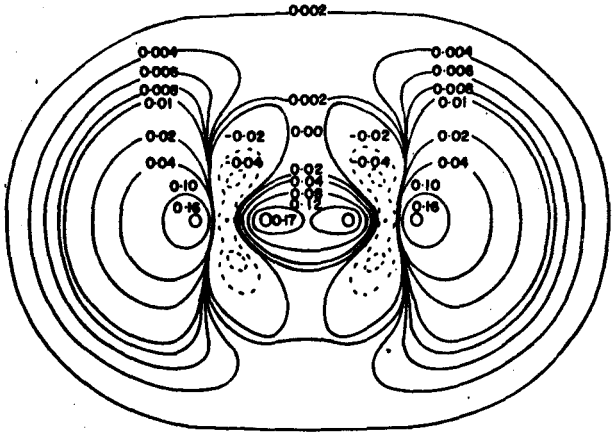

$N_2(X^1\Sigma_g^+) - N_2^+(X^2\Sigma_g^+)$

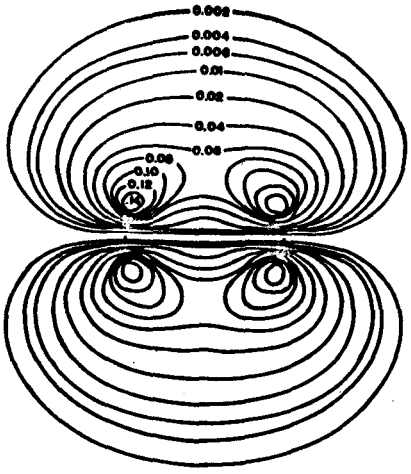

$N_2(X^1\Sigma_g^+)$ $1\pi_u$

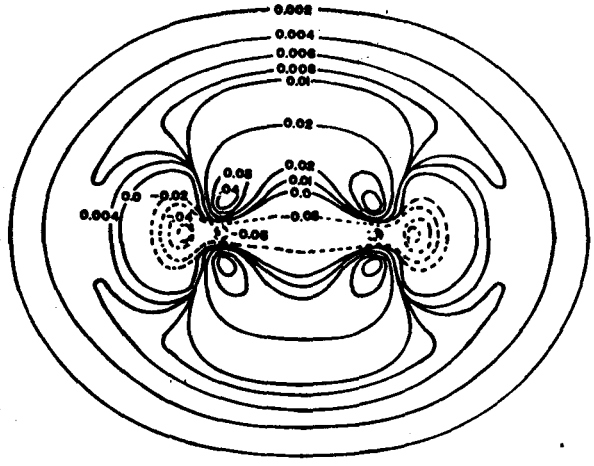

$N_2(X^1\Sigma_g^+) - N_2^+(A^2\Pi_u)$

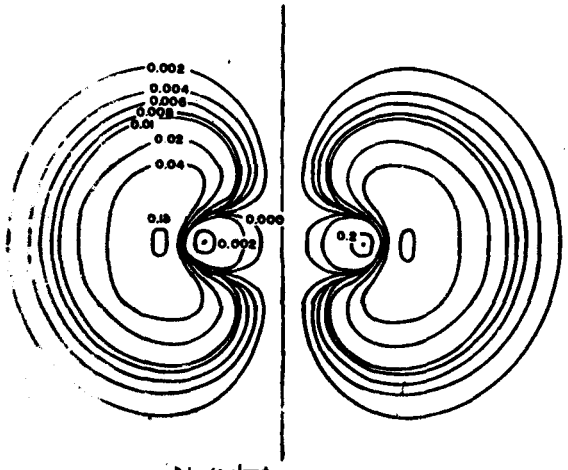

$N_2(X^1\Sigma_g^+)$ $2\sigma_u$

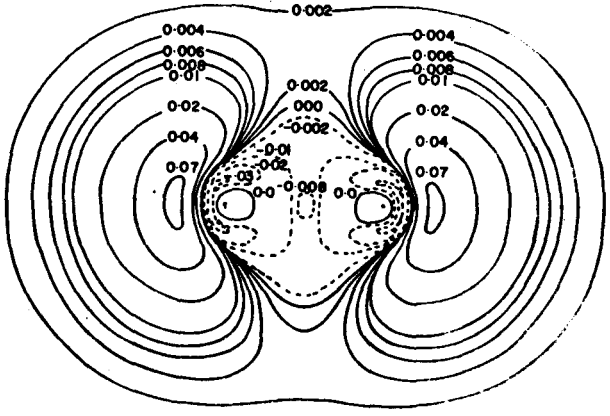

$N_2(X^1\Sigma_g^+) - N_2^+(B^2\Sigma_u^+)$

energies of the ionized state and the ground state. The ionization energies obtained from the second method are consistently smaller. The loss of an electron during the ionization process can be depicted by a density difference contour map in which the density function of the molecular ion is subtracted from that of the neutral species. Positive $\Delta\rho_I(\vec{r})$ contours indicate regions from which electron density has been removed during the vertical ionization. Similarly, negative $\Delta\rho$ contours indicate regions which become electron-rich as a result of the vertical ionization. An integration of $\Delta\rho_I(\vec{r})$ over all space yields the value one as the ionization process results in the loss of one electron. If the rigid orbital model is chosen, then

$$\Delta\rho_I(\vec{r}) = \phi_i^*(\vec{r})\phi_i(\vec{r})$$

where ϕ_i is the molecular orbital from which the electron is removed. Such a $\Delta\rho_I(\vec{r})$ function can be compared with that one obtained by subtracting the true Hartree-Fock densities of both molecular species. Figure 12 shows such a comparison for the $^2\Sigma_g^+$, $A^2\Pi_u$ and $B^2\Sigma_u^+$ states of N_2^+. The $\Delta\rho_I(\vec{r})$ map makes it evident that the bond length will change as a result of the ionization of a $2\sigma_u$ electron. Not only is density removed from the antibinding region in the formation of the molecular ion but also density is accumulated in the internuclear region. From this point of view, it is obvious that the equilibrium distance of $N_2^+(B^2\Sigma_u^+)$ will be shorter than

TABLE VI

Orbital Forces for States of N_2 and N_2^+ for a vertical Ionization[a] R=2.0132 a.u.

State	$f(1\sigma_g)$	$f(1\sigma_u)$	$f(2\sigma_g)$	$f(2\sigma_u)$	$f(1\pi_u)$[b]	$f(3\sigma_g)$	$\tilde{f}_i$	Rigid Orbitals	ΔR_e[c]
$X^1\Sigma_g^+$	1.154	1.080	2.628	-0.439	2.403	0.160	-	-	-
$X^2\Sigma_g^+$	1.086	1.046	2.569	-0.417	2.560	0.102	0.040	0.080	0.039
$A^2\Pi_u$	1.226	1.101	2.790	-0.388	2.003	0.106	0.148	0.600	0.148
$B^2\Sigma_u^+$	1.047	1.006	2.712	-0.039	2.502	0.070	-0.312	-0.220	-0.042

[a] Multiplication of the $\tilde{f}_i$ or f_i values by $Ze^2/R^2a_o^2 = 1.423 \times 10^{-2}$ will convert them to a force in dynes.

[b] These values are calculated for the total occupation number of the Π_u orbital.

[c] These values are the experimentally observed changes in R_e.

MILLS MEMORIAL LIBRARY
McMASTER UNIVERSITY

that of $N_2(X^1\Sigma_g^+)$. Such definite conclusions cannot be drawn from the $\Delta\rho_I(\vec{r})$ maps describing the $X^2\Sigma_g^+$ and $A^2\Pi_u$ states of N_2^+. The ionization of an electron from the $1\pi_u$ orbital of N_2 results in a loss of electron density from both the binding and the antibinding regions. In the ion $N_2^+(A^2\Pi_u)$, there is an accumulation of charge along the internuclear axis both in the binding region and directly behind the nuclei. Such an effect could be the result of a significant reorganization of the charge density in a σ molecular orbital. The ionization of an electron from the $3\sigma_g$ orbital of N_2 is pictured in the $\Delta\rho_I(\vec{r})$ map as a large diffuse group of positive contours in the antibinding regions and a smaller more concentrated group of positive contours in the binding region. The sets of negative contours which form toroidal rings about each nucleus seem to suggest a reorganization of charge density in the π molecular orbitals as a result of the ionization.

Force calculations involving N_2 and the three previously discussed states of N_2^+ should serve to corroborate the qualitative descriptions which the $\Delta\rho_I(\vec{r})$ maps present. Further such calculations permit a determination of the various $\tilde{f}_i$ values and thus a definite physical picture of the bond length changes occurring because of ionization. The orbital forces for the $X^2\Sigma_g^+$, $A^2\Pi_u$, and $B^2\Sigma_u^+$ states of N_2^+ and for the $X^1\Sigma_g^+$ state of N_2 are listed in Table VI.

All are calculated for the internuclear distance corresponding to the Hartree-Fock minimum for the ground state of N_2, a value of 2.0132 a.u. Cade, Sales, and Wahl[58] have previously shown that the H artree-Fock results for the ions do correctly reflect the changes in bond length predicted by the terms bonding and antibonding.

The $A^2\Pi_u$ state of N_2^+ results from the loss of a π_u electron from N_2. The rigid orbital model demands that $\tilde{f}_i$ be equal to 0.6 - a value one-quarter that of $f(1\pi_u)$ in N_2. In reality $\tilde{f}_i = 0.148$. The value of $f(1\pi_u)$ is calculated to be 2.0 whereas the rigid orbital model predicts a value of 1.8 for $f(1\pi_u)$ in this state of N_2^+. The ionization also produces a large increase in the $f(2\sigma_g)$ value. Thus the binding of the $2\sigma_g$ density and of the remaining $1\pi_u$ density increases on ionization of a $1\pi_u$ electron. The $1\pi_u$ molecular orbital in N_2 is bonding by definition. Moreover it can be termed binding because its f_i value is greater than one. More important than the value of $f(1\pi_u)$ is the value of $\tilde{f}_i$. It is positive in this case. The vertical ionization thus results in a net descreening of the nuclei, a repulsive force acting on the nuclei and a net increase in the internuclear distance. This is the situation pictured in Figure 11a.

The $B^2\Sigma_u^+$ state of N_2^+ results from the ionization of an electron from the $2\sigma_u$ orbital of N_2. This $2\sigma_u$ orbital is

antibonding by nature, and, in addition, it is strongly antibinding. It exerts a force which tends to draw the nuclei apart. The removal of an electron from the $2\sigma_u$ orbital causes a decrease in the internuclear distance of the ionized product as pictured in Figure 11b. This can be seen as a result of the decreased electronic force tending to separate the nuclei. The rigid orbital model suggests that the ionization process should increase $f(2\sigma_u)$ from -0.439 to -0.220. Table VI indicates that $f(2\sigma_u)$ has been increased almost to zero and that $\tilde{f}_i$ has a value of -0.312 rather than the rigid orbital value of -0.220. The net attractive force acting on the nitrogen nuclei in the vertical ionization state is accentuated and the reason for the decrease in bond length is evident. All the remaining orbitals undergo changes in their f_i values approximately one-quarter as large as the change in $f(2\sigma_u)$ the binding ability of the $1\sigma_g$, $1\sigma_u$ and $3\sigma_g$ orbitals being decreased and that of the $2\sigma_g$ and $1\pi_u$ orbitals being increased.

The $X^2\Sigma_g^+$ state of N_2^+ arises from the ionization of an electron from the $3\sigma_g$ orbital. This orbital is bonding by definition; moreover, it is antibinding as it no longer shields one unit of nuclear charge. The $3\sigma_g$ density does exert an attractive force on the nuclei, and, in the rigid orbital approximation, the removal of such density should lead to a descreening of the nuclei and a

TABLE VII

Orbital Forces for the Ground States of O_2, O_2^+ and O_2^-.

State	$f(1\sigma_g)$	$f(1\sigma_u)$	$f(2\sigma_g)$	$f(2\sigma_u)$	$f(1\pi_u)$	$f(3\sigma_g)$	$f(1\pi_g)$	R_e
O_2 $X^3\Sigma_g^-$	1.232	1.138	2.934	-0.518	2.604	0.174	0.426	2.282
O_2^+ $X^2\Pi_g$	1.244	1.138	3.056	-0.492	2.783	0.082	0.215	2.122
O_2^- $X^2\Pi_g$	1.220	1.136	2.810	-0.514	2.410	0.277	0.557	2.400

resultant force of repulsion. The calculations in Table VI corroborate this argument. The rigid orbital model predicts a value of 0.080 for $f(3\sigma_g)$ in N_2^+ while the calculations show a value of 0.102 for $f(3\sigma_g)$ in this same molecule. The calculated value of $\tilde{f}_i$ is 0.040 and, as shown in Figure 11a there is a net force of repulsion tending to increase the bond length in N_2^+. There is a significant increase in $f(1\pi_u)$ for this ionized state of N_2. In fact this increase is equal to $f(3\sigma_g)$ in N_2. The remaining orbitals individually undergo much smaller changes, but the net change is a decrease in their binding large enough in magnitude to counteract the increase in the binding of the $1\pi_u$ density.

From the preceding results the absolute sign of the f_i value would appear to determine the subsequent increase or decrease in the internuclear distance that follows ionization. This is not the case as can be seen from an examination of the f_i values for the $^2\Pi_g$ state of O_2^+ listed in Table VII. The forces listed in Table VII are calculated for the experimental equilibrium value of the internuclear distance. Thus the sum of the f_i values is equal to Z in each case and the figures for O_2^+ refer to an adiabatic ionization as depicted by the horizontal arrow in Figure 11b. The data for O_2^+ illustrate that the removal of a $1\pi_g$ electron results in a decrease in the value of R_e even though the $1\pi_g$ density exerts an attractive

force on the nuclei in the neutral molecule. The figures in Table VII show that the removal of an electron from the $1\pi_g$ molecular orbital reduces $f(1\pi_g)$ by a factor of one-half. However there are significant increases in the $f(1\pi_u)$ and $f(2\sigma_g)$ values during the ionization process, and it is evident that in a vertical excitation, the increase in the force exerted by these orbitals more than compensates for the decrease in the force exerted by the $1\pi_g$ density. Although $f(1\pi_g)$ is positive, the vertical ionization of an electron from the $1\pi_g$ molecular orbital yields a negative $\tilde{f}_i$ value. Thus the removal of an electron from this antibonding molecular orbital results in a net decrease of charge in the antibinding region and a decrease in the bond length of $O_2^+ \; X^2\Pi_g$. The term antibinding fulfills the same definition as the term antibonding in this case even though the orbital density exerts an attractive force on the nuclei. The observed change in R_e attendant upon the removal of an electron from a given orbital does not in general provide an accurate isolated measure of the role the orbital plays in the binding of the neutral molecule.

Also included in Table VII are the orbital forces for the $X^2\Pi_g$ state of the O_2^- ion. This ion is obtained by the addition of an electron to the $1\pi_g$ orbital of O_2. As is expected the addition of an electron to an antibonding orbital leads to an increased bond length. From another

perspective, the increase of $f(1\pi_g)$ should lead to a greater attraction of the nuclei and a resultant decrease in the bond length of O_2^-. However, although $f(1\pi_g)$ and $f(3\sigma_g)$ are increased in magnitude, there are significant decreases in $f(2\sigma_g)$ and $f(1\pi_u)$. These latter changes counteract the former effect. The overall result of adding an electron to the $1\pi_g$ orbital is an addition of charge to the anti-binding region. This addition of charge to regions behind the nuclei gives rise to a net force tending to pull the nuclei apart. The result is a larger internuclear distance in O_2^-.

CHAPTER V

A COMPARISON OF COVALENT AND IONIC BINDING

The development of the quantum mechanical formulation of ionic character had its basis in valence bond theory[76]. The amount of ionic character depends on the contribution of the structure $\Psi_{A^+B^-}$ to the total wave function describing the molecule AB.

In a series of papers, Shull[77] has devoted himself to the problem of ionic character. In particular, he points out that an understanding of the concept of the ionic or covalent bond cannot be gained until the chemical bond itself is understood. He criticizes the formulation of the concept of ionic character in terms of valence bond theory and insists that any theoretical foundation for this concept should be independent of a particular model. Further, he points out that the structures $\Psi_{A:B}$ and $\Psi_{A^+B^-}$ in the wavefunction

$$\Psi = C_A\Psi_{A:B} + C_B\Psi_{A^+B^-} \qquad (1)$$

are not independent of each other; that is, they are not orthogonal[78,79]. If

$$\langle\Psi_{A:B}|\Psi_{A^+B^-}\rangle \neq 0 \qquad (2)$$

then the ionic character of the bond between atoms A and B in the molecule AB cannot be quantitatively described by the fractional number C_B^2.

Shull[80,81] has attempted to find answers to the problems that he poses. He uses as his starting point a well-defined approximation to the hydrogen molecule and separates the wavefunction derived in this approximation into orthogonal independent parts Ψ_I and Ψ_A which, respectively have the optimum characteristics associated with the names ionic" and "atomic". With these orthogonal functions, he can rightly calculate and discuss ionic and atomic character. Further, he finds a correlation between his overlap distribution $\Psi_I\Psi_A$ and the intuitive concept of covalence.

Shull's discussion is still couched in terms of ionic structure contributions to a total wavefunction. However, if the concept of the ionic bond and along with it, the concept of ionic character are to have any general validity, they should be independent of a particular type of wavefunction. The form of any approximate Ψ is not unique. In valence bond theory the wavefunction is given as equation (1) of this section. In molecular orbital theory, the total wavefunction can be approximated by a linear combination

$$\Psi = \sum_i C_i \Psi_i \qquad (3)$$

The Ψ_i describe various electronic configurations. If both approximations are carried to their respective limits, they yield the same energies. However an ionic character can be easily derived from the valence bond wavefunction but not from the molecular orbital wavefunction. It is desirable to avoid definition of ionic character in terms of wavefunctions.

The original purpose in defining ionic and covalent character was to obtain some crude estimate of how the valence electrons are distributed or shared in a molecule. This can now be done by means of the calculated molecular charge density distribution. Such a charge distribution is unique; that is, it is an observable of the system. It is one of the principle aims of this thesis to provide definitions of the concepts of the ionic and covalent bond in terms of their respective charge distributions. Indeed the molecule LiF is analyzed in terms of its electron density distribution and the force which this distribution exerts on the nuclei. This analysis is then compared with a similar one for the homonuclear molecule N_2.

LiF is a molecule whose properties closely approximate those of the ionic model. It possesses a diple moment of 6.284 D[83]. This value is 84% of the ideal dipole moment obtained for e separation of equal and opposite charges in LiF at the observed internuclear distance of 2.956 a.u.[83].

Figure 13. The total molecular charge distribution of LiF

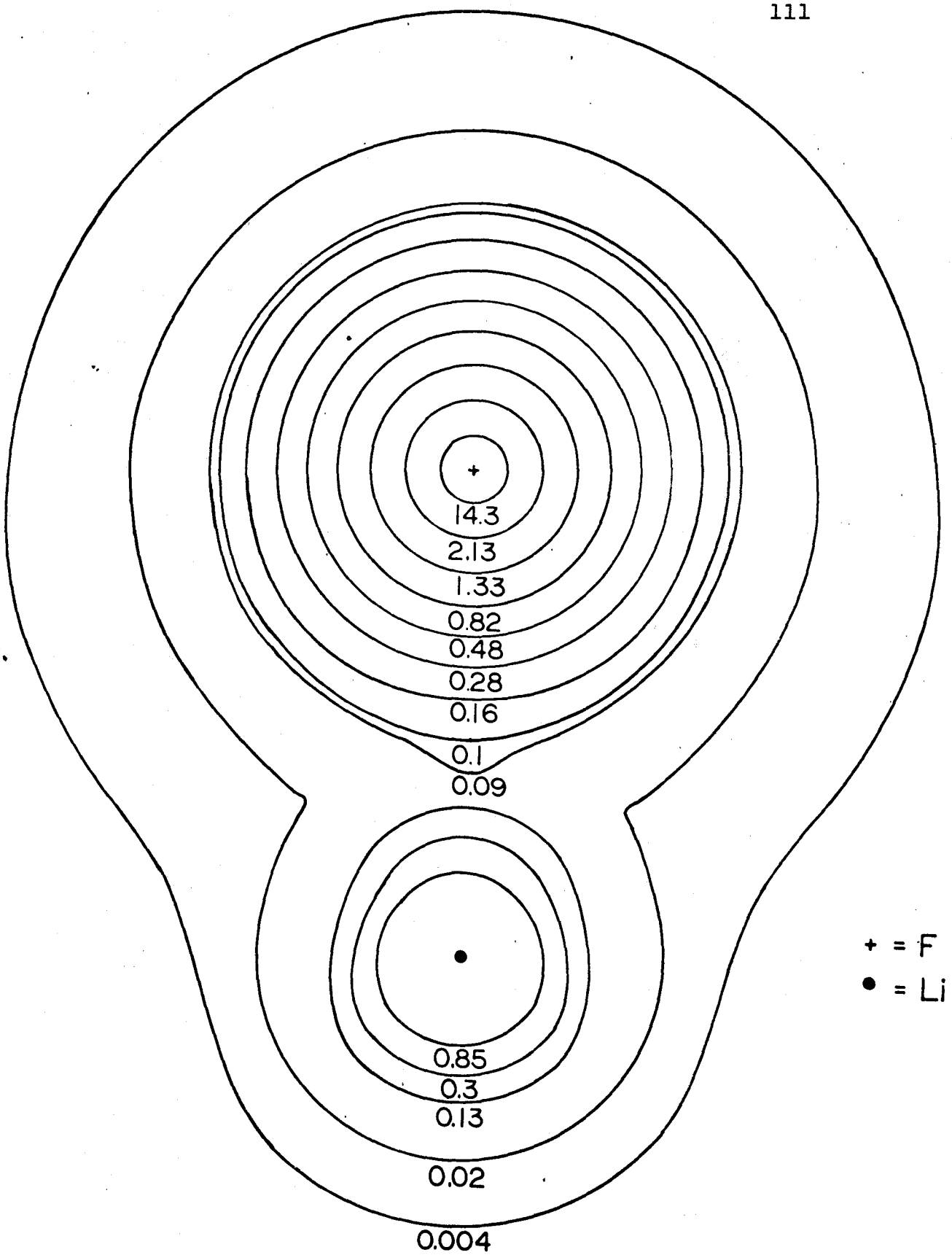
14.3
2.13
1.33
0.82
0.48
0.28
0.16
0.1
0.09
0.85
0.3
0.13
0.02
0.004
+ = F
• = Li

In Pauling's[76] view, such a percentage is one way of measuring the ionic character of a bond. McLean[82] has obtained a wavefunction for LiF with an energy of -106.9885 a.u. at the calculated internuclear distance of 2.8877 a.u. He estimates that this energy is within 0.005 of the Hartree-Fock limit and calculates a dipole moment of 6.30 D.

Figure 13 shows the total molecular charge contour map derived from McLean's[82] wavefunction for LiF. This contour map has the appearance of two nonoverlapping spheres of unequal charge density. It is interesting to compare this charge distribution with that shown for C_2 in Figure 3. These two molecules are isoelectronic. In C_2, the first contour which encircles the entire molecule is the 0.26 contour. However in LiF, the first contour which encircles the entire molecule is the 0.0^8 contour*. Also in the F_2 molecule the first contour localized about the F nucleus is the 0.30 contour while in LiF the first contour localized about the F nucleus is the 0.0^9 contour. Similarly in the Li_2 molecule, the first contour localized about the Li nucleus is the 0.013 contour while in LiF the first contour localized about the Li nucleus is the 0.0^9 contour. Ransil and Sinai[45] have discussed charge density contours localized about given nuclei as a function of the

*This has been confirmed although the 0.08 contour is not shown in Figure 13.

Figure 14. A contrast of the density difference distributions for ionic and covalent binding. The total amount of charge within the zero contour encompassing the F is $9.81e^-$. A total of $0.85e^-$ and $0.51e^-$ migrate to the regions of charge increase in LiF and N_2 respectively.

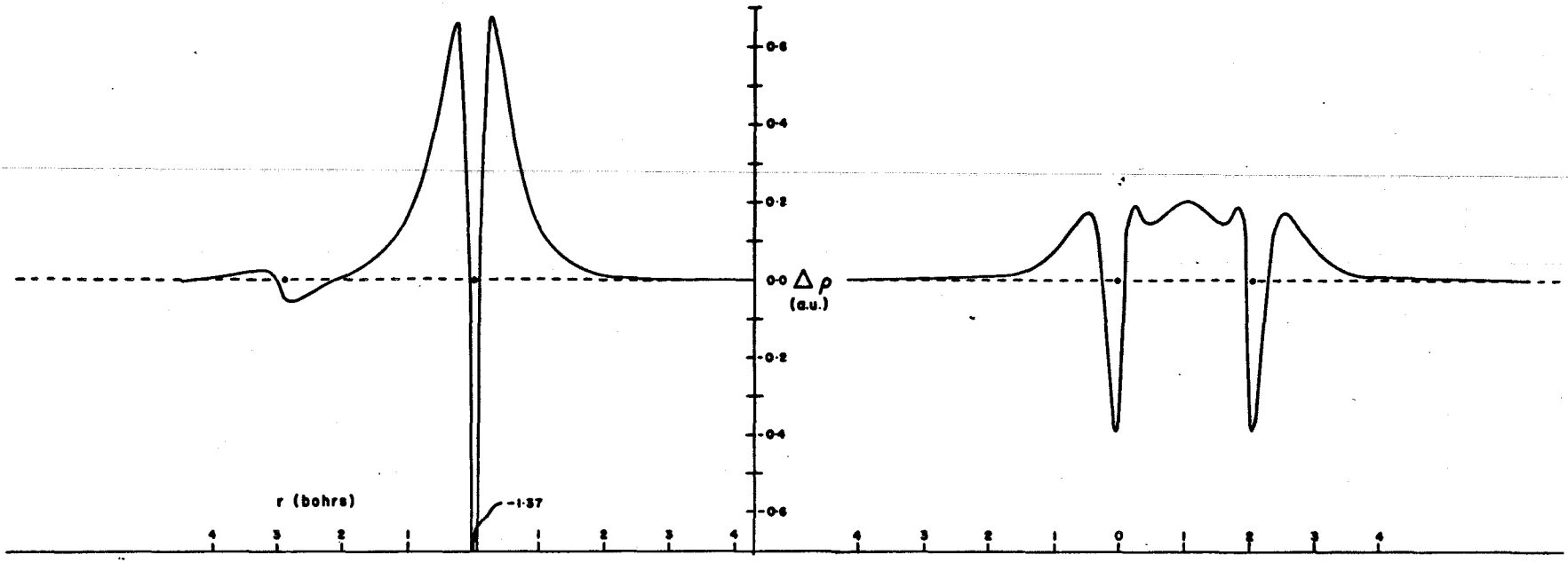
0·6
0·4
0·2
0·0 Δρ
(a.u.)
-0·2
-0·4
-0·6
r (bohrs)
-1·37
4
3
2
1
0
1
2
3
4

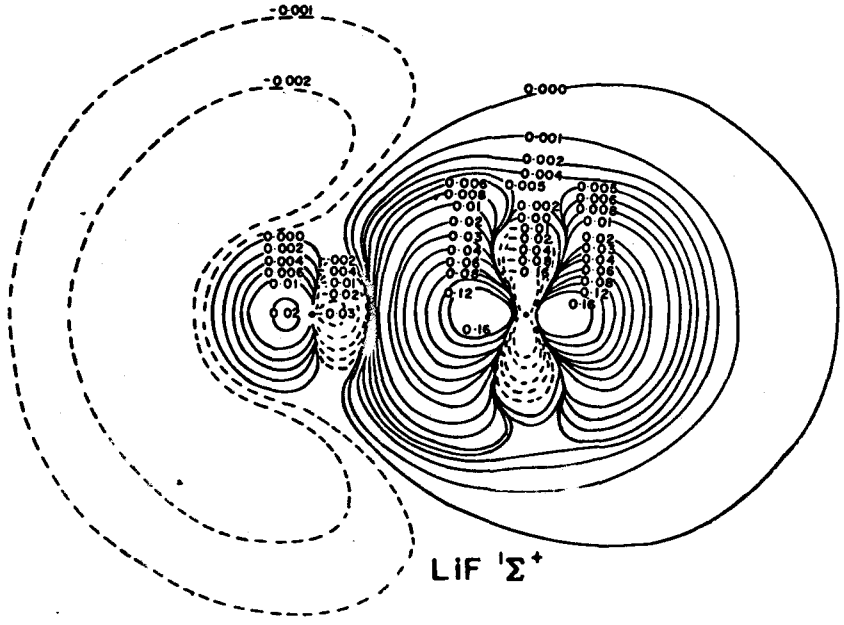
LiF ¹Σ⁺

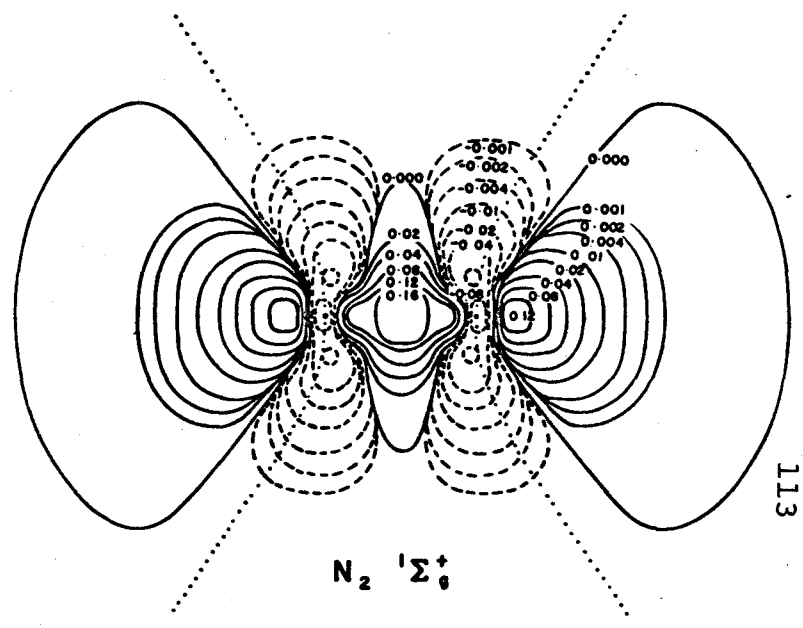
N₂ ¹Σ⁺g

electron populations within these contours. They show that within the 1.0 contour surrounding F in LiF, there is a total charge of 3.5 electrons while within the same contour in F_2 there is a total charge of 3.0 electrons. Similarly within the 0.1 contour of Li in Li_2 there is a total charge of 1.6 electrons while within the 0.1 contour of Li in LiF there is a total charge of 1.4 electrons. It is evident that a great portion of the total charge in LiF is localized in spherical regions about the nuclei while in C_2 a large fraction of the total charge is delocalized about the entire molecule. There is more charge localized about the F nucleus in LiF than there is localized about the F nucleus in F_2. Similarly there is less charge localized about the Li nucleus in LiF than there is localized about the Li nucleus in Li_2.

Figure 14 contrasts the electron density difference maps for LiF and N_2. Above each contour map is a profile of $\Delta\rho(\vec{r})$ in the plane of the nuclei. LiF contains two regions where charge is built up in the molecule relative to the separated atoms. One region is localized about the fluorine nucleus while the other region is localized behind the lithium nucleus. N_2 contains three regions where charge is built up in the molecule relative to the separated atoms. Two of these areas of charge buildup are localized in the antibinding regions behind the N nuclei. The third area of charge buildup is shared between the nuclei in the binding

region. The profile of the LiF $\Delta\rho(\vec{r})$ function indicates contours of a high value about the F nucleus. These positive contours stretch three-quarters of the way to the Li nucleus. There is a much greater amount of total charge localized about F than there is localized behind Li. On the other hand, the profile of the N_2 $\Delta\rho(\vec{r})$ function indicates two equal amounts of charge built up in the anti-binding regions behind the nuclei and a relatively larger amount of charge concentrated in the binding region between the nuclei.

The $\Delta\rho(\vec{r})$ map has been interpreted as a bond map which describes the reorganization of charge that must occur during the formation of a stable molecule in order to balance the force of repulsion owing to the nuclei. If such an interpretation is applied here, then it is clear that LiF achieves electrostatic equilibrium through a localized increase of charge about the F nucleus. N_2 achieves electrostatic equilibrium by means of a shared increase of charge in the binding region between the N nuclei.

In previous discussions concerning the electronic force acting on the nucleus in a diatomic molecule, the total density has been partitioned into atomic and overlap distributions. As a result of this breakdown of the total density, the electronic force acting on nucleus A in the molecule AB is composed of atomic, overlap, and screening

contributions. Such a partitioning of the total density, although arbitrary, follows naturally from the form of the molecular orbitals used. It is now desirable to obtain a different division of the total density, a division based upon an analysis of the $\Delta\rho(\vec{r})$ contour map. In the case of LiF it would be of interest to know the electronic force acting on the Li nucleus because of the total charge density within the 0.0 contour describing the localized charge buildup about the F nucleus. An idea of this partitioning of charge can be gained by superimposing the zero contours of the $\Delta\rho$ map on the total molecular charge density contour map. The region of the total density map within the zero contour surrounding F is the region of interest. Such total electronic density screens F nuclear charge from Li and is therefore termed an atomic density surrounding F. The remaining molecular density is termed an atomic density surrounding Li. In the case of N_2 it would be of interest to know the electronic force acting on the N nucleus because of the positive density difference contours within the 0.0 contour describing the shared charge buildup in the binding region between the N nuclei. Such $\Delta\rho(\vec{r})$ contours are shared by both nuclei and the $\Delta\rho(\vec{r})$ density distribution is termed a shared density distribution. The remaining total density is atomic in nature and is divided between the two nitrogen nuclei.

Figure 15. The overlap density distributions in LiF and N_2

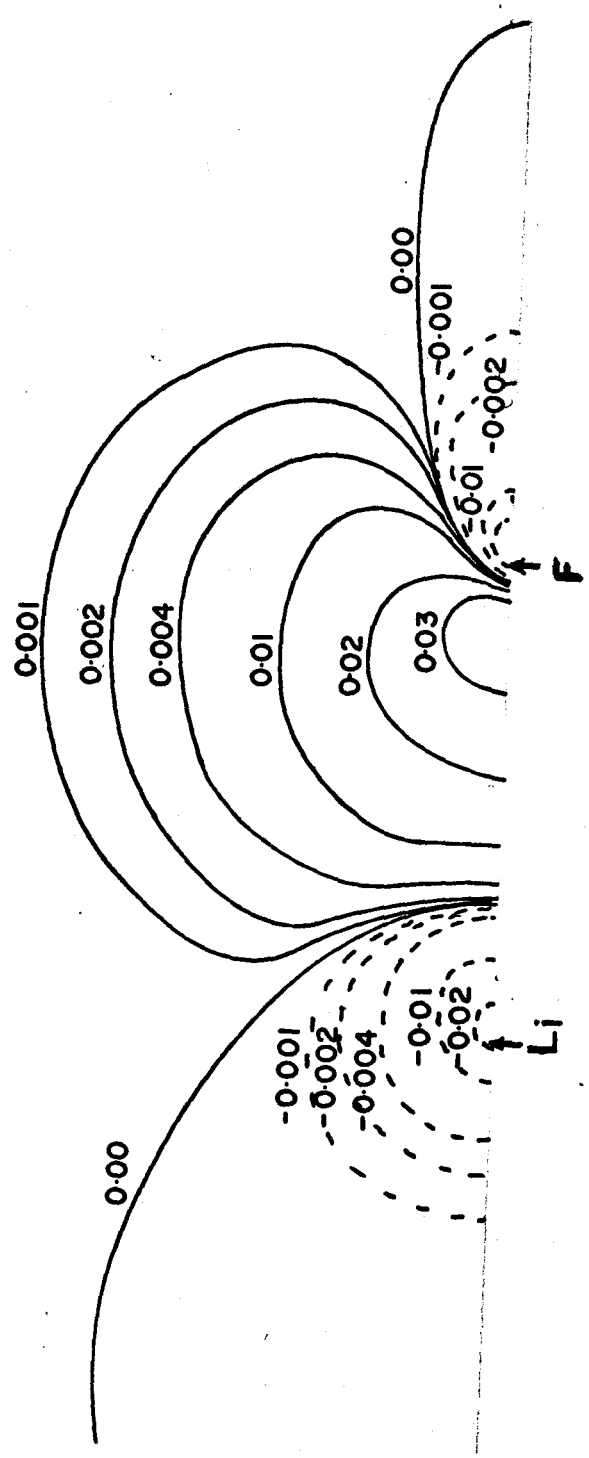
0·00
0·001
0·002
0·004
0·01
0·02
0·03
-0·001
-0·002
-0·01
F
-0·001
-0·002
-0·004
-0·01
-0·02
Li

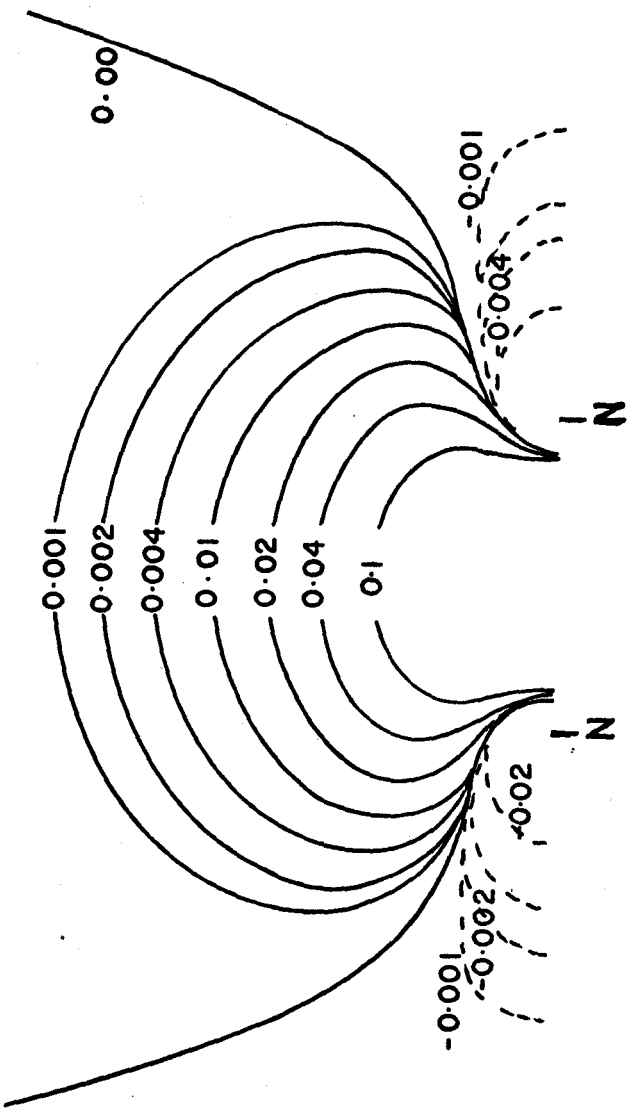
0·00
0·001
0·002
0·004
0·01
0·02
0·04
0·1
-0·001
-0·004
N
-0·001
-0·002
-0·02
N

Such a partitioning of the total density is theoretically possible but in practice, a suitable method for calculating the electronic force resulting from such regions of density has not been developed. Thus it is necessary to make an identification between the above defined atomic and shared densities and the molecular orbital atomic and overlap densities. Figure 15 shows the overlap density distributions derived from the Hartree-Fock wavefunctions for LiF and N_2 respectively. The overlap density of the N_2 molecule places a symmetrical increase of charge in the binding region. Further charge density is also removed from the antibinding regions. This overlap density is concentrated about the internuclear axis and is shared between the two nuclei. It is here identified with the shared density distribution which was previously defined in terms of the $\Delta\rho(\vec{r})$ map. The overlap density of the LiF molecule places an asymmetric increase of charge in the binding region. Charge is removed from a symmetric region surrounding the Li nucleus while charge is removed from the region directly behind the F nucleus. The positive contours of this overlap distribution lie within the 0.0 contour describing the localized charge buildup surrounding the F nucleus in the LiF $\Delta\rho(\vec{r})$ contour map. Thus in reality, this overlap density screens F nuclear charge from the lithium nucleus. It is identified as part of the atomic

density defined previously as the total density within the 8.0 contour of the localized charge increase surrounding the F nucleus in the LiF $\Delta\rho(\vec{r})$ contour map.

With this above partitioning of the total density distribution, a comparison of the force acting on the nucleus in both an ionic and a covalent molecule is discussed. Consider a classical model for the ionic bond which involves the transfer of one electronic charge from the electropositive atom A to the electronegative atom B. This model thus consists of two nuclei A and B possessing respectively nuclear charges Z_A and Z_B. Nucleus A is surrounded by a spherical distribution of Z_A-1 electrons while nucleus B is surrounded by a spherical distribution of Z_B+1 electrons. The result is two spherical nonoverlapping charge distributions separated at the observed internuclear distance. The force acting on nucleus A is given as

$$F_A = \frac{Z_A}{R^2}\,[Z_B - Z_B - 1] = -\frac{Z_A}{R^2} \qquad (4)$$

is the internuclear distance. Similarly the force acting on nucleus B is given as

$$F_B = \frac{Z_B}{R^2}\,[Z_A - Z_A + 1] = \frac{Z_B}{R^2} \qquad (5)$$

There is an attractive force acting on nucleus A while there is a repulsive force acting on nucleus B. The classical model predicts instability. The important feature

TABLE VIII

Force Contributions in LiF

	Contribution from localized charge[a]	
	on F	on Li
Force on F	1.05	2.04
Ideal ionic binding	1.00	2.00 ($=Z_{Li}-1$)
Force on Li	9.86	-0.71
Ideal ionic binding	10.00 ($=Z_F+1$)	-1.00

[a] The charge density localized on F exerts an atomic force on F and a screening force on Li. Similarly the charge density localized on Li exerts an atomic force on Li and a screening force on F.

of the model is the transfer of unit charge from A to B. It is possible to maintain this feature in the model and to obtain electrostatic equilibrium if the charge distributions are polarized in directions opposite to that of charge transfer. A polarization of the charge density surrounding nucleus A into the antibinding region counteracts the force of attraction experienced by this nucleus because of the charge density surrounding nucleus B. Similarly a polarization of the charge density surrounding nucleus B into the binding region counteracts the repulsive force experienced by this nucleus owing to the unscreened nuclear charge centred on A.

If LiF approaches this classical model, then the lithium nucleus should experience a repulsive force owing to nine F nuclear charges and an attractive force owing to $Z_F+1=10$ effective electronic charges centred on the F nucleus. The b ack polarization of the electronic density surrounding Li is represented by an effective electronic charge of -1 unit centred at the fluorine nucleus. Similarly the fluorine nucleus should experience a repulsive force owing to three Li nuclear charges and an attractive force owing to $Z_{Li}-1=2$ effective electronic charges centred on the lithium nucleus. The polarization of the fluorine density into the binding region is represented by 1 unit of effective electronic charge centred at the lithium nucleus. Table VIII shows how closely the electron density distri-

bution derived from McLean's wavefunction approaches this limit. The atomic charge density localized about fluorine exerts a force on the lithium nucleus which is equivalent to 9.86 effective electronic charges centred on the F nucleus. This effective charge is obtained as previously suggested by combining the overlap and screening force populations acting on the Li nucleus. This is equivalent to identifying the overlap and screening force populations with an atomic density about F. This atomic density has previously been defined as the total molecular charge lying within the zero contour of the localized charge buildup surrounding the F nucleus in the LiF $\Delta\rho(\vec{r})$ map. Indeed the values in this table show that the Li nucleus has been descreened by one unit of effective electronic charge. The transfer of charge is almost complete as the Li nucleus now experiences an attractive force owing to 9.86 effective electronic charges centred on the F nucleus. The lithium core density is polarized into the antibinding region. The force acting on the lithium nucleus owing to this remaining electronic density surrounding Li is represented by an effective charge of -0.71 units compared to the ideal value of -1.0 units. The fluorine atomic density is polarized into the binding region. The force acting on the fluorine nucleus as a result of this polarization is represented by an effective charge of 1.05 units compared to the ideal value of 1.0 units.

TABLE IX

THE TOTAL ATOMIC, OVERLAP AND SCREENING CONTRIBUTIONS TO THE FORCES

	Atomic Contribution $\Sigma_i f_i^{(AA)}$	Overlap Contribution $\Sigma_i f_i^{(AB)}$	Screening Contribution $\Sigma_i f_i^{(BB)}$	Z minus Screening $Z-\Sigma_i f_i^{(BB)}$	D_e (ev)
Li_2	-0.563	0.927	2.591	0.409	1.106
B_2	-0.644	1.708	3.887	1.113	2.884
C_2	-0.735	2.198	4.523	1.477	6.251
N_2	-1.943	3.853	5.136	1.864	9.909
O_2	-2.284	3.486	6.788	1.212	5.181
F_2	-1.949	2.505	8.381	0.619	1.647

Table IX shows the partitioning of the total electronic force into its atomic overlap and screening populations for the molecules Li_2 B_2, C_2, N_2, O_2 and F_2 . As previously discussed the overlap force population is to be identified with the shared density defined by the positive $\Delta\rho(\vec{r})$ contours in the binding region of each molecule. In every case the nuclei are descreened. The sum

$$\sum_i f_i^{(BB)} \tag{6}$$

is always less than the nuclear charge. The expression

$$Z - \sum_i f_i^{(BB)} \tag{7}$$

provides a measure of this nuclear descreening and is listed in column four of this table. For example, in the Li_2 molecule there is an effective charge of +0.409 units situated on the Li nucleus because the atomic density surrounding this Li nucleus no longer shields an equivalent number of nuclear charges. As indicated by the various overlap populati ons, the shared density found in the binding region is indeed responsible for molecular stability. In fact so much charge is transferred to the binding region, that the remaining atomic density must be polarized into the antibinding region in order to achieve electrostatic equilibrium. This polarized atomic density gives rise to the positive $\Delta\rho(\vec{r})$ contours in the antibinding regions of

Figure 16. The total density difference contour map for HF.

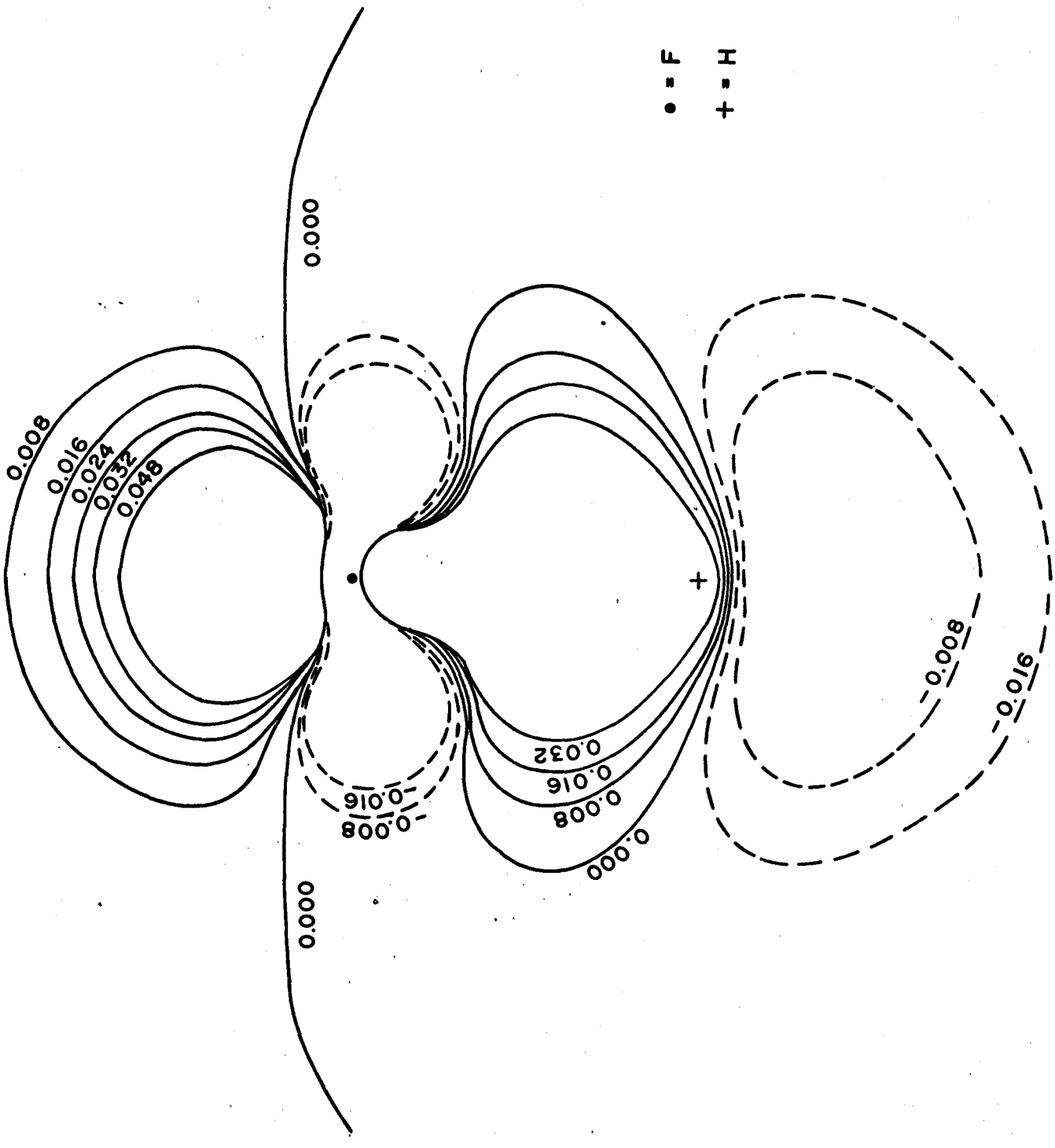
I
F
0.000
0.008
0.016
0.024
0.032
0.048
0.008
0.016
0.032
0.016
0.008
0.000
0.008
0.016
0.000

Figure 17. The total density difference contour map for LiH.

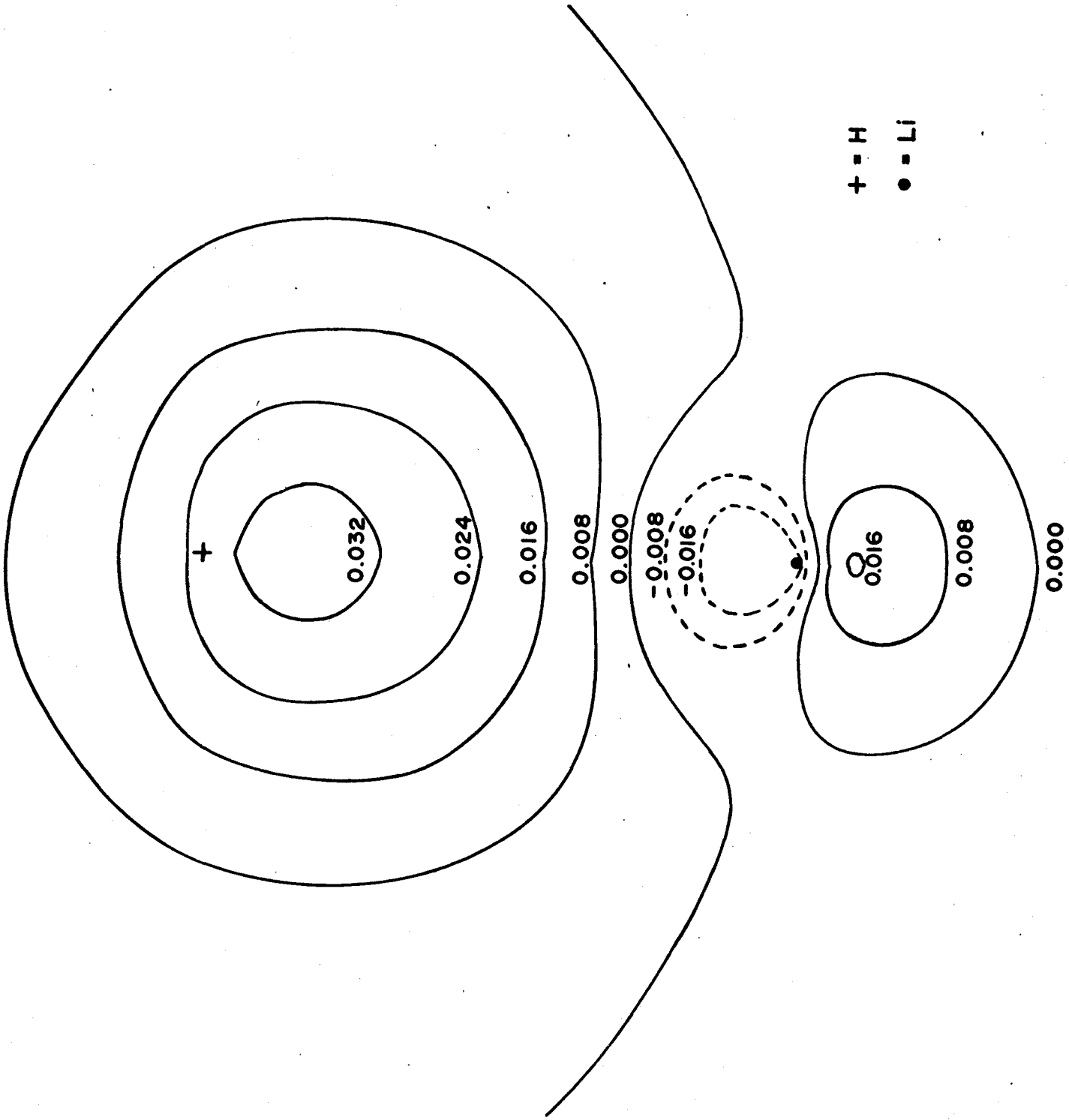
+ = H
● = Li
0.032
0.024
0.016
0.008
0.000
-0.008
-0.016
0.016
0.008
0.000

each molecule.

Thus in ionic binding both nuclei are bound by the charge localized about one of them while in covalent binding, the nuclei are bound by a density increase which is shared equally between them.

The analysis presented in the preceding pages for LiF can be extended to include other heteronuclear diatomic molecules. Figures 16 and 17 show respectively the $\Delta\rho(\vec{r})$ contour maps for HF and LiH. The wavefunction for HF is from Nesbet[84] and the wavefunction for LiH is from Kahalas and Nesbet[85]. These $\Delta\rho(\vec{r})$ maps provide an interesting comparison between two heteronuclear diatomic molecules, one in which the nuclei are bound by a localized increase of charge density and one in which the nuclei are bound by a shared increase of charge density. In HF the $\Delta\rho(\vec{r})$ contour map shows two regions of charge buildup. One is localized in the antibinding region behind F while the other is shared between the nuclei in the binding region. The zero contour which describes this charge increase in the binding region encloses the H nucleus. This is to be contrasted with LiF where the Li nucleus is excluded from the charge increase that binds the nuclei. Similarly the $\Delta\rho(\vec{r})$ map for LiH shows two regions of charge increase. But these regions are localized about the H nucleus and in the antibinding region behind Li.

If the zero contours of the $\Delta\rho(\vec{r})$ map for LiH are superimposed upon the total density distribution of this molecule, they suggest a partitioning of this total charge density. That density contained within the zero contour which is localized about the H nucleus defines an atomic density surrounding H. The remaining density is termed an atomic density surrounding Li. In HF, where the nuclei are bound by a shared density, the positive $\Delta\rho(\vec{r})$ contours in the binding region provide a measure of this shared density.

As noted before, there is no practical way of calculating the force acting on the nucleus owing to such regions of density. However, the atomic, overlap, and screening force contributions in these molecules have been calculated. They are listed in the appendix. In LiH, the overlap and screening force acting on the Li nucleus are combined. Their sum is identified with the previously defined atomic density surrounding H. Thus at equilibrium, the Li nucleus experiences a repulsive force owing to one H nuclear charge. However the atomic density localized about H exerts a force on Li which is equivalent to 1.638 units of effective charge centred on the nucleus. The atomic density localized about Li exerts a force on Li which is equivalent to placing -0.335 units of effective charge on the H nucleus. This result indicates that the atomic density surrounding Li is polarized away from H into the antibinding

region. Similarly this atomic density localized about Li exerts a force on the H nucleus which is equivalent to placing 2.210 units of effective charge on the Li nucleus. This attractive force is not enough to balance the repulsive force owing to the Li nuclear charge. The H atomic density is polarized into the binding region. It exerts an attractive force on the H nucleus which is equivalent to placing 0.688 units of effective charge on the Li nucleus. The conclusions are evident. The Li nucleus is descreened and its remaining density is polarized into the antibinding region. The nuclei are bound by a localized increase in charge defined by the zero contour surrounding the H nucleus in the LiH $\Delta\rho(\vec{r})$ contour map . LiH is an example of ionic binding.

For HF, the overlap force is identified with the shared increase in density defined by the positive $\Delta\rho(\vec{r})$ contours found between the nuclei in the binding region. The force analysis shows that this shared density binds the nuclei. In fact so much of the F atomic density is transferred to the overlap region, that its remaining density is strongly polarized into the antibinding region. If the overlap and screening forces acting on the H nucleus are combined, they exert an attractive force which is equivalent to placing 8.776 units of effective charge on the F nucleus. Even this effective charge does not succeed in balancing

the repulsive force owing to nine F nuclear charges. The F nucleus is still descreened. The hydrogen nucleus is descreened as its density exerts an attractive force which is equivalent to placing 0.390 effective charges on the H nucleus. This effective charge is not sufficient to counterbalance the repulsive force owing to the hydrogen nuclear charge. However this descreening of the H nucleus is not sufficient to reverse the direction of the polarization of the remaining H density. This density is polarized into the internuclear region. HF is an example of polar covalent binding.

One might expect to observe a correlation between the dissociation energy for a molecule and the magnitude of the attractive force which binds the nuclei together. Since the total force acting on the nuclei at the equilibrium internuclear distance is zero, one must decide on a breakdown of the total force into equal and opposite components of attraction and repulsion which will reflect the changes in the density and the forces which occur in the formation of the molecule. For example setting the attractive force equal to the total electronic force will certainly not give a correlation with D_e as this force increases as does Z^2. The total electronic force operative at R_e does not, of course, take into account the fact that most of the density continues to simply screen nuclear charge in the molecule as in the separated atoms and in no

Figure 18. A plot of $\sum_i [f_i^{(AA)} + f_i^{(AB)}]/R_e^2$ versus the dissociation energy for homonuclear diatomic molecules and molecular ions.

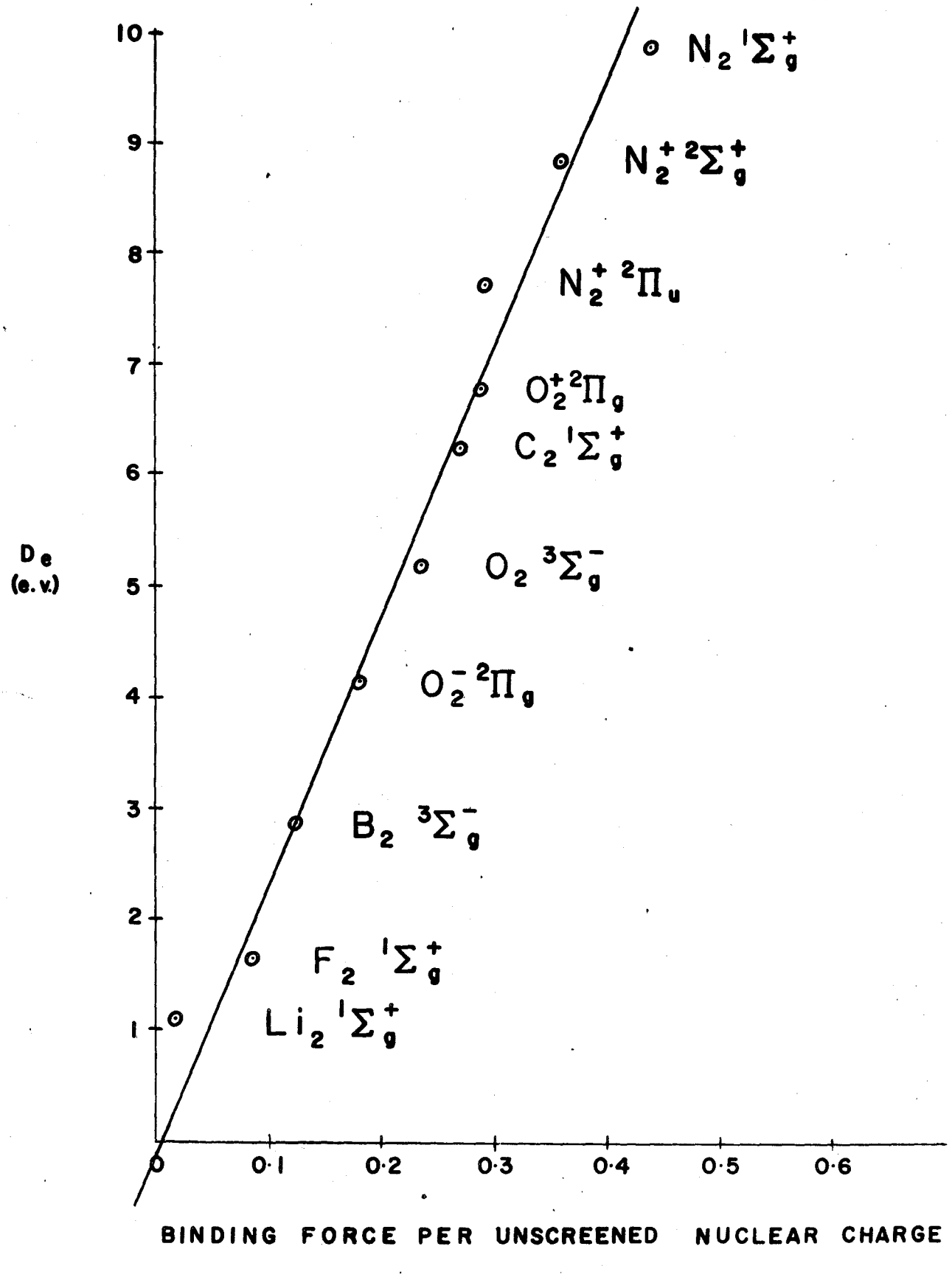
10
9
8
7
6
5
4
3
2
1
De
(e.v.)
$N_2\ ^1\Sigma_g^+$
$N_2^+\ ^2\Sigma_g^+$
$N_2^+\ ^2\Pi_u$
$O_2^+\ ^2\Pi_g$
$C_2\ ^1\Sigma_g^+$
$O_2\ ^3\Sigma_g^-$
$O_2^-\ ^2\Pi_g$
$B_2\ ^3\Sigma_g^-$
$F_2\ ^1\Sigma_g^+$
$Li_2\ ^1\Sigma_g^+$
0
0·1
0·2
0·3
0·4
0·5
0·6
BINDING FORCE PER UNSCREENED NUCLEAR CHARGE

way reflects the change in the density or the forces and hence the change in energy arising from the formation of the molecule. A covalent molecule has here been defined as one in which the transfer of charge results in a descreening of both nuclei. The magnitude of the force of repulsion generated by this descreening of the nuclei is thus a direct reflection of the change in the charge density which arises because of the formation of the molecule. This force of repulsion is balanced by the atomic and overlap contributions which provide a measure of the net attractive force which binds the nuclei. The sum of the overlap and atomic contributions when multiplied by $(1/R_e^2)$ is thus equal to the force binding each of the unscreened nuclear charges by the electron density which has been redistributed in the formation of the molecule. A plot of this quantity versus the dissociation energy is given in Figure 18. There is indeed a correlation between these two quantities, one which is best described by a linear relationship.

The only molecule which is seriously out of line is Li_2. It was noted earlier that the bond in this molecule differs from the others in the series in that it is formed primarily from the overlap of s orbitals and it does not involve π orbitals. There could well be a distinct slope for bonds of differing type. Included in the plot are

points for the states of the molecular ions O_2^+, O_2^- and N_2^+. The sum of the atomic and overlap contributions for these species are corrected by the addition of 0.5 for the negative ions and by the subtraction of 0.5 for the positive ions. These corrections take account of the fact that there is initially present a force of repulsion equivalent to one-half of a positive charge on each nucleus in the positive ions and a net force of attraction on the nuclei of similar magnitude for the negative ions.

CHAPTER VI

CONCLUDING SUMMARY

Many conclusions can be drawn from the results presented in this thesis. The one-electron density distribution is a three-dimensional function and can be represented by charge contour maps. Further these maps provide a physically significant picture of the distribution of electronic charge in a molecule. Estimates of molecular dimensions have been derived from the contour maps describing the molecules Li_2, B_2, C_2, N_2, O_2 and F_2 and these estimates are in agreement with the results derived from equation of state data. Such molecular dimensions are predictive in nature. They can be used in studies of molecular crystals to determine the validity of proposed crystal structures and to provide molecular dimensions. No correlation has been found between the fraction of charge in the binding region and the experimental dissociation energy. Molecular length is found to be related to the internuclear separation and the rate at which density falls off from the nucleus in the isolated atom. In fact, it has been proposed that the length of a peripheral atom in a molecule can be estimated by taking the sum of $\frac{1}{2} R_e$ from a suitable source

plus the atomic radius as defined by the 0.002 contour of the isolated atom. For atoms such as Li and Na the atomic radius is defined by the 0.002 contour of the core density.

The $\Delta\rho(\vec{r})$ contour maps present a picture of the reorganization of charge density attendant upon the formation of the chemical bond. From another point of view such contour maps describe the changes in density that must occur in order that the molecular system may reach electrostatic equilibrium. These maps are useful as they permit a classification of diatomic molecules according to their bond type. The Li_2 molecule is representative of an s-type bond. Such a bond presents a diffuse buildup of charge in the binding region. The remaining stable homonuclear diatomic molecules studied in this thesis are representative of p-type bonds. For such bonds there is a much more concentrated buildup of charge along the internuclear axis. Further such bonds show a significant accumulation of charge density in the antibinding regions as well as in the binding region. This accumulation of charge in the antibinding regions is certainly contrary to the classical picture of charge buildup in the binding region at the expense of charge removal from the antibinding regions. It is a nonclassical effect which owes its origin to interactions between electrons possessing angular momentum. The chemical bond is a result of an

accumulation of charge density in the binding region - an accumulation which balances the force of repulsion owing to the nuclei. However the chemical bond is also a result of the balance between electron-electron repulsion and electron-nucleus attraction. Consider two atoms whose valence electrons possess angular momentum. As such atoms approach each other during the formation of a bond, the valence electrons interact. Under the influence of such interactions, the atomic density distributions acquire a directional character. The concentrated increase of molecular charge density in the binding region emphasizes the importance of electronic-nuclear attraction in binding the nuclei together. But because of the directional nature of the atomic densities, electron-electron repulsion between the atomic charge clouds takes the form of a large increase of molecular density in the antibinding regions behind the nuclei. For atoms whose valence electrons possess no angular momentum, this electron-electron repulsion is indicated by a large <u>diffuse</u> buildup of charge in the binding region. The $\Delta\rho(\vec{r})$ maps are not predictive in nature as they do not present distinct differences between stable and unstable molecules.

The analysis of the force acting on the nucleus in a diatomic molecule is found to corroborate the results obtained from the total density and density difference maps.

Force calculations verify the stability of all the molecules studied in this thesis with the exception of Be_2. Be_2 is correctly predicted to be unstable in its ground state at an internuclear distance of 3.5 a.u. It is not possible to predict the number of electron-pair bonds in a diatomic molecule as the difference in the number of binding and antibinding molecular orbitals. This is a result of the fact that there is no correlation between the terms binding and bonding[73 74,68] in the case of the $3\sigma_g$ molecular orbital. It is not desirable to change the definition of binding because such a redefinition results in a loss of the physical picture presented by the f_i values. The charge density of a molecular orbital whose f_i value is greater than one is built up in the binding region and exerts a force of attraction on the nucleus in excess of the force of repulsion owing to one nuclear charge.

Finally the $\Delta\rho(\vec{r})$ contour maps provide new definitions for ionic and covalent bonds in terms of localized and shared density increases. The density difference contour map describing an ionic bond shows a localized buildup of charge about the electronegative atom while the $\Delta\rho(\vec{r})$ contour map describing a covalent bond shows a shared increase of charge in the binding region. If the $\Delta\rho(\vec{r})$ contour map is interpreted as a bond map, then a localized increase of charge binds the nuclei in an ionic molecule while a shared increase of charge binds the nuclei in a covalent molecule. Future studies should involve calculations of the force acting on the nucleus owing to these localized and shared densities. It is heartening to note that the analysis suggested in this thesis and originally applied to the molecules LiF, HF, and LiH has general applicability. The first and second row hydride molecules have been discussed by Bader, Keaveny, and Cade[88]. They find that the $\Delta\rho(\vec{r})$ maps for these molecules indeed show a gradual transition from an ionic mechanism of binding in LiH and NaH to a polar covalent mechanism of binding in HF and HCl. Bader and Bandrauk[89] have analyzed two iso-electronic series of molecules. The one includes BF, CO and N_2 while the other includes LiF, BeO, and C_2. They conclude that LiF, and BeO are ionic while BF appears to be a mixture of both bond types.

APPENDIX

THE CALCULATION OF INTEGRALS

Consider a diatomic molecule AB described by a Hartree-Fock wavefunction Ψ where

$$\Psi = \sqrt{\frac{1}{N!}} \, ||\phi_1(1)\alpha(1)\phi_1(2)\beta(2) \ \ldots\ \phi_{\frac{N}{2}}(N)\beta(N)|| \qquad (1)$$

The operator

$$O = \frac{Z_A \cos\Theta_A}{r_A^2} \qquad (2)$$

describes the x component of the force acting on nucleus A owing to an electronic charge at a distance r_A units from nucleus A. The situation is pictured in figure 1 of the text. The expectation value of this operator is given as

$$F_A^{(ELEC)} = Z_A \sum_i N_i \left\langle \phi_i \left| \frac{\cos\Theta_A}{r_A^2} \right| \phi_i \right\rangle \qquad (3)$$

The sum is over all occupied molecular orbitals. Z_A is the nuclear charge. N_i is the occupation number of molecular orbital ϕ_i. If the one-electron molecular orbitals are approximated as linear combinations of atomic orbitals, then the calculation of $F_A^{(ELEC)}$ involves the calculation of three types of integrals. These are listed below as

$$1.\ \left\langle \chi_A \left| \frac{\cos\Theta_A}{r_A^2} \right| \chi_A \right\rangle \qquad (4)$$

$$2.\ \left\langle \chi_A \left| \frac{\cos\Theta_A}{r_A^2} \right| \chi_B \right\rangle \qquad (5)$$

$$3.\ \left\langle \chi_B \left| \frac{\cos\Theta_A}{r_A^2} \right| \chi_B \right\rangle \qquad (6)$$

χ_A is a Slater-type function centred on nucleus A while χ_B is a Slater-type function centred on nucleus B. Integrals one, two, and three are referred to respectively as atomic, overlap and screening integrals. They are discussed in the text.

The atomic integrals are easily evaluated as they are simple one-centre integrals. The overlap and screening integrals involve two centres. A prolate spheroidal coordinate system is used in the evaluation of these integrals. The variables in such a coordinate system are designated λ, μ, and ϕ. ϕ is a rotation about the x axis. Some relations between these coordinates and those shown in Figure 1 of the text are given below.

$$\lambda = (r_A + r_B)/R \tag{7}$$

$$\mu = (r_A - r_B)/R \tag{8}$$

$$r_A = [\lambda + \mu]R/2 \tag{9}$$

$$r_B = [\lambda - \mu]R/2 \tag{10}$$

$$\cos\theta_A = \frac{1+\lambda\mu}{\lambda+\mu} \tag{11}$$

$$\cos\theta_B = \frac{1-\lambda\mu}{\lambda-\mu} \tag{12}$$

$$\sin\theta_A = \left[(\lambda^2-1)(1-\mu^2)\right]^{\frac{1}{2}}/\lambda+\mu \tag{13}$$

$$\sin\theta_B = \left[(\lambda^2-1)(1-\mu^2)\right]^{\frac{1}{2}}/\lambda-\mu \tag{14}$$

$$\sin\theta_A\sin\theta_B = (\lambda^2-1)(1-\mu^2)/(\lambda^2-\mu^2) \tag{15}$$

The volume element in a spherical coordinate system is given as

$$r_A^2 \sin\theta_A dr d\theta d\phi \qquad (16)$$

while the volume element in a prolate spheroidal coordinate system is given as

$$\frac{R^3}{8} (\lambda^2-\mu^2) d\lambda d\mu d\phi \qquad (17)$$

The two-centre force integrals in this new coordinate system can be expressed as sums of integrals of the type

$$F_{kmn}(\alpha,\beta) = \int_1^{\infty} \int_{-1}^{1} \frac{(\lambda^2-1)^k}{(\lambda+\mu)^{k+1}} \lambda^m \mu^n e^{-\alpha\lambda} e^{-\beta\mu} d\lambda d\mu \qquad (18)$$

where

$$\alpha = (\zeta_A+\zeta_B) R/2 \qquad (19)$$

$$\beta = (\zeta_A-\zeta_B) R/2 \qquad (20)$$

The symbol ζ_A and ζ_B are the effective nuclear charges of the Slater-type functions centred on A and B.

Kotani[86] et al list general expressions for the integral (18). These expressions were made the basis of a computer programme designed by Dr. J. Goodisman at the University of Illinois. This programme was modified in order to be of use in the calculations discussed in this thesis, is a subroutine and has the name FØRINT . It has as input data the values of α and β and calculates values for $F_{0mn}(\alpha,\beta)$, $F_{1mn}(\alpha,\beta)$, and $F_{mn}(\alpha,\beta)$ where

$$F_{mn}(\alpha,\beta) = F_{0,m+1,n}(\alpha,\beta) - F_{1,m,n}(\alpha,\beta) \qquad (21)$$

The computational method does not apply to the case where ζ_A is equal to ζ_B. All force integrals where ζ_A is not equal to ζ_B have been expressed in terms of F_{0mn}, F_{1mn} and F_{mn}. Each integral is programmed in a separate function subprogramme with a call statement to FØRINT. Thus any programme to calculate two centre integrals consists of a main deck with call statements to the various force function subprogrammes. These function subprogrammes and the FØRINT subprogramme are always loaded with the main deck.

In the subroutine FØRINT, the F_{mn} values are designated by the subscripted variable FMN(I,J). Thus the indices I and J are always one unit higher than the m and n values. For example

$$F_{20} = \text{FMN}(3,1) \qquad (22)$$

Also

$$F_{020} = \text{FO}(3,1) \qquad (23)$$

and

$$F_{120} = \text{F1}(3,1) \qquad (24)$$

Listed below are all formulae used in this work. The code is as follows:

O = overlap force

S = screening force

A = atomic force

For example O1S1S means the force on nucleus A owing to the overlap of a 1s orbital on A with a 1s orbital on B. P1S1S means the force on nucleus A owing to the 1s density on B. A2P1S is the force on nucleus A owing to the overlap of the 2p and 1s orbitals on atom A. The symbol Z is used to indicate the effective nuclear charge. For overlap integrals

$$Z_A = \zeta_A = Z_1 \tag{25}$$

and

$$Z_B = \zeta_B = Z_2 \tag{26}$$

R is the internuclear distance.

The overlap integrals are listed below. They are designated with an "O". Thus, the notation is

$$O2S_A(Z_1)\ 2S_B(Z_2) = O2S2S$$

$$O1S1S = Z_1^{3/2} Z_2^{3/2} R [F_{10}-F_{01}]$$

$$O2S1S = \frac{Z_1^{5/2} Z_2^{3/2} R^2}{2.0 \sqrt{3}} [F_{20}-F_{02}]$$

$$O2P1S = \frac{Z_1^{5/2} Z_2^{3/2} R^2}{2.0} [F_{10}+F_{21}-F_{01}-F_{12}]$$

$$O3S1S = \frac{Z_1^{7/2} Z_2^{3/2} R^3}{12} \sqrt{\frac{2}{5}} [F_{30}+F_{21}-F_{12}-F_{03}]$$

$$O3D1S = \frac{Z_1^{7/2} Z_2^{3/2} R^3}{24} \sqrt{2} [3(F_{10}+2F_{21}+F_{32}-F_{01}-2F_{12}-F_{23}) - F_{30}-F_{21}+F_{03}+F_{12}]$$

$$O4F1S = \frac{Z_1^{9/2} Z_2^{3/2} R^4}{48.0} \sqrt{\frac{1}{5}} [5(F_{10}+F_{43})+12(F_{21}+F_{32})+3(F_{14}+F_{03}) -5(F_{01}+F_{34})-12(F_{12}+F_{23})-3(F_{41}+F_{30})]$$

$$O1S2S = \frac{Z_1^{3/2} Z_2^{5/2} R^2}{2\sqrt{3}} [F_{02}+F_{20}-2F_{11}]$$

$$O2S2S = \frac{Z_1^{5/2} Z_2^{5/2} R^3}{12} [F_{30}+F_{03}-F_{12}-F_{21}]$$

$$O2P2S = \frac{Z_1^{5/2} Z_2^{5/2} R^3}{4.0\sqrt{3}} [F_{20}+F_{02}+F_{13}+F_{31}-2(F_{11}+F_{22})]$$

$$O3S2S = \frac{Z_1^{7/2} Z_2^{5/2} R^4}{24} \sqrt{\frac{2}{15}} [F_{40}-2F_{22}-F_{04}]$$

$$O3D2S = \frac{Z_1^{7/2} Z_2^{5/2} R^4}{48.0} \sqrt{\frac{2}{3}} [3(F_{20}+2F_{31}+F_{42}+F_{02}+2F_{13}+F_{24} - 2(F_{11}+2F_{22}+F_{33}))-F_{40}-F_{04}+2F_{22}]$$

$$O4D2S = \frac{Z_1^{9/2}\, Z_2^{5/2}\, R^5}{96.0}\sqrt{\frac{1}{15}}\,[5(F_{20}+F_{02}+F_{53}+F_{35})+15(F_{31}+F_{13}+F_{42}$$

$$+F_{24})-10(F_{11}+F_{44})-24(F_{22}+F_{33})-3(F_{51}+F_{15}+F_{40}+F_{04})]$$

$$O1S2P = \frac{Z_1^{3/2}\, Z_2^{5/2}\, R^2}{2}\,[F_{10}+F_{12}-F_{01}-F_{21}]$$

$$O2S2P = \frac{Z_1^{5/2}\, Z_2^{5/2}\, R^3}{4\sqrt{3}}\,[F_{20}+F_{13}-F_{31}-F_{02}]$$

$$O2P2P = \frac{Z_1^{5/2}\, Z_2^{5/2}\, R^3}{4}\,[F_{23}+F_{10}-F_{01}-F_{32}]$$

$$O3S2P = \frac{Z_1^{7/2}\, Z_2^{5/2}\, R^4}{24}\sqrt{\frac{2}{5}}\,[F_{30}+F_{21}+F_{23}-F_{41}-F_{32}-F_{12}-F_{03}+F_{14}]$$

$$O3D2P = \frac{Z_1^{7/2}\, Z_2^{5/2}\, R^4\,\sqrt{2}}{48.0}\,[3(F_{10}+F_{21}+F_{23}+F_{34}-F_{32}-F_{43}$$

$$-F_{01}-F_{12})-F_{30}-F_{23}-F_{21}-F_{14}+F_{41}+F_{12}+F_{32}+F_{03}]$$

$$O4F2P = \frac{Z_1^{9/2}\, Z_2^{5/2}\, R^2}{96}\sqrt{\frac{1}{5}}\,[5(F_{10}+F_{45})+7(F_{21}+F_{34})+3(F_{52}-F_{03})$$

$$-5(F_{01}+F_{54})-7(F_{12}+F_{43})-3(F_{25}+F_{30})]$$

$$O1S3S = \frac{Z_1^{3/2}\, Z_2^{7/2}\, R^3}{12}\sqrt{\frac{2}{5}}\,[F_{30}+3F_{12}-3F_{21}-F_{03}]$$

$$O2S3S = \frac{Z_1^{5/2}\, Z_2^{7/2}\, R^4}{24}\sqrt{\frac{2}{15}}\,[F_{40}+2F_{13}-2F_{31}-F_{04}]$$

$$O2P3S = \frac{Z_1^{5/2}\, Z_2^{7/2}\, R^4}{24}\sqrt{\frac{2}{5}}\,[F_{30}+3F_{12}+F_{41}+3F_{23}-3F_{21}-F_{03}-3F_{32}-F_{14}]$$

$$O3S3S \quad \frac{Z_1^{7/2}\, Z_2^{7/2}\, R^5}{360}\,[F_{50}+F_{14}+2F_{23}-2F_{32}-F_{41}-F_{05}]$$

$$O3D3S = \frac{Z_1^{7/2}\, Z_2^{7/2}\, R^5}{288}\sqrt{\frac{4}{5}}\,[3(F_{30}+3F_{12}+2F_{41}+6F_{23}+F_{52}$$

$$+3F_{34}-3F_{21}-F_{03}-6F_{32}-2F_{14}-3F_{43}-F_{25})$$

$$-F_{50}-F_{14}-2F_{23}+2F_{32}+F_{41}+F_{05}]$$

$$O4F3S = \frac{Z_1^{9/2}\, Z_2^{7/2}\, R^6\,\sqrt{2}}{2880}\,[5(F_{30}+F_{63})+15(F_{12}+F_{45})$$

$$+18(F_{41}+F_{52})+39(F_{23}+F_{34})+3(F_{16}+F_{05})-5(F_{03}+F_{36})$$

$$-15(F_{21}+F_{54})-18(F_{14}+F_{25})-39(F_{32}+F_{43})-3(F_{61}+F_{50})]$$

$$O1S3D = \frac{Z_1^{3/2}\, Z_2^{7/2}\, R^3\,\sqrt{2}}{24}\,[3(F_{10}+F_{32}+2F_{12}-F_{23}-F_{01}-2F_{21})$$

$$-F_{30}-3F_{12}+3F_{21}+F_{03}]$$

$$O2S3D = \frac{Z_1^{5/2} Z_2^{7/2}\, R^4}{48}\sqrt{\frac{2}{3}}\,[3(F_{20}+F_{42}+2F_{13}-2F_{31}-F_{02}$$

$$-F_{24})-F_{40}-2F_{13}+2F_{31}+F_{04}]$$

$$O2P3D = \frac{Z_1^{5/2}\, Z_2^{7/2}\, R^4\,\sqrt{2}}{48}\,[3(F_{12}+F_{23}+F_{10}+F_{43}-F_{01}-F_{34}$$

$$-F_{21}-F_{32})-F_{30}-3F_{12}-F_{41}-3F_{23}+3F_{21}+F_{03}+3F_{32}+F_{14}]$$

$$O3S3D = \frac{Z_1^{7/2}\, Z_2^{7/2}\, R^5}{288}\sqrt{\frac{4}{5}}\,[3(F_{30}+F_{52}+F_{43}+2F_{23}+2F_{14}+F_{21}$$

$$-2F_{41}-2F_{32}-F_{12}-F_{34}-F_{03}-F_{25})-F_{50}-F_{14}$$

$$-2F_{23}+2F_{32}+F_{41}+F_{05}]$$

$$O3D3D = \frac{2\,Z_1^{7/2}\,Z_2^{7/2}\,R^5}{576}\,[9(F_{10}+F_{54}+2F_{23}-2F_{32}-F_{01}-F_{45})$$

$$-6(F_{30}+F_{52}+F_{12}+F_{34}+4F_{23}-4F_{32}-F_{43}-F_{03}$$

$$-F_{25}-F_{21})+(F_{040}+F_{051}+2F_{013}+2F_{024}-2F_{031}$$

$$-2F_{042}-F_{004}-F_{015}]$$

$$O4F3D = \frac{Z_1^{9/2}\,Z_2^{7/2}}{1152}\sqrt{\frac{2}{5}}\,R^6\,[15(F_{10}+F_{65})+18(F_{32}+F_{43})$$

$$+21(F_{21}+F_{54})+14(F_{03}+F_{36})+9(F_{14}+F_{25})+3(F_{50}+F_{61})$$

$$-15(F_{01}+F_{56})-18(F_{23}+F_{34})-21(F_{12}+F_{45})$$

$$-14(F_{30}+F_{63})-9(F_{41}+F_{52})-3(F_{05}+F_{16})]$$

$$O1S4F = \frac{Z_1^{3/2}\,Z_2^{9/2}\,R^4}{48\sqrt{5}}\,[5(F_{10}+F_{34})+6(F_{32}+F_{12})+3(F_{41}+F_{03})$$

$$-5(F_{01}+F_{43})-6(F_{23}+F_{21})-3(F_{14}+F_{30})]$$

$$O2S4F = \frac{Z_1^{5/2}\,Z_2^{9/2}\,R^5}{96\sqrt{15}}\,[5(F_{20}+F_{35})+9(F_{42}+F_{13})+3(F_{04}+F_{51})$$

$$-5(F_{02}+F_{53})-9(F_{24}+F_{31})-3(F_{40}+F_{15})]$$

$$O2P4F = \frac{Z_1^{5/2}\,Z_2^{9/2}\,R^5}{96\sqrt{5}}\,[5(F_{10}+F_{45})+3(F_{52}+F_{03})+F_{43}+F_{12}$$

$$-5(F_{01}+F_{54})-3(F_{25}+F_{30})-F_{34}-F_{21}]$$

$$O3D4F = \frac{Z_1^{7/2}\,Z_2^{9/2}\,R^6}{1152}\sqrt{\frac{2}{5}}\,[15(F_{10}+F_{56})+6(F_{32}+F_{34})$$

$$+7(F_{21}+F_{45})+14(F_{03}+F_{63})+3(F_{41}+F_{16}+F_{25}+F_{50})$$

$$-15(F_{01}+F_{65})-6(F_{23}+F_{43})-7(F_{12}+F_{54})-14(F_{30}+F_{36})$$

$$-3(F_{14}+F_{61}+F_{52}+F_{05})]$$

$$O3S4F = \frac{Z_1^{7/2} Z_2^{9/2} \sqrt{2} R^6}{2880} [3(F_{61}+F_{05})+5(F_{30}+F_{21}+F_{45})+12(F_{52}+F_{14})+9(F_{43}+F_{23})-3(F_{16}+F_{50}-5(F_{03}+F_{12}+F_{54}+F_{63}-F_{36})+12(F_{25}+F_{41})+9(F_{34}+F_{32})]$$

$$O4F4F = \frac{Z_1^{9/2} Z_2^{9/2} R^7}{11520} [25(F_{10}+F_{67})+27(F_{45}+F_{32})+9(F_{50}+F_{14}+F_{63}+F_{27})+30(F_{03}+F_{21}+F_{74}+F_{56})-25(F_{01}+F_{76})-27(F_{54}+F_{23})-9(F_{05}+F_{41}+F_{36}+F_{72})-30(F_{30}+F_{12}+F_{47}+F_{65})]$$

Π OVERLAP FUNCTIONS

$$O2P2P = \frac{Z_1^{5/2} Z_2^{5/2} R^3}{8.0} [F_{110}+F_{121}+F_{103}+F_{114}-F_{101}-F_{123}-2F_{112}]$$

$$O2P3D = \frac{Z_1^{5/2} Z_2^{7/2} R^4}{8.0} \sqrt{\frac{1}{6}} [F_{110}+F_{103}+F_{134}+F_{123}-F_{112}-F_{101}-F_{132}-F_{125}]$$

$$O2P4F = \frac{Z_1^{5/2} Z_2^{9/2} R^5}{64\sqrt{30}} [6(F_{30}+F_{52})+5(F_{01}+F_{45})+4F_{23}+7F_{14}+2(F_{21}+F_{43})+F_{05}-6(F_{03}+F_{25})-5(F_{10}+F_{54})-4F_{32}-7F_{41}-2(F_{12}+F_{34})-F_{50}]$$

$$O3D2P = \frac{Z_1^{7/2} Z_2^{5/2} R^4}{8\sqrt{6}} [F_{110}+2F_{121}+F_{132}+F_{103}+2F_{114}+F_{125}-3F_{112}-3F_{123}-F_{134}-F_{101}]$$

$$O3D3D = \frac{Z_1^{7/2} Z_2^{7/2} R^5}{48} [F_{110}+F_{121}+F_{103}+F_{114}+2F_{134}+F_{145}-2F_{112}-F_{101}-F_{132}-F_{143}-F_{125}-F_{136}]$$

$$O3D4F = \frac{Z_1^{7/2} Z_2^{9/2} R^6}{384\sqrt{5}} [6(F_{30}+F_{63})+2(F_{23}+F_{34})+5(F_{01}+F_{56})$$
$$+3(F_{12}+F_{45})+F_{14}+F_{25}+F_{16}+F_{05}-6(F_{03}+F_{36})-2(F_{32}+F_{43})$$
$$-5(F_{10}+F_{65})-3(F_{21}+F_{54})-F_{41}-F_{52}-F_{61}-F_{50}]$$

$$O4F2P = \frac{Z_1^{9/2} Z_2^{5/2} R^5}{64\sqrt{30}} [6(F_{30}+F_{52})+20\ F_{23}+5F_{01}+14(F_{12}+F_{34})$$
$$+9F_{41}+5F_{45}+F_{05}-6(F_{03}+F_{25})-20F_{32}-5F_{10}$$
$$-14(F_{21}+F_{43})-9F_{14}-5F_{54}-F_{50}]$$

$$O4F3D = \frac{Z_1^{9/2} Z_2^{7/2} R^6}{384\sqrt{5}} [6(F_{30}+F_{43}+F_{23}+F_{36})+5(F_{01}+F_{65})$$
$$+3(F_{41}+F_{25})+9(F_{12}+F_{54})+F_{05}+F_{61}$$
$$-6(F_{03}+F_{34}+F_{32}+F_{63})-5(F_{10}+F_{56})-3(F_{14}+F_{52})$$
$$-9(F_{21}+F_{45})-F_{50}-F_{16}]$$

$$O4F4F = \frac{Z_1^{9/2} Z_2^{9/2}}{15360} [35(F_{30}+F_{74}+F_{12}+F_{56})+F_{70}+F_{16}$$
$$+11(F_{05}+F_{63}+F_{41}+F_{27})+9(F_{52}+F_{34})+33(F_{23}+F_{45})$$
$$+25(F_{01}+F_{67})-35(F_{03}+F_{65}+F_{47}+F_{21})-F_{07}-F_{61}$$
$$-11(F_{50}+F_{36}+F_{14}+F_{72})-9(F_{25}+F_{43})-33(F_{32}+F_{54})$$
$$-25(F_{10}+F_{76})] \times R^7$$

The penetration force integrals are designated with a "P". The notation is, for example,

$$P2S(Z_1)1S(Z_2) = P2S1S$$

$$P1S1S = Z_1^{3/2} Z_2^{3/2} R [F_{10}-F_{01}]$$

$$P2S1S = \frac{Z_1^{5/2} Z_2^{3/2} R^2}{2\sqrt{3}} [F_{20}+F_{02}-2F_{11}]$$

$$P2S2S = \frac{Z_1^{5/2} Z_2^{5/2} R^3}{12} [3(F_{12}-F_{21})+F_{30}-F_{03}]$$

$$P2P1S = \frac{Z_1^{5/2} Z_2^{3/2} R^2}{2} [F_{10}-F_{01}+F_{12}-F_{21}]$$

$$P2P2S = \frac{Z_1^{5/2} Z_2^{5/2} R^3}{4\sqrt{3}} [2(F_{22}-F_{11})+F_{20}+F_{02}-F_{13}-F_{31}]$$

$$P2P2P = \frac{Z_1^{5/2} Z_2^{5/2} R^3}{4} [2(F_{12}-F_{21})+F_{10}+F_{32}-F_{01}-F_{23}]$$

$$P3S1S = \frac{Z_1^{7/2} Z_2^{3/2} R^3}{12} \sqrt{\frac{2}{5}} [F_{30}+3F_{12}-3F_{21}-F_{03}]$$

$$P3S2S = \frac{Z_1^{7/2} Z_2^{5/2} R^4}{24} \sqrt{\frac{2}{15}} [F_{40}+6F_{22}+F_{04}-4(F_{31}+F_{13})]$$

$$P3S2P = \frac{Z_1^{7/2} Z_2^{5/2} R^4}{24} \sqrt{\frac{2}{5}} [F_{30}+3F_{12}-F_{41}-3F_{23}-3F_{21} -F_{03}+3F_{32}+F_{14}]$$

$$P3S3S = \frac{Z_1^{7/2} Z_2^{7/2} R^5}{144} \frac{2}{5} [F_{50}+10F_{32}+5F_{14}-10F_{23}-5F_{41}-F_{05}]$$

$$P3D1S = \frac{Z_1^{7/2} Z_2^{3/2} R^3 \sqrt{2}}{24} [3(2(F_{12}-F_{21})+F_{10}+F_{32}-F_{23}-F_{01}) -3(F_{12}-F_{21})-F_{30}+F_{03}]$$

$$P3D2S = \frac{Z_1^{7/2} Z_2^{5/2} R^4}{48.0} \sqrt{2} \, [3(4F_{22}+F_{20}+F_{02}+F_{42}+F_{24} -2(F_{31}+F_{13}+F_{33}+F_{11}))-6F_{22}+4(F_{31}+F_{13}) -F_{04}-F_{40}]$$

$$P3D2P = \frac{Z_1^{7/2} Z_2^{5/2} R^4 \sqrt{2}}{48} \, [3(3(F_{12}+F_{32}-F_{23}-F_{21})+F_{10} +F_{34}-F_{01}-F_{43})-3(F_{12}+F_{32}-F_{21}-F_{23})-F_{14} -F_{30}+F_{41}+F_{03}]$$

$$P3D3S = \frac{Z_1^{7/2} Z_2^{7/2} R^5}{228} \sqrt{\frac{4}{5}} [3(F_{30}-3F_{21}-6F_{23}+2F_{14}+F_{52} -3F_{43}+3F_{12}-F_{03}-2F_{41}+6F_{32}+3F_{34}-F_{25})-F_{50} -5F_{14}-10F_{32}+5F_{41}+10F_{23}+F_{05}]$$

$$P3D3D = \frac{2 Z_1^{7/2} Z_2^{7/2} R^5}{9\times 64} \, [9(6(F_{32}-F_{23})+4(F_{34}+F_{12}-F_{43} -F_{21})+F_{10}+F_{54}-F_{45}-F_{01})-6(3(F_{34}+F_{12} -F_{43}-F_{21})+6(F_{32}-F_{23})+2(F_{14}-F_{41})+F_{30} -F_{03}+F_{52}-F_{25})+F_{50}+10(F_{32}-F_{23})+5(F_{14}-F_{41})-F_{05}]$$

$$P4F1S = \frac{Z_1^{9/2} Z_2^{3/2} R^4}{48\sqrt{5}} \, [5(F_{10}+F_{34})+6(F_{32}+F_{12})+3(F_{41}+F_{03}) -5(F_{01}+F_{43})-6(F_{23}+F_{21})-3(F_{14}+F_{30})]$$

$$P4F2S = \frac{Z_1^{9/2} Z_2^{5/2} R^5}{95\sqrt{15}} [5(F_{20}+F_{02})+3(F_{42}+F_{24}+F_{51}+F_{15})+12F_{22}+10F_{44}-3(F_{13}+F_{31}+F_{04}+F_{40})-5(F_{53}+F_{35})-10F_{11}-12F_{33}]$$

$$P4F2P = \frac{Z_1^{9/2} Z_2^{5/2} R^5}{96\sqrt{5}} [5(F_{10}+F_{54})+12F_{32}+6F_{41}+3(F_{03}+F_{25})+11(F_{12}+F_{34})-5(F_{01}+F_{45})-12F_{23}-6F_{14}-3(F_{30}+F_{52})-11(F_{21}+F_{43})]$$

$$P4F3S = \frac{Z_1^{9/2} Z_2^{7/2} R^6}{2880}\sqrt{2} [5(F_{30}+F_{36})+15(F_{12}+F_{32}+F_{34}+F_{54})+3(F_{61}+F_{05})-5(F_{03}+F_{63})-15(F_{21}+F_{23}+F_{43}+F_{45})-3(F_{16}+F_{50})]$$

$$P4F3D = \frac{Z_1^{9/2} Z_2^{7/2} R^6}{1152}\sqrt{\frac{2}{5}} [15(F_{10}+F_{56})+54F_{32}+33(F_{12}+F_{54})+54F_{34}+14(F_{03}+F_{63})+27(F_{41}+F_{25})+3(F_{50}+F_{16})-15(F_{01}+F_{65})-54F_{23}-33(F_{21}+F_{45})-54F_{43}-14(F_{30}+F_{36})-27(F_{14}+F_{52})-3(F_{05}+F_{61})]$$

$$P4F4F = \frac{Z_1^{9/2} Z_2^{9/2} R^7}{11520} [25(F_{10}+F_{76})+105(F_{32}+F_{54})+60F_{12}+140F_{34}+30(F_{03}+F_{47})+75(F_{41}+F_{63})+90F_{25}+9(F_{50}+F_{72})+60F_{56}+18F_{16}-25(F_{01}+F_{67})-105(F_{23}+F_{45})-140F_{43}-60F_{21}-30(F_{30}+F_{74})-75(F_{14}+F_{36})-90F_{52}-9(F_{05}+F_{27})-60F_{65}-18F_{61}]$$

For Π Integrals, one easily obtains

$$P2P2P = \frac{Z_1^{5/2} Z_2^{5/2} R^3}{8} [F_{110}+F_{121}+F_{103}+F_{114}-F_{101}-F_{123} -2F_{112}]$$

$$P3D2P = \frac{Z_1^{7/2} Z_2^{5/2} R^4}{8\sqrt{6}} [F_{110}+F_{103}+F_{134}+F_{123}-F_{112}-F_{101} -F_{132}-F_{125}]$$

$$P3D3D = \frac{Z_1^{7/2} Z_2^{7/2} R^5}{48} [F_{110}+F_{103}+F_{143}+F_{136}+2F_{123} -F_{121}-F_{101}-F_{114}-F_{132}-F_{145}-F_{125}]$$

$$P4F2P = \frac{Z_1^{9/2} Z_2^{5/2} R^5}{64\sqrt{30}} [6F_{30}+F_{05}+5(F_{01}+F_{45})+4F_{23} +2(F_{21}+F_{43})+7F_{14}+6F_{52}-6F_{03}-F_{50} -5(F_{10}+F_{54})-4F_{32}-2(F_{12}+F_{34})-7F_{41}-6F_{25}]$$

$$P4F3D = \frac{Z_1^{9/2} Z_2^{7/2} R^6}{384\sqrt{5}} [6(F_{30}+F_{43}+F_{23}+F_{36})+5(F_{01}+F_{65}) +13(F_{14}+F_{52})+7(F_{21}+F_{45})+F_{61}+F_{05} -6(F_{03}+F_{34}+F_{32}+F_{63})-5(F_{10}+F_{56})-13(F_{41}+F_{25}) -7(F_{12}+F_{54})-F_{16}-F_{50}]$$

$$P4F4F = \frac{Z_1^{9/2} Z_2^{9/2} R^7}{15360} [35(F_{30}+F_{74})+121F_{52}+F_{70}+55F_{43} +85(F_{14}+F_{36})+11(F_{05}+F_{27})+65(F_{23}+F_{45}) +15F_{61}+25(F_{01}+F_{67})+45(F_{21}+F_{65})-35(F_{03}+F_{47}) -121F_{25}-F_{07}-55F_{34}-85(F_{41}+F_{63})-11(F_{50}+F_{72}) -65(F_{32}+F_{54})-15F_{16}-25(F_{10}+F_{76})-45(F_{12}+F_{56})]$$

The Atomic force integrals are designed with an "A". The notation is for example

$$A2P(Z_1)1S(Z_2) = A2P1S$$

$$A2P1S = \frac{4}{3}\frac{Z_1^{5/2} Z_2^{3/2}}{(Z_1+Z_2)^2}$$

$$A2P2S = \frac{8}{3}\frac{Z_1^{5/2} Z_2^{5/2}}{\sqrt{3}\,(Z_1+Z_2)^3}$$

$$A3S2P = \frac{8}{3}\sqrt{\frac{2}{5}}\frac{Z_1^{7/2} Z_2^{5/2}}{(Z_1+Z_2)^4}$$

$$A3D2P = \frac{16}{15}\frac{\sqrt{2}\, Z_1^{7/2} Z_2^{5/2}}{(Z_1+Z_2)^4}$$

$$A3D4F = \frac{32}{7}\sqrt{\frac{2}{5}}\frac{Z_1^{7/2} Z_2^{9/2}}{(Z_1+Z_2)^6}$$

The Π atomic integrals are

$$A3D2P = \frac{16}{5}\frac{1}{\sqrt{6}}\frac{Z_1^{7/2} Z_2^{5/2}}{(Z_1+Z_2)^4}$$

$$A4F3D = \sqrt{\frac{1}{5}}\;\frac{128}{21}\;\frac{Z_1^{9/2} Z_2^{7/2}}{(Z_1+Z_2)^6}$$

In the case of homonuclear diatomic molecules, electronic overlap force integrals occur in which Z_A, the effective nuclear charge of the orbital centred on nucleus A equals Z_B, the effective nuclear charge of the orbital centred on nucleus B. Such integrals cannot be evaluated by the method of Kotani et al[86]. The Barnett-Coulson[87] zeta-function technique was used during the course of this work to evaluate such integrals. In this technique, the function centred on nucleus B is expanded in terms of a co-ordinate system centred on nucleus A. The expansion is

$$r_B^{m-1} e^{-Z_B r_B} = \sum_{n=0}^{\infty} \frac{(2n+1)}{\sqrt{r_A R}} P_n(\cos\theta_A) \zeta_{mn}(Z_B, r_A, R) \quad (27)$$

$$= Z_B^{-m+1} \sum_{n=0}^{\infty} \frac{(2n+1)}{\sqrt{t\,\tau}} P_n(\cos\theta_A) \cdot \zeta_{mn}(1, t, \tau) \quad (28)$$

The variables t and τ are dimensionless. Further

$$t = Z_B r_A \quad (29)$$

$$\tau = Z_B R \quad (30)$$

R is the internuclear distance and P_n is the Legendre Polynomial of order n. Each $\zeta_{m,n}(Z_B, r_A; R)$ is a function of three variables. These are Z_B, r_A, and R. For m=0,

$$\zeta_{o,n} = \gamma_n (Z_B, r_A; R) \quad (31)$$

where

$$\gamma_n(Z_B, r_A, R) = I_{n+\frac{1}{2}} (Z_B, r_A)\, K_{n+\frac{1}{2}} (Z_B, R) \text{ for } r_A \leq R \quad (32)$$

The I and K are standard Bessel functions of purely imaginary argument. When $r_A > R$, the positions of r_A and R on the right hand side of equation (32) are interchanged. Any $\zeta_{m,n}$ can be expressed in terms of lower ζ. Thus

$$\zeta_{1,n}(1,t,\tau) = p_n(1,t;\tau) = \frac{t\tau}{2n+1}\left[\gamma_{n-1}(1,t;\tau)-\gamma_{n+1}(1,t;\tau)\right] \quad (33)$$

or in general

$$\zeta_{m+2,n}(1,t;\tau) = (t^2+\tau^2)\zeta_{m,n}(1,t;\tau)$$

$$- \frac{2t\tau}{(2n+1)}\left\{n\zeta_{m,n-1}(1,t;\tau) + (n+1)\,\zeta_{m,n+1}(1,t;\tau)\right\} . \quad (34)$$

For the work considered in this thesis, the force integrals are expressed in terms of J integrals where

$$J(k,\ell,m) = \int e^{-Z_A r_A}\, e^{-Z_B r_B}\, \cos^k\theta_A\, r_A^{\ell-1}\, r_B^{m-1}\, d\tau \quad (35)$$

Further

$$Z_B^{(\ell+m+1)} J(k,\ell,m) = \frac{4\pi}{\sqrt{\tau}} \int_0^\infty e^{-\kappa t}\, t^{\ell+\frac{1}{2}}\, f(m,k;t)\, dt \quad (36)$$

where

$$\kappa = \frac{Z_1}{Z_2} \quad (37)$$

The f(m,k:t) functions are linear combinations of the $\zeta_{m,n}$ functions. Thus the J(k,ℓ,m) integrals can be calculated as sums of Z integrals where

$$Z_{m,n,\ell+\frac{1}{2}}(\kappa,\tau) = \int_0^\infty e^{-\kappa t}\, \zeta_{m,n}(1,t,\tau)\, t^{\ell+\frac{1}{2}} dt \quad (38)$$

In particular

$$G_{n,\ell+\frac{1}{2}}(\kappa,\tau) = \int_0^\infty e^{-\kappa t}\gamma_n(1,t,\tau)\,t^{\ell+\frac{1}{2}}dt \qquad (39)$$

$$P_{n,\ell+\frac{1}{2}}(\kappa,\tau) = \int_0^\infty e^{-\kappa t}\,p_n(1,t,\tau)\,t^{\ell+\frac{1}{2}}\,dt \qquad (40)$$

The force integrals are expressed as sums of these $G_{n,\ell+\frac{1}{2}}$ and $P_{n,\ell+\frac{1}{2}}$ functions. A general subroutine called Ø VLINT was designed to calculate these $G_{n,\ell+\frac{1}{2}}$ and $P_{n,\ell+\frac{1}{2}}$ functions. In the programme

$$G_{N,L+\frac{1}{2}} = G(N+2,L+2) \qquad (41)$$

$$P_{N,L+\frac{1}{2}} = CP(N+2,L+2) \qquad (42)$$

G, and CP are doubly subscripted variables. Expressions for the integrals evaluated by this technique are given below.

$$O1S1S = \frac{Z_1^{3/2}\,Z_2^{1/2}}{\sqrt{\tau}}\,4\,P_{1,-1+\frac{1}{2}}$$

$$O2S2S = \frac{Z_1^{5/2}}{Z_2^{1/2}}\,\frac{4}{3\sqrt{\tau}}\,[G_{1,2+\frac{1}{2}}+\tau^2 G_{1,0+\frac{1}{2}}-\frac{2\tau}{3}\,[G_{0,1+\frac{1}{2}}+2G_{2,1+\frac{1}{2}}]]$$

$$O3S3S = \frac{8}{45}\,\frac{Z_1^{7/2}}{Z_2^{3/2}\sqrt{\tau}}\,[P_{1,3+\frac{1}{2}}+\tau^2 P_{1,1+\frac{1}{2}}-\frac{2\tau}{3}\,(P_{0,2+\frac{1}{2}}+2P_{2,2+\frac{1}{2}})]$$

$$O3D3D = \frac{2Z_1^{7/2}}{9}\sqrt{\frac{Z_2}{\tau}}\,[\frac{6}{5}\,R^2(2P_{1,1+\frac{1}{2}}+3P_{3,1+\frac{1}{2}})-\frac{4}{35}\,\frac{R}{Z_2}\,(14P_{0,2+\frac{1}{2}}+55P_{2,2+\frac{1}{2}}$$
$$+36P_{4,2+\frac{1}{2}})+\frac{1}{Z_2^2}(\frac{44}{35}\,P_{1,3+\frac{1}{2}}+\frac{56}{35}P_{3,3+\frac{1}{2}}+\frac{8}{7}\,P_{5,3+\frac{1}{2}}-\frac{\tau^2}{5}\,(4P_{1,1+\frac{1}{2}}$$
$$+6P_{3,1+\frac{1}{2}})+\frac{\tau}{105}(56P_{0,2+\frac{1}{2}}+220P_{2,2+\frac{1}{2}}+144P_{4,2+\frac{1}{2}}))]$$

$$O4F4F = \frac{Z_1^{9/2}\, Z_2^{9/2}}{45\sqrt{\tau}} \left[(4.2857142R^3 - 2.5714285 \frac{R\tau^2}{Z_2^2}) P_{2,2+\frac{1}{2}}/Z_2^4 \right.$$

$$+ \frac{P_{4,2+\frac{1}{2}}}{Z_2^4} [5.7142857R^3 - 3.4285714 \frac{R\tau^2}{Z_2^2}] + \frac{P_{1,3+\frac{1}{2}}}{Z_2^5} [2.0571428 \frac{R\tau}{Z_2}$$

$$-5.1428571R^2 + 1.0285714 \frac{\tau^2}{Z_2^2}] + \frac{P_{3,3+\frac{1}{2}}}{Z_2^5} [6.1333333 \frac{R\tau}{Z_2} - 15.3333333R^2$$

$$+3.0666666 \frac{\tau^2}{Z_2^2}] + \frac{P_{5,3+\frac{1}{2}}}{Z_2^5} [3.8095238 \frac{R\tau}{Z_2} - 9.5238095R^2 + 1.9047619 \frac{\tau^2}{Z_2^2}]$$

$$+ \frac{P_{0,4+\frac{1}{2}}}{Z_2^6} [1.7142857R - 0.6857142 \frac{\tau}{Z_2}] + \frac{P_{2,4+\frac{1}{2}}}{Z_2^6} [7.4285715R - \frac{4\tau}{Z_2}]$$

$$+ \frac{P_{4,4+\frac{1}{2}}}{Z_2^6} [9.6623377R - 5.2363636 \frac{\tau}{Z_2}] + \frac{P_{6,4+\frac{1}{2}}}{Z_2^6} [5.1948051R - 2.0779220$$

$$\frac{\tau}{Z_2}] - 0.8761905 \frac{P_{1,5+\frac{1}{2}}}{Z_2^7} 0.8727273 \frac{P_{3,5+\frac{1}{2}}}{Z_2^7} - 1.3186813 \frac{P_{5,5+\frac{1}{2}}}{Z_2^7}$$

$$\left. -0.9324009 \frac{P_{7,5+\frac{1}{2}}}{Z_2^7} \right]]$$

For the Π overlap integrals, one obtains

$$P2P2P = \frac{4Z_1^{5/2}}{5\sqrt{Z_2\tau}} [P_{1,1+\frac{1}{2}} - P_{3,1+\frac{1}{2}}]$$

$$O3D3D = \frac{4}{3} \frac{Z_1^{7/2}}{\sqrt{Z_2\tau}} [\frac{2R}{15} P_{0,2+\frac{1}{2}} + \frac{2R}{21} P_{2,2+\frac{1}{2}} - \frac{8}{35} R P_{4,2+\frac{1}{2}}$$

$$- \frac{6}{35} \frac{P_{1,3+\frac{1}{2}}}{Z_2} + \frac{2}{45} \frac{P_{3,3+\frac{1}{2}}}{Z_2} + \frac{8}{63} \frac{P_{5,3+\frac{1}{2}}}{Z_2}]$$

$$O4F4F = \frac{Z_1^{9/2}}{60\sqrt{Z_2\tau}} [P_{1,3+\frac{1}{2}} (\frac{16R^2}{7} - \frac{16\tau^2}{35Z_2^2}) + P_{3,3+\frac{1}{2}} (\frac{8}{9} R^2 - \frac{8}{45} \frac{\tau^2}{Z_2^2}$$

$$+ P_{5,3+\frac{1}{2}} (\frac{40}{63} \frac{\tau^2}{Z_2^2} - \frac{200}{63} R^2) + \frac{P_{0,4+\frac{1}{2}}}{Z_2} (-\frac{32}{21} R + \frac{32}{105} \frac{\tau}{Z_2})$$

$$+\frac{P_{2,4+\frac{1}{2}}}{Z_2}\left[-\frac{80}{21}R+\frac{80}{105}\frac{\tau}{Z_2}\right]+\frac{P_{4,4+\frac{1}{2}}}{Z_2}\left[\frac{144}{77}R-\frac{1008}{2695}\frac{\tau}{Z_2}\right]$$

$$+\frac{P_{6,4+\frac{1}{2}}}{Z_2}\left[\frac{800}{231}R-\frac{160}{231}\frac{\tau}{Z_2}\right]+\frac{112}{105Z_2^2}P_{1,5+\frac{1}{2}}+\frac{272}{495Z_2^2}P_{3,5+\frac{1}{2}}$$

$$-\frac{1680}{2457Z_2^2}P_{5,5+\frac{1}{2}}-\frac{400}{429Z_2^2}P_{7,5+\frac{1}{2}}]$$

Also for the sigma overlap integral O2P2P, one obtains

$$O2P2P = Z_1^{5/2}\,Z_2^{5/2}\,\frac{4}{\sqrt{\tau}}\left[\frac{R}{3.0Z_2^2}\left(P_{0,0+\frac{1}{2}}+2P_{2,0+\frac{1}{2}}\right)-\frac{1}{5Z_2^3}\right.$$

$$\left.\left(3P_{1,1+\frac{1}{2}}+2P_{3,1+\frac{1}{2}}\right)\right]$$

Figure 19. Computer output describing a molecular density contour map. The maximum contour is 1.8 a.u. and is represented by the integer 9. The minimum contour is 0.0 a.u. and is represented by the integer 0. The arrow designates the origin of the co-ordinate system. For this particular example the nucleus H is situated at this origin.

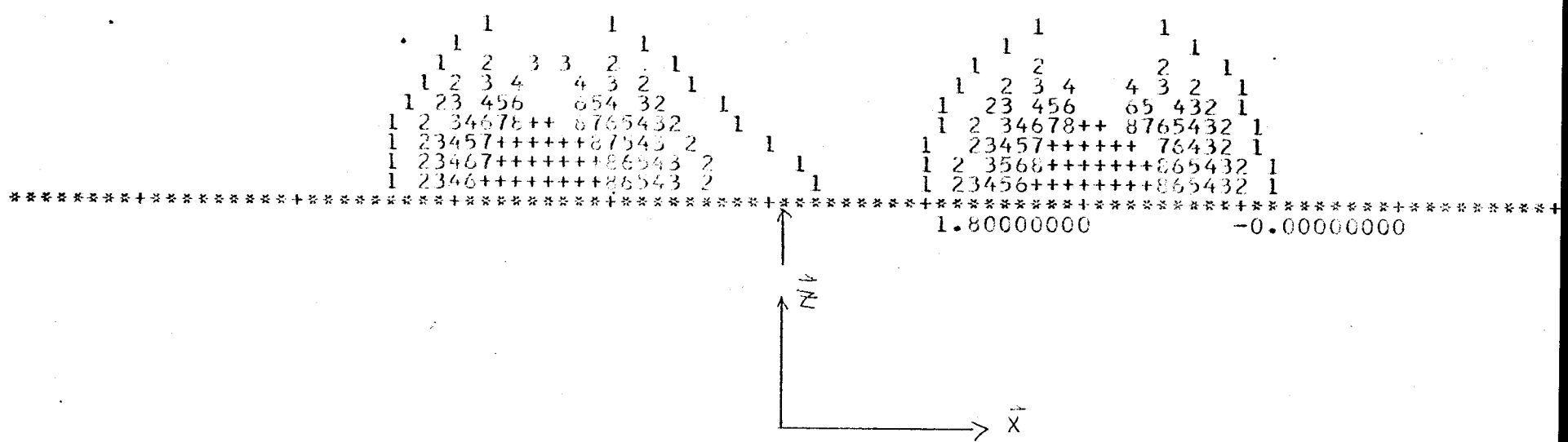
1.80000000
-0.00000000
N
X

Figure 20. Computer output describing a density difference contour map. The integer 5 represents the zero contour. The integers 0, 1, 2, 3 and 4 represent negative contours. The integers 6, 7, 8 and 9 represent positive contours. The symbol plus represents a region of contours having higher values than DMAX. The symbol - indicates a region of contours having more negative values than DMIN. The arrow represents the origin of the co-ordinate system and one of the nuclei (B in this case) is situated at this origin.

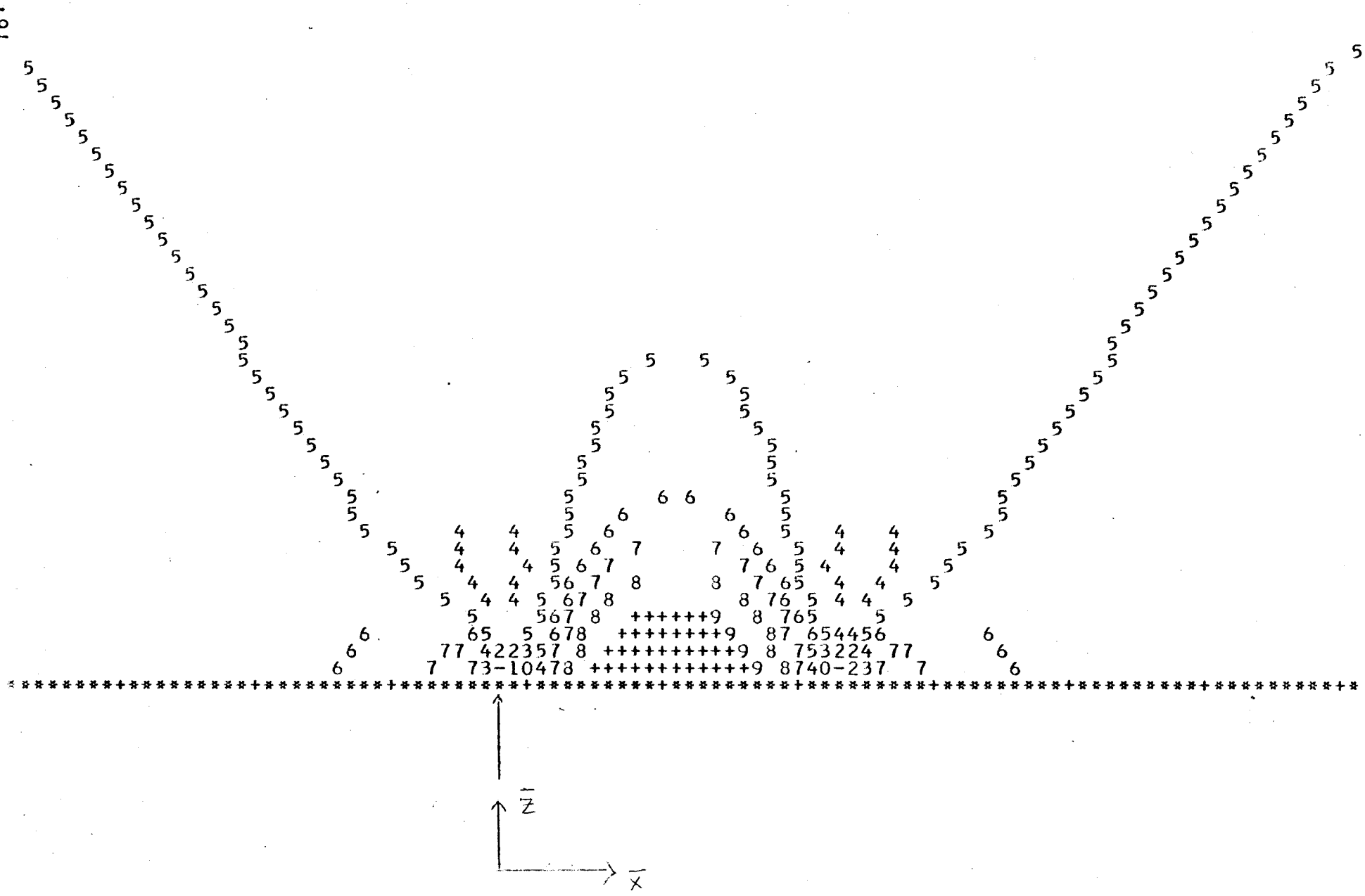
Z
X

THE DENSITY AND DENSITY DIFFERENCE CONTOUR MAPS

The one-electron density computed from a molecular Hartree-Fock function is given by

$$\rho(\vec{r}) = \sum_{i=1}^{N} n_i \phi_i \phi_i \qquad (43)$$

where N is the number of occupied molecular orbitals and n_i is the occupation number of the ith molecular orbital. Similarly the density difference function is given by

$$\Delta\rho(\vec{r}) = \rho(\vec{r}) - \rho_A(\vec{r}) \qquad (44)$$

The symbol $\rho(\vec{r})$ is defined above while the symbol $\rho_A(\vec{r})$ designates the density of the noninteracting atoms brought up to the observed internuclear distance. It is a relatively simple task to set up a programme to calculate these density functions for a diatomic molecule at a number of points in the regions surrounding the nuclei. This in fact was done and the computed density values were stored on the disc. At the end of the calculation the density values were fed into the library subroutine CØNTØR. This subroutine produced as output integer contours such as those shown in Figure 19 for the total density of the $(FHF)^{-1}$ ion and Figure 20 for the density difference function o f B_2. The path traced out by each repeated integer represents a curve of constant density. A maximum of ten integers from 0 to 9 is available for each separate map. Noted below is the section of the FØRTRAN programme devoted to the plotting of contours.

```
      ———
      ———
      ———
      ———
      REWIND 3
      READ 30, DMAX, DMIN
   30 FØRMAT (2F8.5)
      DØ 150 kI1 = 1,41
      READ (3) DX
  150 CALL CØNTØR(DX,DMAX,DMIN,M,N).
      ———
      ———
      ———
      ———
      ———
```

DX is a subscripted variable representing the density. It must have as its dimension the integer M. DMAX and DMIN represent respectively the maximum and minimum values of contours which appear in the plot. For example, if DMAX=0.9 and DMIN=0.0, then one can label the contours in the following way

Integer	Contour
0	0.0
1	0.1
2	0.2
3	0.3
4	0.4
5	0.5
6	0.6
7	0.7
8	0.8
9	0.9

M is an integer which in this work was always set equal to 101. It represents the length along the x axis defined in Figure 1 in dimensionless units and can have a maximum value of 132. In the programmes discussed here a multiplication of the number M by 0.12 yields the range of values along the x axis in atomic units. N is another integer which indicates the number of contours which will be plotted. The number 41 in the segment programme above represents the number of computer lines printed per contour map. It is a dimensionless number describing the range of Z values as defined in Figure 1. Multiplication of this dimensionless number by 0.15 gives the range of Z values in atomic units. The last computer line in each contour map is the internuclear axis. Thus the first 101 calculated density points

have a Z co-ordinate of 6.0 atomic units. In a total calculation 101×41 = 4141 density points are stored in the disc during the execution of the programme. These points are then read in groups of 101 into the library function CØNTØR Contour maps such as those shown in Figures 19 and 20 represent the computer output.

THE POPULATION NUMBERS

The population numbers reported in this thesis are just integrated forms of the total density and density difference functions. The numbers listed in Table I and labelled as the fractions of the charge in the binding regions of the various molecules are defined by the equation

$$P_B = \frac{1}{N} \int_{Q=0} \rho(\vec{r})\, d\vec{r} \qquad (45)$$

N is the total number of electrons. The restriction Q=0 indicates that $\rho(\vec{r})$ is integrated over all values of r_A and r_B in the binding region.

The numbers in Table II are labelled as the increase in the number of electronic charges in Berlin's[34] binding and antibinding regions. These numbers are defined by the equation

$$P_L = \int_{\Delta\rho(\vec{r}) = 0} \Delta\rho(\vec{r})\, d\vec{r} \qquad (46)$$

Thus P_L is equal to the integral of $\Delta\rho(\vec{r})$ over the various regions where $\Delta\rho(\vec{r})$ is positive.

The density and density difference contour maps define regions over which the various integrals are to be evaluated. Each region is divided into a grid of rectangles. The density at the midpoint of each rectangle is calculated.

The segment program below describes the evaluation of P_L

```
      ____
      ____
      ____
     PA=0.0
     X = XINII
     DØ 150 kI1 = 1,N
     Z = ZINIT
     DØ 149 kI2 = 1,M
     ____
     ____
     ____
     ____
     _____
     RØUT = Z + RECZ/2.0
     RIN = Z-RECZ/2.0
     QA = DELTA * [RØUT**2.0-RIN**20]* 3.14159
     PA = QA+PA
     1F (DELTA.LE.0.0) GØ TØ 150
149  Z = Z+RECZ
150  X = X+RECX
160  PA =PA*RECX
```

DELTA is a variable describing the density. The expression QA is the number of electrons in the annular ring whose outer radius is RØUT and whose inner radius is RIN. This annular ring is in a plane perpendicular to the internuclear axis and the radii RIN and RØUT describe the distances from the internuclear axis to the inner and outer edges of this annular ring respectively. Each of these annular ring populations is added to PA. RECZ is the length of the rectangle in the Z direction. RECX is the length of the rectangle in the X direction. XINIT and ZINIT are initial values of X and Z. The integers N and M describe the dimensions of the total grid of rectangles. The final value of PA in statement 160 is the desired population number.

TABLES

Forces on Lithium ($X^1\Sigma_g^+$) R = 5.05 1 a.u.

Orbital	Atomic Force	Overlap Force	Screening Force	f_i
$1\sigma_g$	-0.2979	0.0052	0.9984	0.7057
$1\sigma_u$	-0.3356	-0.0056	0.9993	0.6581
$2\sigma_g$	+0.0708	0.9271	0.5932	1.5911
Total	-0.5627	0.9267	2.5909	2.9549

$$\sum_i f_i = 2.9549$$

$$\text{Net Force} = \frac{3}{R^2}\,[3-2.9549] = [0.0451]\frac{3}{R^2} = 0.005$$

Force on Boron ($X^3\Sigma_g^-$) R = 3.005 a.u.

Orbital	Atomic Force	Overlap Force	Screening Force	f_i
$1\sigma_g$	-0.0263	0.0056	0.9992	0.9785
$1\sigma_u$	-0.0242	-0.0062	1.0011	0.9707
$2\sigma_g$	0.0841	1.4260	0.7947	2.3048
$2\sigma_u$	-0.8755	-0.1987	0.5823	-0.4919
$1\pi_u$	0.1980	0.4809	0.5095	1.1884
Total	-0.6439	1.7076	3.8868	4.9505

$$\sum_i f_i = 4.9505$$

$$\text{Net Force} = \frac{5}{R^2}\,[5-4.9505] = 0.027$$

Forces on Carbon ($a^1\Sigma_g^+$) R = 2.3481 a.u.

Orbital	Atomic Force	Overlap Force	Screening Force	f_i
$1\sigma_g$	-0.0381	0.0082	0.9990	0.9691
$1\sigma_u$	-0.0397	-0.0068	1.0008	0.9543
$2\sigma_g$	-0.0388	1.4869	0.8021	2.2502
$2\sigma_u$	-0.9402	-0.1920	0.6958	-0.4364
$1\pi_u$	0.3215	0.9018	1.0257	2.2490
Total	-0.7353	2.1983	4.5234	5.9864

$$\sum_i f_i = 5.9864$$

$$F_A = \frac{6}{R^2}[6-5.9864] = 0.015$$

Force on Nitrogen $(X\,^1\Sigma_g^+)$ R = 2.068 a.u.

Orbital	Atomic Force	Overlap Force	Screening Force	f_i
$1\sigma_g$	0.1519	0.0080	0.9997	1.1596
$1\sigma_u$	0.0738	0.0137	0.9972	1.0847
$2\sigma_g$	-0.0425	1.8418	0.8824	2.6817
$2\sigma_u$	-0.7754	-0.1666	0.4791	-0.4629
$3\sigma_g$	-1.7664	1.2206	0.6961	0.1503
$1\pi_u$	0.4156	0.9355	1.0816	2.4327
Total	-1.9430	3.8530	5.1361	7.0461

$$\sum_i f_i = 7.0461$$

$$\text{Net Force} = \frac{7}{R^2}\,[7\text{-}7.0461] = -0.075$$

Forces on Oxygen ($X^3\Sigma_g^-$) R = 2.282 a.u.

Orbital	Atomic Force	Overlap Force	Screening Force	f_i
$1\sigma_g$	0.2309	0.0005	1.0005	1.2319
$1\sigma_u$	0.1288	0.0098	0.9991	1.1377
$2\sigma_g$	0.4036	1.6277	0.9029	2.9342
$2\sigma_u$	-1.0478	-0.2674	0.7971	-0.5181
$3\sigma_g$	-2.3335	1.6930	0.8147	0.1742
$1\pi_u$	0.4341	0.8410	1.3287	2.6038
$1\pi_g$	-0.1003	-0.4187	0.9449	0.4259
Total	-2.2842	3.4859	6.7879	7.9896

$$\sum_i f_i = 7.9896$$

$$\text{Net Force} = \frac{8}{R^2}\,[8-7.9896] = 0.016$$

Force on Fluorine ($X^1\Sigma_g^+$) R = 2.68

Orbital	Atomic Force	Overlap Force	Screening Force	f_i
$1\sigma_g$	0.2425	0.0004	1.0002	1.2431
$1\sigma_u$	0.1207	0.0028	0.9999	1.1234
$2\sigma_g$	0.6079	0.9084	0.9307	2.4470
$2\sigma_u$	-0.7478	-0.4079	0.9878	-0.1679
$3\sigma_g$	-2.4587	2.0669	0.9081	0.5163
$1\pi_u$	0.3082	0.5640	1.5908	2.4630
$1\pi_g$	-0.0221	-0.6301	1.9639	1.3117
Total	-1.9493	2.5045	8.3814	8.9366

$$\sum_i f_i = 8.9366$$

$$\text{Net Force} = \frac{9}{R^2}[9-8.9366] = 0.080$$

Forces on Beryllium ($^1\Sigma_g^+$) R = 3.5 a.u.

Orbital	Atomic Force	Overlap Force	Screening Force	f_i
$1\sigma_g$	0.0434	0.0088	0.9991	1.0513
$1\sigma_u$	0.0342	-0.0077	1.0012	1.0277
$2\sigma_g$	-0.0870	1.3617	0.7281	2.0028
$2\sigma_u$	-0.8666	-0.3457	0.8137	-0.3986
Total	-0.8760	1.0171	3.5421	3.6832

$$\sum_i f_i = 3.6832$$

$$\text{Net Force} = \frac{4}{R^2}[4-3.6832] = 0.103$$

Forces on $N_2(X^1\Sigma_g^+)$ R = 2.01320 a.u.

Orbital	Atomic Force	Overlap Force	Screening Force	f_i
$1\sigma_g$	0.1448	0.0095	0.9995	1.1538
$1\sigma_u$	0.0698	0.0137	0.9969	1.0804
$2\sigma_g$	-0.1040	1.8513	0.8808	2.6281
$2\sigma_u$	-0.7256	-0.1742	0.4607	-0.4391
$3\sigma_g$	-1.7022	1.1792	0.6829	0.1599
$1\pi_u$	0.4077	0.9356	1.0593	2.4026
Totals	-1.9095	3.8151	5.0801	6.9857

$$\sum_i f_i = 6.9857$$

$$\text{Net Force} = \frac{7}{R^2}[7-6.9857] = 0.025$$

$N_2^+(X^2\Sigma_g^+)$ R = 2.0132 a.u.

Orbital	Atomic Force	Overlap Force	Screening Force	f_i
$1\sigma_g$	0.0788	0.0076	0.9995	1.0859
$1\sigma_u$	0.0464	-0.0002	0.9997	1.0459
$2\sigma_g$	-0.0627	1.7520	0.8792	2.5685
$2\sigma_u$	-0.6426	-0.2209	0.4464	-0.4171
$3\sigma_g$	-0.8500	0.5989	0.3532	+0.1021
$1\pi_u$	+0.4494	0.9769	1.1341	2.5604
Total	-0.9807	3.1143	4.8121	6.9457

$$\sum_i f_i = 6.9457$$

$$\text{Net Force} = \frac{7}{R^2}[7-6.9457] = 0.0094 \text{ a.u.}$$

$N_2^+(A^2\Pi_u)$ R = 2.01320 a.u.

Orbital	Atomic Force	Overlap Force	Screening Force	f_i
$1\sigma_g$	0.2169	0.0092	1.0000	1.2261
$1\sigma_u$	0.0993	0.0018	0.9996	1.1007
$2\sigma_g$	-0.1256	1.9924	0.9234	2.7902
$2\sigma_u$	-0.6085	-0.2277	0.4484	-0.3878
$3\sigma_g$	-1.6074	1.0400	0.6738	0.1064
$1\pi_u$	0.3894	0.7674	0.8465	2.0033
Total	-1.6359	3.5831	4.8917	6.8389

$$\sum_i f_i = 6.8389$$

$$\text{Net Force} = [7-6.8389]\frac{7}{R^2} = 0.278$$

$N_2^+(B^2\Sigma_u^+)$ R = 2.01320 a.u.

Orbital	Atomic Force	Overlap Force	Screening Force	f_i
$1\sigma_g$	0.0381	0.0096	0.9992	1.0469
$1\sigma_u$	0.0069	-0.0008	0.9997	1.0058
$2\sigma_g$	-0.1415	1.9460	0.9075	2.7120
$2\sigma_u$	-0.0663	-0.1766	0.2042	-0.0387
$3\sigma_g$	-1.6624	1.0610	0.6710	0.0696
$1\pi_u$	0.4196	0.9614	1.1211	2.5021
Total	-1.4056	3.8006	4.9027	7.2977

$$\sum_i f_i = 7.2977$$

$$\text{Net Force} = \frac{7}{R^2}[7-7.2977] = -0.514$$

$O_2^+(X^2\Pi_g)$ R = 2.12200 a.u.

Orbital	Atomic Force	Overlap Force	Screening Force	f_i
$1\sigma_g$	0.2422	0.0017	1.0006	1.2445
$1\sigma_u$	0.1286	0.0101	0.9990	1.1377
$2\sigma_g$	0.3225	1.8055	0.9277	3.0557
$2\sigma_u$	-1.0029	-0.2026	0.7131	-0.4924
$3\sigma_g$	-2.1760	1.4752	0.7830	+0.0822
$1\pi_u$	0.5368	0.9245	1.3218	2.7831
$1\pi_g$	0.0453	-0.2067	0.4671	0.2151
Totals	-1.9941	3.8077	6.2123	8.0259

$$\sum_i f_i = 8.0259$$

$$\text{Net Force} = \frac{8}{R^2}[8-8.0259] = -0.045$$

O_2^- ($^2\Pi_g$) R = 2.40 a.u.

Orbital	Atomic Force	Overlap Force	Screening Force	f_i
$1\sigma_g$	0.2198	+0.0000	1.0005	1.2203
$1\sigma_u$	0.1280	0.0087	0.9993	1.1360
$2\sigma_g$	0.4288	1.4982	0.8827	2.8097
$2\sigma_u$	-1.0386	-0.3550	0.8800	-0.5136
$3\sigma_g$	-2.4155	1.8602	0.8327	0.2774
$1\pi_u$	0.3272	0.7707	1.3122	2.4101
$1\pi_g$	-0.0998	-0.9002	1.5570	0.5570
Total	-2.4501	2.8826	7.4644	7.8969

$$\sum_i f_i = 7.8969$$

$$\text{Net Force} = \frac{8}{R^2}[8-7.8969] = 0.1798$$

Forces in HF

	Molecular Orbital	Atomic Force	Overlap Force	Screening Force	f_i
Force on H	1σ	0.	0.	2.0	2.000
	2σ	0.058	0.526	1.664	2.248
	3σ	0.213	0.553	1.142	1.908
	1π	0.004	0.134	2.757	2.985
	Total	0.275	1.213	7.563	9.051

$$\text{Net Force} = \frac{1}{R^2}[9-9.051] = -0.017 \text{ a.u.}$$

Force on F	1σ	0.146	0.002	0.000	0.148
	2σ	0.394	0.382	0.057	0.833
	3σ	-2.476	+1.827	0.327	-0.322
	1π	0.187	0.114	0.006	0.307
	Total	-1.749	2.325	0.390	0.966

$$\text{Net Force} = \frac{9}{R^2}[1-0.966] = 0.104 \text{ a.u.}$$

Forces on LiH

	Molecular Orbital	Atomic force	Overlap force	Screening force	f_i
Force on Li	1σ	-0.325	0.066	0.002	-0.257
	2σ	-0.010	0.730	0.840	1.560
	Total	-0.335	0.796	0.842	1.303

$$\text{Net Force} = \frac{3}{R^2}[1-1.303] = -0.010 \text{ a.u.}$$

Force on H	1σ	0.002	0.028	1.963	1.993
	2σ	0.062	0.589	0.247	0.898
	Total	0.064	0.617	2.210	2.891

$$\text{Net Force} = \frac{1}{R^2}[3-2.891] = 0.012 \text{ a.u.}$$

Forces in LiF

	Molecular Orbital	Atomic force	Overlap force	Screening force	f_i
Force on Li	1σ	0.	0.	2.0	2.0
	2σ	-0.362	0.070	0.003	-0.289
	3σ	-0.064	0.016	2.004	1.956
	4σ	-0.296	0.080	2.200	1.984
	1π	0.010	0.180	3.304	3.494
	Total	-0.712	0.346	9.511	9.145

$$\text{Net Force} = \frac{3}{R^2}[9-9.145] = -0.052$$

Force on F	1σ	0.099	0.001	0.000	0.100
	2σ	0.007	0.028	1.972	2.007
	3σ	0.636	0.081	0.014	0.731
	4σ	-1.148	0.739	0.043	-0.366
	1π	0.474	0.136	0.012	0.622
	Total	0.068	0.985	2.041	3.094

$$\text{Net Force} = \frac{9}{R^2}[3-3.094] = -0.101$$

BIBLIOGRAPHY

1. P.A.M. Dirac, Proc. Roy. Soc., A123, 714 (1929).
2. J. H. Van Vleck and A. Sherman, Rev. Mod. Phys. 7, 167 (1935).
3. R. S. Mulliken, Spectroscopy, Molecular Orbitals and Chemical Bonding. Technical Report, Laboratory of Molecular Structure and Spectra, Dept. of Physics, The University of Chicago, 1966.
4. R. P. Feynman, Phys. Rev., 56, 340 (1939); H. Hellmann, "Einfuhrung indie Quantenchemie", F. Deuticke, Leipzig, 1937, p. 285.
5. G. N. Lewis, J. Am. Chem. Soc., 38, 762 (1916).
6. R.F.W. Bader and W.H. Henneker, J. Am. Chem. Soc., 87, 3063 (1965).
7. R.F.W. Bader and W.H. Henneker, J. Am. Chem. Soc., 88, 280 (1966).
8. R.F.W. Bader, W. H. Henneker and P. E. Cade, J. Chem. Phys. 46, 3341 (1967).
9. D. R. Hartree, The Calculation of ATomic Structures. New York: John Wiley and Sons, Inc., 1957.
10. P. O. Löwdin, Phys. Rev., 97, 1474 (1955).
11. A. J. Coleman, Rev. Mod. Phys. 35, 668 (1963).
12. D. R. Hartree, Proc. Cambridge Phil. Soc. 24, 89 (1927).

13. E. Clementi, Tables of Atomic Functions, published by International Business Machines Corporation.

14. V. Fock, Z. Physik, 61, 126 (1930).

15. J. C. Slater, Phys. Rev., 35, 210 (1930).

16. M. Born and R. Oppenheimer, Ann. Physik, 87, 457 (1927).

17. R. G. Parr, Quantum Theory of Molecular Electronic Structure, New York, W. A. Benjamin, Inc. 1964.

18. C.C.J. Roothaan, Rev. Mod. Phys., 23, 69 (1951).

19. A. C. Hurley, Proc. Roy. Soc., A226, 179 (1954).

20. C. W. Scherr, J. Chem. Phys., 23, 569 (1955).

21. B. J. Ransil, Rev. Mod. Phys., 32, 245 (1960).

22. J. W. Richardson, J. Chem. Phys., 35, 1829 (1961).

23. A. C. Wahl, J. Chem. Phys., 41, 2600 (1964).

24. P. E. Cade, K.D. Sales, and A. C. Wahl, J. Chem. Phys. 44, 1973 (1966).

25. J. Hinze and C.C.J. Roothaan (reprint)

26. L. Brillouin, Actualités Sci et Ind., No. 71 (1933); No. 159 (1934).

27. C. Moller and M. S. Plesset, Phys. Rev., 46, 618 (1934).

28. R. E. Stanton, J. Chem. Phys. 36, 1298 (1962).

29. R. K.Nesbet, Rev. Mod. Phys. 33, 28 (1961).

30. Reference 69, page 171.

31. W. M. Huo, J. Chem. Phys., 45, 1554 (1966).

32. S. T. Epstein, A. C. Hurley, R. E. Wyatt, and R. G. Parr, J. Chem. Phys. 47, 1275 (1967).

33. M. Cohen and A. Dalgarno, Proc. Phys. Soc. (London), 77, 748 (1961).

34. T. Berlin, J. Chem. Phys., 19, 208 (1951).

35. M. Roux, S. Besnainou, and R. Daudel, J. Chim. Phys., 53, 218 (1956).

36. M. Roux, S. Besnainou, and R. Daudel, J. Chim. Phys., 53, 939 (1956).

37. M. Roux, J. Chim. Phys., 55, 754 (1958).

38. M. Roux, J. Chim. Phys., 57, 53 (1960).

39. M. Roux, M. Cornille, and G. Bessis, J. Chem. Phys., 58, 389 (1961).

40. M. Roux, M. Cornille, and L. Burnelle, J. Chem. Phys., 37, 933 (1962).

41. G. Bessis and S. Bratoz, J. Chim. Phys. 57,769 (1960).

42. J.L.J. Rosenfeld, Acta Chem. Scand., 18, 1719 (1964).

43. P. R. Smith and J. W. Richardson, J. Phys. Chem., 69, 3346 (1965).

44. P.R. Smith and J. W. Richardson, J. Phys. Chem., 71, 924 (1967).

45. B. J. Ransil' and J. J. Sinai, J. Chem. Phys. 46, 4050 (1967).

46. R. S. Mulliken, J. Chem. Phys., 23, 1833 (1955).

47. R. S. Mulliken, J. Chem. Phys., 23, 1841 (1955).

48. E. R. Davidson, J. Chem. Phys. 46, 3320 (1967).

49. K. Ruedenberg, Rev. Mod. Phys., 34, 326 (1962).

50. C. Edmiston and K. Ruedenberg, Rev. Mod. Phys., 35, 457 (1963).

51. C. Edmiston and K. Ruedenberg, J. Chem. Phys., 43, S97 (1965).

52. L. S. Bartell and R. M. Gavin, J. Am. Chem. Soc. 86, 3493 (1964).

53. R. M. Gavin and L. S. Bartell, J. Chem. Phys., 44, 3687 (1966).

54. L. S. Bartell and R. M. Gavin, J. Chem. Phys. ,43, 856 (1965).

55. L. S. Bartell (private communication).

56. P. E. Cade, K. D. Sales, and A. C. Wahl (unpublished results for $Li_2(X\,^1\Sigma_g^+)$.

57. J. B. Greenshields (unpublished results).

58. P. E. Cade, K. D. Sales, and A. C. Wahl, J. Chem. Phys. 44, 1973 (1966).

59. P. E. Cade and G. Malli (unpublished results for $O_2^+(X^2\Pi_g)$, $O_2(X^3\Sigma_g^-)$ and $O_2^-(^2\Pi_g)$.

60. A. C. Wahl, J. Chem. Phys. 41, 2600 (1964).

61. J. O. Hirschfelder, C. F. Curtiss, and R. B. Bird, Molecular Theory of Gases and Liquids (John Wiley and Sons, Inc., New York, 1954). Appendix I-A, pp 1111 and 185 ff.

62. R.F.W. Bader, J. Am. Chem. Soc., 86, 5070 (1964).

63. E. Clementi, C.C.J. Roothaan, and M. Yoshimine, Phys. Rev., 127, 1618 (1962).

64. R.F.W. Bader and A.K. Chandra (private communication).

65. G. Das and A. C. Wahl, J. Chem. Phys., 44, 87 (1966).

66. P. E. Cade and K. D. Sales (unpublished calculations for $Be_2\ ^1\Sigma_g^+$).

67. R.F.W. Bader and A.K. Chandra (private communication).

68. G. Herzberg, Z. Physik, 57, 601 (1929).

69. A. C. Hurley, in Molecular Orbitals in CHemistry, Physics and Biology, P. O. Löwden and B. Pullman, Eds. (Academic Press Inc., New York 1964) pp. 161-191.

70. R.F.W. Bader and G. A. Jones, Can. J. Chem. 39, 1253 (1961).

71. C. W. Kern and M. Karplus, J. Chem. Phys., 40, 1374 (1964).

72. A. C. Wahl, Science 151, 961 (1966).

73. R. S. Mulliken, Rev. Mod. Phys. 4, 1 (1932).

74. R. S. Mulliken, Phys. Rev. 56, 778 (1939).

75. W. L. Clinton and W. C. Hamilton, Rev. Mod. Phys. 32, 422 (1960).

76. L. Pauling, The Nature of the Chemical Bond. (Cornell University Press, Ithaca, New York), 3rd edition.

77. H. Shull, J. Appl. Phys. Suppl. 33, 240 (1962).

78. J. Braunstein and W. T. Simpson, J. Chem. Phys. 23, 176 (1955).

79. J. Braunstein and W. T.Simpson, J. Chem. Phys. 23, 174 (1955).

80. H. Shull, J. Am. Chem. Soc. 82, 1287 (1960).

81. H. Shull, J. Phys. Chem. 66, 2320 (1962).

82. A. D. McLean, J. Chem. Phys. 39, 2653 (1963).

83. L. Wharton, W. Klemperer, L. P. Gold, R. Strauch, J. J. Gallagher and V. E. Derr, J. Chem. Phys., 38, 1203 (1963).

84. R. K. Nesbet, J. Chem. Phys. 36, 1518 (1962).

85. S. L. Kahalas and R. K. Nesbet, J. Chem. Phys. 39, 529 (1963).

86. M. Kotani, A. Amemiya, E. Ishiguro, and T. Kimura, Table of Molecular Integrals, (Tokyo, Maruzen Co., Limited. 1955).

87. M. P. Barnett and C. A. Coulson, Phil. Trans. Roy. Soc. A243, 221 (1951).

88. R.F.W. Bader, I. T. Keaveny and P. E. Cade (to be published).

89. R. F. W. Bader and A. D. Bandrauk (to be published).

90. T. A. Koopmans, Physica 1, 104 (1933).